Modeling Dynamic Ground Reaction to Predict Motion of and Loads on Stranded Ships in Waves

Jeffrey McQuillan

A thesis submitted to the faculty of

Virginia Polytechnic Institute and State University

in partial fulfillment of the requirements for the degree of

MASTER OF SCIENCE
in
Ocean Engineering

Dr. Alan J. Brown, Chairman

Dr. Michael J. Allen

Dr. Marte S. Gutierrez

December 2002

Blacksburg, Virginia

Keywords: stranded, grounded, ship, motion, soil, reaction

Modeling Dynamic Ground Reaction to Predict Motion of and Loads on Stranded Ships in Waves

Jeffrey McQuillan

Abstract

Ship groundings are a low probability event, but can create severe environmental and financial consequences. The objective of this thesis is to provide knowledge and understanding of the grounded ship condition to salvors and ship owners so they can reduce the possible negative consequences of future ship groundings. There has been very little research on the motions of and loads on a grounded ship in waves. In this thesis, a model of the ground reaction forces due to the steady state motions of a grounded ship is developed. This model is derived from civil engineering applications but tailored to the stranded ship problem. The ground reaction sub-model is part of a ship motion model that predicts grounded ship motions and loads in waves. The model input specifies the static grounded equilibrium condition and static grounded forces. The model calculates steady state motions and loads around the equilibrium condition. This thesis describes a preliminary version of the full six degree of freedom model in which soil reactions are accounted for in two degrees of freedom, heave and pitch, assuming a rectangular shaped hull. Bottom types are categorized as sand, mud, coral and rock. The ship can be embedded or resting on the surface of the bottom.

Dedication

To my family,
loving wife Jaimee
and supportive son Scott

Acknowledgements

I would like to thank Dr. Alan J. Brown for his guidance and advice throughout this thesis. He is a great mentor and I appreciated working with him. I would like to thank Dr. Marte S. Gutierrez for all his help with the soil model. I would like to thank my research partner LT Mike Simbulan, USCG for all his work in developing the Stranded Ship Motions and Loads Program and for his help in writing this thesis.

Table of Contents

List of Figures and Tables

Figures

Tables

Chapter 1 Introduction

1.1 Motivation and Background

Ship groundings are a low probability event, but when they do occur it is big news, with potentially major consequences for the environment and the shipping industry. Significant work has been done and continues on predicting structural damage suffered by a ship while grounding, but little work has been done to predict the motion of and loads on a ship after it has grounded. A review of ship groundings was conducted to identify some generalities about historic grounding events. A summary of this review is provided in Table 1.1, which lists a variety of grounding events documented mostly by the U.S. Navy Supervisor of Salvage [1], [2], [3], [4], and [5]. Based on this data, the following general conclusions and observations about the range and scope of these events are:

1. Groundings occur on a range of bottom types. The general types of bottom are:
    - Sand, as shown in Figure 1.1
    - Clay (mud)
    - Soft rock (coral), as shown in Figure 1.2
    - Hard rock

Figure 1.1 Warship grounded in sand [6]

Figure 1.2 Cargo ship grounded in coral [7]

Table 1.1-Ship Grounding Incidents

Ship	Orientation	Type of Bottom	Waves	Time	Hull Shape (Idealized)	Year	Location
New Carissa	Broached	Sandy, in surf zone	*15-26ft, breaking, longshore current 8-10kts, wind 25-45kts gusts 70kts, *15-20ft, wind calm	*4 days, *3 days	Rectangle	4-Feb-99	Coos Bay, OR
Valdivia (LST 93) LST 1179 class	Broached, 7ft trim, 2.5deg list to stbd	Sand, small rocks	breaking, in surf zone	55 days	wedge	17-May-97	North Chile Coast
USS La Moure County LST 1194 (LST 1179 Class)		Rock	5-7ft, flood tide, SS2, wind 18-22kts	1.5 hours	wedge	12-Sep-00	Cifuncho Bay, Chile
M/V Kuroshima	Broached	Rocks then sand			rectangle	26-Nov-97	Unalaska Island, Alaska
M/V Concorde Spirit	Entire ship embedded	Mud			rectangle	23-Oct-98	Hampton, VA
T/B Bayou Zachary	Broached	Mud			rectangle		Harvey Canal Intercoastal
USNS Bob Hope				1 day	wedge	19-Sep-01	Chesapeake Bay
Liberty Spirit		Sand			rectangle	29-Mar-99	Columbia River
M/V Sergo Zakariadze	Broached	Rocks	7-10ft (12ft high)		rectangle	18-Nov-99	San Juan, Puerto Rico
Bunga Terati Satu		Coral			rectangle	2-Nov-00	Sudbury Reef, Australia
Monssen DD 798	Broached-fully embedded, 5 deg list	Sand, 7ft deep		45 days	wedge	5-Mar-62	Beach Haven, NJ
Dona Ouriana	180ft of 483 ft aground	Coral			rectangle	27-Apr-62	Pocklington Reef
Frank Knox DDR 742		Coral	Tyhpoon Gilda, Harriet strong lateral current	37 days	wedge	18-Jul-65	Pratas Reef, South China Sea
Terrell County LST 1157	Broached	Sand			wedge		Tuy Hoa, Vietnam
Summit County LST 1146		Sand			wedge		Chu Lai, Vietnam
T-AK 276		Coral	4 typhoons		wedge	23-Sep-73	Triton Island, South China Sea
Mahnomen County LST 912	Broached	Rocky shore	Breaking, 18ft, wind 25kts		wedge	31-Dec-66	Chu Lai, Vietnam
USNS General Daniel I. Sultan		Coral			wedge		Rukon Shoal, Okinawa
Submarine Tiru SS 416		Coral			cylinder	19-Nov-67	Frederick Reef, Australia
Guardfish SSN 612		Coral		3 days	cylinder	24-Dec-67	Pearl Harbor, Hawaii
Regulus AP 57		Hard rock and Sand	Typhoon		rectangle	Aug-73	Hong Kong Harbor
Tucumcari PGH 2	25 deg down by bow, 3 deg list to port	Coral, 3ft of water				fall 1972	Caballo Blanco Reef, Puerto Rico
Solar Trader		Coral			rectangle	Dec-71	West Fayu Islands, atoll in Pac
Garfish H-3 (SS30)	Broached	Sand			cylinder	14-Dec-16	Samoa Beach Eureka, CA
Milwaikee C 2	Broached	Sand			wedge	13-Jan-17	Samoa Beach Eureka, CA

DeLong DD129				16 days	wedge	1-Dec-21	Halfmoon Bay, CA
S-19 (SS124)		Sand		64 days	cylinder	13-Jan-25	Nauset Beach near Orleans, MA
S-48 (SS159)		Rocks then Sand			cylinder	29-Jan-25	Jaffrey Point, NH
Omaha (CL4)	1/2 length embedded, 2453 tons on reef (of 8993)	Coral	small tide range	10 days	wedge	19-Jul-37	Castle Is, Bahamas
SS Lancaster		Rocks			wedge	31-Dec-42	El Hank Light
SS Sea Flyer		Sand			wedge	21-Jul-41	Eniwetok Atoll
Seize ARS26	Broached	Sand			wedge		Clipperton Is, Pacific atoll
Missouri-Battleship	whole length embedded	Sand	calm, protected	14 days	wedge	17-Jan-50	near Old Point Comfort
Thai Frigate HMTS Prasae	Broached-7 ft in sand	Sand	6ft		wedge	Jan-51	North Korea
North Korean LST M-370	Broached	Rock			wedge	Mem day'51	Taechong-do, Korea
Cornhusker Mariner-535ft		Rock		over 3 months	rectangle	7-Jul-53	Pusan, Korea
San Mateo Victory		Rock					Cheju-do Pusan
SS Quartette	Broached	Sand			rectangle		Pearl & Hermes Reef, near Midway
Korean LST Suyong (LST677)	Broached			16 days	wedge	13-Mar-83	Tok Son Ri, Korea
Gumi ARS26		Rocks	high seas, high winds	12 days	wedge	13-Mar-83	Tok Son Ri, Korea
LindenBank	Broached	Coral			rectangle	late'75	Fanning Is, 1,000miles south HI
Anangel Liberty		Coral			rectangle	Apr-80	French Frigate Shoals, HI
USNS Chauvenet T-AG529	hard aground at bow	Coral			wedge	mid 1982	Dauisan Reef in Sulu Sea
Torrey Canyon	8 deg stbd list	Rocks	bad weather, almost gale force winds		rectangle	Mar-67	Seven Stones in Scilly Isles
Amoco Cadiz		Rocks	Breaking		rectangle	Mar-77	Portsall on Brittany coast
Exxon Valdez		Coral			rectangle	24-Mar-89	Bligh Reef, Prince William sound, Ak

2. The grounding event is divided into 4 distinct phases, as shown in Figure 1.3:

   a. Ship underway-Phase 1

   b. Grounding impact event (t = 0 to t = 5 sec)-Phase 2

   c. Orientation and translation (t = 5 sec to t = 24^{+} hours)-Phase 3

   d. The steady-state grounded position with steady-state periodic motion in response to waves (t = after one extreme tidal or extreme weather cycle), (statistically stationary process)-Phase 4

Grounded ship can go back to phase 3 and then re-enter phase 4

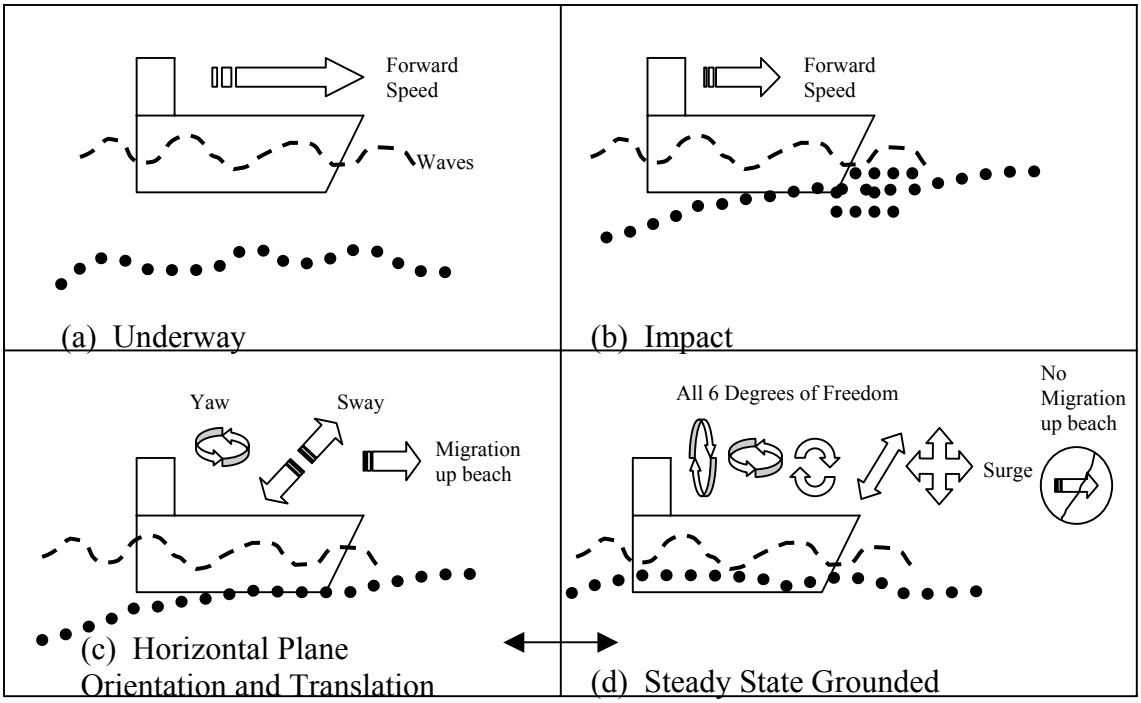

Figure 1.3 Four Phases of Ship Groundings

3. Ships are most often in a surf zone close to shore with waves, as shown in Figure 1.1.

4. Ship orientation cannot be generalized. A ship that grounds may broach if conditions are right, but it does not always broach. Since ship operators and

salvors try to prevent broaching, it cannot be assumed that a ship will broach after grounding.

5. Ships usually run aground bow first with some portion of the ship length either embedded in the bottom or resting on the bottom exchanging buoyancy for an equal ground reaction.
6. Groundings may last several days to several months. This emphasizes the need to understand the ship's motions and loads during this time, because important decisions have to be made about its rescue and salvage.

Most grounding research has focused on the grounding event, phase two. Few researchers have investigated the third and fourth phases of grounding. This thesis analyzes the fourth phase of ship grounding. The steady-state grounded motions of the stranded ship in waves around the quasi-equilibrium position are treated as a steady dynamic problem. The equilibrium condition without waves is calculated after one extreme tidal or extreme weather cycle (which includes direction of the waves, wind speed and direction). Calculations are made at a discrete number of tidal stages. If another large tide or extreme weather cycle does occur that changes the equilibrium position of the stranded ship then the ship may go back to the third phase. After it re-orients itself and finishes any translation it will enter the fourth phase again. As a preliminary study, this thesis calculates the forces and moments necessary to analyze motions of and loads on the grounded ship in two degrees of freedom, heave and pitch. After troubleshooting and assessment of this model, it will be expanded to a full six degree of freedom model. **Our hypothesis is that a grounded ship in waves may have significantly higher loads and bending moments than predicted by static analysis.**

1.1.1 Salvage Operations

It is important for salvors to know and understand the motions of and loads on a ship after it has grounded. There is often significant damage caused during grounding. Hull structure residual strength may be marginal. Understanding current and potential loads on the ship is important in determining ship safety and the potential for further damage or breaking up. By the time salvage vessels arrive on-scene, immediate decisions are required for a successful operation. These decisions are often made in the face of adverse waves and weather so they need to be based on the best and most accurate information available.

Until freeing, the ship is often stabilized. This is done using anchors (beach gear) or by flooding down. Currently, the basic techniques used in the salvage industry to free a stranded ship are:

- reducing the draft of the ship,
- pushing or pulling the ship into deeper water,
- increasing the depth of water at the site of the stranded ship, or
- some combination of these techniques.

Removing loads like cargo, fuel, mud and floodwater reduces the draft of a stranded ship. If the ship is partially grounded then adjusting its trim by moving weights or adjusting ballast may free it. Pushing or pulling the stranded ship requires enough force to overcome the forces of friction, suction and soil buildup. Friction in sand is a function of the ground reaction force so reducing the ground reaction by lightering the ship can aid in the operation. Friction in mud is the product of shear strength and contact area so loosening the mud around the hull will aid in the operation. The suction force can be

decreased by rocking the ship or by scouring the surrounding soil, which will allow water to flow to the hull. Dredging and scouring can be used to increase the water depth at the stranded ship. Sometimes channels are created for the ship to float into deeper water. Tides may also increase the water depth at the stranded ship site, but only temporarily. Examples of typical decisions that need to be made by the salvor are:

- hurry the operation to avoid adverse weather or tides,
- stabilize the stranded ship,
- remove/destroy some or all of the cargo,
- request more help and money, or
- a combination of these choices.

Currently these decisions are made in an ad hoc manner based on a simplified use of static analysis along with experience and sound engineering/seamanship judgment. Some courses of action intended to avoid disaster may have significant adverse pollution, safety and cost impacts. Examples of these actions are:

- efforts to refloat or ballast,
- rigging of anchors, cables and support vessels that are necessary to stabilize the stranded ship,
- lightering or burning of fuel, and
- use of explosives.

The salvor must have all the necessary information to accurately predict the impact of alternative plans of action or no action. Ships are not designed for the motions and loads they experience in the grounded condition such as partially constrained hydrodynamic motions and soil reactions. After grounding damage, the ship structure

may have only limited residual strength. The longer the ship stays grounded, the worse the situation gets. The *U.S. Navy Salvage Engineer's Handbook* [8] states, "Stranding salvage is time-critical; environmental conditions may improve or worsen with time, but the condition of a stranded ship steadily deteriorates". The continued wave loading and soil reaction on a stranded ship will eventually cause structural damage even on a hull that was initially undamaged from the grounding event.

1.1.2 Ground Reaction

At sea, buoyant force equals total ship weight, but if a ship runs aground then a ground reaction is created. At equilibrium the ground reaction is defined as the difference between the ship weight and the available buoyancy. It acts approximately through the centroid of the grounded area [8]. The ground reaction can increase if the ship takes on more weight from flooding either by seas or hull damage. If the ship is partially aground then the ship is free to heel and change its trim about the grounded area until both forces and moments are in equilibrium.

When a ship grounds in mud, the mud is forced down by the weight of the ship, which causes pore water to displace and the mud to condense. The condensed mud severely restricts water flow to the hull. This makes the pressure below the stranded ship constant. If hydrostatic pressure then increases around the ship because of a high tide or waves, then a low-pressure region is created below the ship that holds the ship down due to suction. Ships with rectangular shaped hulls experience greater suction effects then wedge shaped ships [8].

1.2 Objectives

The primary objective of this thesis is to develop a practical methodology and model to predict motions of and loads on a stranded ship in waves as a function of the stranded ship scenario, sea and weather conditions. As a preliminary, a Stranded Ship Motions & Loads Program (SSMLP) with two degrees of freedom is developed that takes into account wave loading and soil reactions. The main focus of this thesis is to apply a simple yet practical soil model to be used in this Stranded Ship Motions & Loads Program. The next phase in this research will expand this program to a full six degree of freedom model.

1.3 Literature Search

A literature search was conducted that indicates there has been very little study on the motions of and loads on a stranded ship in Phase 4 of ship groundings (Figure 1.3). Most of the research in ship grounding involves damage to the ship structure in Phase 2 as a ship grounds, but this research does not extend to the motion of and loads on a ship after it has grounded. The only specific study on the motions of a grounded ship is by McCormick [9] and McCormick and Hudson [10]. Both studies address Phase 3 of ship grounding events. In McCormick's study, the planar motions of a grounded broached ship are linearized and solved, with the hydrodynamic reactions analyzed using linear wave theory, and the seabed treated elastically using a quasi-elastic discrete model. McCormick and Hudson developed a two-degree of freedom model to predict the wave-induced migration of a partially embedded, structurally intact, grounded and broached ship up a sandy mildly sloping sea bottom without rock. They compare results from their

model to results obtained from an experimental study using a wave tank with a sand bottom middle section with no slope and a rectangular ship model.

The most relevant work involving a suitable model of grounding soil reactions comes from civil engineering where the soil-structure interaction is very important for structures subjected to earthquakes, machine vibrations, and offshore structures subjected to wave loading. These disciplines have studied soil dynamic behavior for some time and have developed simple and consistent methods to model the soil reactions. These same techniques are used here, but tailored to the grounded ship application.

1.4 Outline

A theoretical analysis of the motions and loads in six-degrees of freedom of a grounded ship in waves is developed. The equations of motion are analytically derived for a stranded ship in waves with an appropriate soil reaction model to generate the soil reaction forces. Results are obtained that compare forces and loads between a free floating and a grounded ship. Chapter One provides an introduction and motivation for solving the grounded ship problem. Background is provided on salvage operations and ground reaction. Chapter Two provides the background and development of soil models in general and then describes, more specifically, lumped parameter models. A six degree-of-freedom soil model is presented and explained. Chapter Three derives the equations of motion for a grounded ship in waves. Chapter Four presents the methods and equations used to calculate the static grounded condition. Chapter Five describes the Stranded Ship Motions & Loads Program (SSMLP). Chapter Six presents motion and load results in the form of bending moment plots and response amplitude operator plots,

provides a parametric study of the soil parameters, and briefly discusses future work required in the grounded ship problem.

Chapter 2 Modeling Soil Reaction

2.1 Background and Development of Soil Models

The following is a brief summary of the historical development of soil models presented by Jose M. Roesset [14]. Initially, soil dynamic analysis did not receive much attention in Civil Engineering, which mainly focused on static analysis. Some work in the area of machine-foundation interaction was made and continues which isolates and deduces the effects of machine vibrations on foundations. Mainstream study and analysis of soil dynamics did not occur until significant damage was suffered by buildings from earthquakes. The earthquake damage needed to be explained by analyzing the vibrations of soil, so researchers started studying soil dynamics and soil-structure interaction. The development of soil models was motivated by the effects earthquakes had on structures and the need to understand the dynamic loads so building and foundation designs could be improved. Also, the development of offshore gravity platforms, which use large heavy concrete foundations to anchor themselves to the ocean floor, has increased the need for understanding dynamic loads on foundations.

Researchers started their study of soil dynamics by developing general equations, which then led to sophisticated calculations. They gained experience over time and discovered the key aspects of soil behavior. This then led to the development of simplified procedures like the one that is presented in this thesis that are still used today. Work began in the area of soil-structure interaction in the 1920's from the need to design structures to support heavy machinery that could cause vibration in the foundation. In the 1930's the first analytical solution for vertical displacement on the surface of a linear

elastic, homogenous and isotropic half-space subject to a harmonic normal stress uniformly distributed over a circular area with torsional vibrations was developed by Reissner [11]. Work continued in the 1940's and the 1950's saw an expansion of research in this area, which led to continued studies on the subject in the 1960's. By 1971, a solution for a rigid circular foundation on the surface of an elastic half-space, covering an extended range of dimensionless frequencies, was presented in graphical and tabular form for coupled horizontal and rocking motions by Veletsos and Wei [12]. By the late 1970's, the capability existed to compute the dynamic stiffness of foundations of arbitrary shape in horizontally stratified soil deposits with any desired degree of accuracy, as long as linear elastic behavior could be assumed.

Work also began on soil-structure interaction on a parallel path in the area of seismic studies. In the 1940's, the effect of soil-structure interaction on the seismic response of buildings was studied. Work continued through the 1950's, 60's and 70's in this area with Kausel [13] developing a substructure approach, that accounts for the response of a rigid foundation to a train of seismic waves using linear analysis. By the late 1970's the basic phenomena of soil-structure interaction was well known and understood. In 1985 the first rigorous and comprehensive treatment of the topic with applications in both machine foundations and seismic problems was addressed by Wolf [18]. Researchers have always tried to use simple models to represent tsoil such as the simple lumped parameter model consisting of a mass, a spring and a dashpot. As early as 1954, researchers substituted a rotational spring for the foundation in their seismic studies of soil-structure interaction. Horizontal and rotational springs were used in 1965 to model the soil. Lumped parameter models were used frequently in the late 60's. Work

has continued on the improvement of the lumped parameter model, and it is still used today to model soil in various civil engineering applications.

The basic Civil Engineering problem that applies to this thesis is the dynamic response of a structure interacting with a soil. The problem is defined as a structure with finite dimensions embedded to some degree in soil, which extends to infinity, with specified loads acting on the structure. It is common to assume the response of the soil and structure will remain linear as is stated by Wolf [14], "In the majority of cases both the structure and the soil [response] will remain linear, but linear analysis is also helpful in more complicated nonlinear areas of application. The results of a nonlinear analysis of certain dynamic systems with strong nonlinearities are often similar to those of a linear calculation." This study assumes linear behavior.

There are two alternate methods for modeling this problem, the direct finite element method and the substructure method. The direct finite element method models the region of linear soil adjacent to the soil-structure interface explicitly with finite elements up to an artificial boundary. The artificial boundary presents some problems in the analysis because it is arbitrary. A large number of degrees of freedom arise from discretizing the adjacent soil region, which requires large computational time. According to Wolf [14], "a loss of physical insight also results. It follows that the direct finite element method is not appropriate for standard projects of moderate and small sizes." The ship-soil interaction falls into the moderate to small size project range on the scale of typical civil engineering applications.

The substructure method decomposes the global soil-foundation-superstructure system into subsystems, each of which can be analyzed separately using the most appropriate techniques. The irregular (nonlinear) structure is modeled with an interconnection of masses, dashpots and springs or equivalently by finite elements. The dynamic equations of motion of the structure discretized at the nodes located on the structure-soil interface and in its interior are then developed. The other substructure, the unbounded soil extending to infinity, has equations that are regular and linear. A boundary-integral equation is used to calculate the interaction force-displacement relationship. Dynamic stiffness is the boundary condition used to model the unbounded soil. The responses of the individual subsystems are combined by imposing the interaction conditions along the separating surfaces. Thus, the overall response of the system is obtained. The substructure method is preferred over the direct finite element method in civil engineering applications.

The equations of motion may be solved in the time domain or the frequency domain. Because ocean waves are a random excitation, frequently described by only a sea state and a corresponding wave energy spectra, a frequency domain solution to the equations of motion is more appropriate and straight-forward to apply. The solution requires some basic assumptions about the random nature of the waves and the linearity of the response. These are discussed in Chapter 3.

In the frequency domain the excitation can be decomposed using a Fourier series and the response determined independently for each Fourier term corresponding to a specific frequency. The dynamic response of the soil is visco-elastic. Damping is modeled using a dashpot. The dynamic stiffness of the unbounded visco-elastic soil can

be modeled using the boundary-element method or sophisticated finite-element procedures, but these procedures are too complicated and require large computation times and large investments. As Wolf [14] states, "for most projects the simple physical models of the unbounded soil developed [in his book] can be used", and lumped parameter models are one of the simple physical models described in his book. This thesis uses a lumped parameter model to develop the soil reactions for the grounded ship condition.

To find the stiffness and damping coefficients, soil properties are needed. Table 2.1 from D`Appolonia Consulting Engineers [15] lists average soil parameter values that are used in the development of the soil model. Hudson [16] used sand mass-density = 1,600 kg/m3, Young's Modulus E = 60 MPa and Poisson's Ratio $\nu = 0.26$.

Table 2.1 Average soil properties used in soil lumped parameter model [15]

	Sand	Clay (Mud)	Soft Rock (Coral)	Hard Rock
Shear wave velocity, V_s (ft/sec)	1,250	625	2,500	5,000
Poisson's Ratio, ν	0.45	0.499	0.35	0.25
Density, ρ ($10^3 lb_f$-sec^2/ft^4)	4.35×10^{-3}	4.04×10^{-3}	4.66×10^{-3}	4.97×10^{-3}
Shear Modulus, G, ($10^3 lb_f/ft^2$)	6.79×10^3	1.58×10^3	29.1×10^3	124.2×10^3

Whitman and Richart [17] recommend the following values for Poisson's ratio:

- Sand (dry, moist, partially saturated) $\nu = 0.35\text{-}0.4$
- Clay (saturated) $\nu = 0.5$
- A good value for most partially saturated soils is $\nu = 0.4$.

2.2 Lumped Parameter Models

The complex behavior of the soil-structure interaction is modeled using a simple lumped parameter model, which consists of a mass, m (slugs), a spring, k (lb_f/ft) and a dashpot, c (lb_f-sec/ft), where the system parameters m, k and c are chosen to match measured response or finite element analysis.

For loads applied statically to the structure, the soil can be represented by a simple spring and dashpot. The lumped parameter model is exact for the static case and for the asymptotic value at infinite frequency. The coefficients are frequency dependent.

Wolf [14] states the model must reflect the following key aspects of the foundation-soil system for all translational and rotational degrees of freedom:

- The shape of the foundation-soil (structure-soil) interface
- The nature of the soil profile
- The amount of embedment
    - Surface-no embedment
    - Embedded-with soil contact along the total height of the wall or only on part of it

As stated in the report by D`Appolonia Consulting Engineers [15], "both the lumped parameter method and the finite element model can be used for assessing the effect of embedment on the response of a structure. Each method has limitations due to assumptions, but may by used effectively for soil-structure interaction analyses. Lumped parameter methods require more assumptions, but can be used with an acceptable level of accuracy by using appropriate models. To improve the effectiveness of the lumped parameter method, parametric analyses are needed to reduce uncertainties in determining soil stiffness and damping coefficients under varying conditions of embedment." The standard lumped parameter method models the static stiffness of the soil half-space using a simple spring with coefficient k. This provides an exact result for static loading. The coefficients of the dashpot, c, and mass, M, are two free parameters that are selected to match as closely as possible the response of the total dynamic system, which may be determined by boundary element or finite element methods. The curve-fitting technique is applied to the total system's dynamic response and not that of the soil alone as in the substructure method. The mass parameter M is added to that of the structure in the foundation node. As Wolf [18] explains, "this added mass does not mean that an identifiable mass of the soil really exists that moves with the same amplitude and in phase with the structure over the whole range of frequency. It is an additional inertia which provides a better fit between the dynamic response of the lumped parameter model and that of the actual soil."

Basic lumped parameter soil models can be developed for each degree of freedom as is shown in Figure 2.1 for translational motion and Figure 2.2 for rotational motion.

The lumped parameter model also allows for coupling effects to be taken into account. Figure 2.3 shows the soil model with coupling effects.

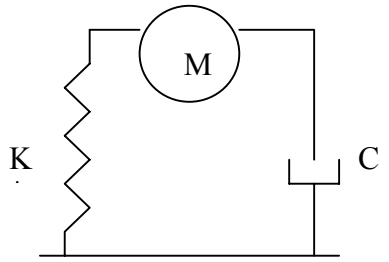

Figure 2.1 Translational Motion

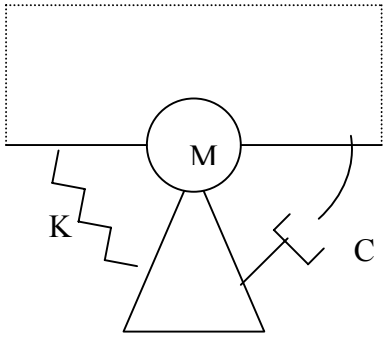

Figure 2.2 Rotational Motion

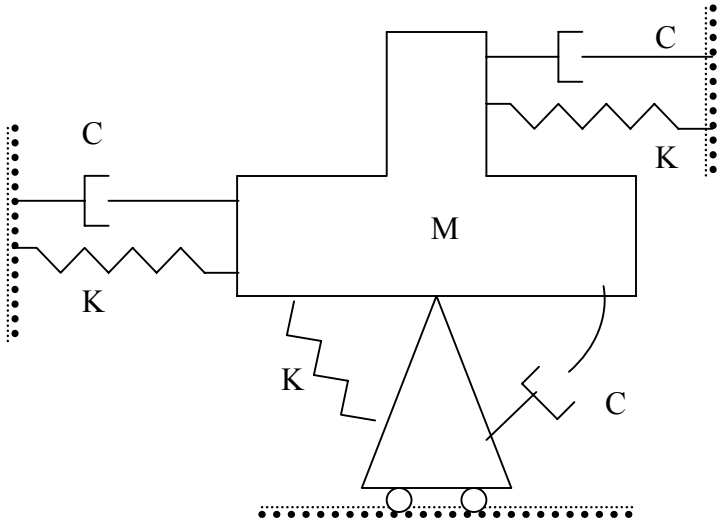

Figure 2.3 Coupling of Horizontal and Rocking Motions

The equation of motion for a single degree of freedom system with vertical motion, heave, as shown in Figure 2.1 is:

$$M\ddot{x} + C\dot{x} + Kx = F\cos(\omega t + \gamma) \tag{2.1}$$

where x = displacement, $\dot{x}$ = velocity, $\ddot{x}$ = acceleration

F = forcing function, ω = frequency, γ = phase shift

with steady state excitation:

$$F = F\cos(\omega t + \gamma) = \overline{F}\, e^{i\omega t} \quad \overline{F} \text{ bar is a complex quantity, its real part is implied} \tag{2.2}$$

we assume the steady state system response:

$$X = X\cos(\omega t + \varepsilon) = \overline{X}\, e^{i\omega t} \tag{2.3}$$

The equation of motion can be rewritten as:

$$(-M\omega^2 + i\,\omega C + K)\,\overline{X}\, e^{i\omega t} = \overline{F}\, e^{i\omega t} \tag{2.4}$$

The harmonic transfer function, which relates the steady-state response of this system to the excitation is:

$$\frac{\overline{X}}{\overline{F}} = H(\omega) = \frac{1}{(K - M\omega^2) + i(C\omega)} \tag{2.5}$$

The magnitude of this response is:

$$H_{mag}(\omega) = \frac{1}{\sqrt{(K - M\omega^2)^2 + (C\omega)^2}} \tag{2.6}$$

And the phase angle relative to the excitation is:

$$\varepsilon = -\tan^{-1}\left(\frac{C\omega}{K - M\omega^2}\right) \tag{2.7}$$

Figure 2.4 shows a typical frequency response for this system.

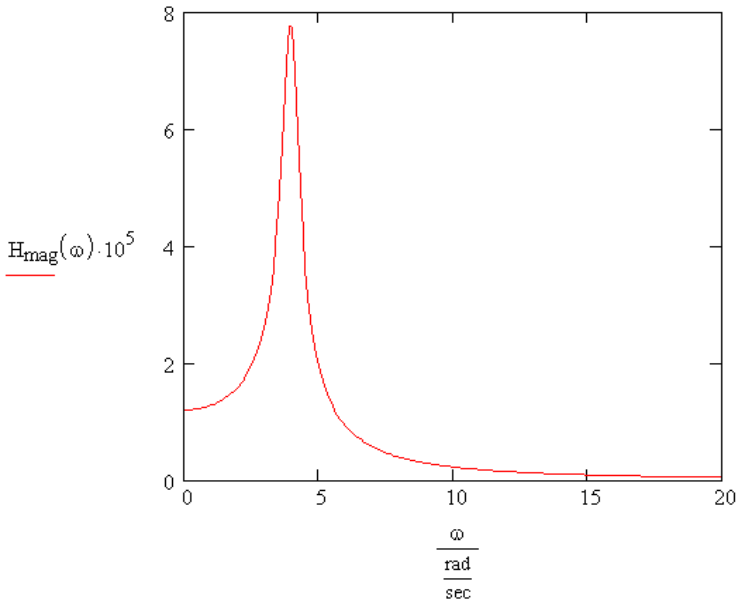

Figure 2.4 Frequency Response Transfer Function

Since the system is linear, forcing functions and responses can be superimposed using Fourier series:

$$F(t) = a_0 + \sum_{r=1}^{\infty} (a_r \cos r\omega t + b_r \sin r\omega t) \tag{2.8}$$

where,

$$a_0 = \frac{1}{T}\int_{-T/2}^{T/2} F(t)\,dt \tag{2.9}$$

$$a_r = \frac{2}{T}\int_{-T/2}^{T/2} F(t)\cos r\omega t\,dt \tag{2.10}$$

$$b_r = \frac{2}{T}\int_{-T/2}^{T/2} F(t)\sin r\omega t\,dt \tag{2.11}$$

$$T = 2\pi/\omega \tag{2.12}$$

The Fourier series is more conveniently expressed as:

$$F(t) = \sum_{-\infty}^{\infty} c_r e^{ir\omega t} \tag{2.13}$$

$$where \quad c_r = \frac{1}{T}\int_{-T/2}^{T/2} F(t) e^{-ir\omega t}\,dt \tag{2.14}$$

The right hand side of the equation of motion can then be represented as a sum of harmonic components:

$$M\ddot{x} + C\dot{x} + Kx = c_1 e^{i\omega t} + c_2 e^{i2\omega t} + \ldots etc \tag{2.15}$$

where c_1, c_2, etc are given by equation (2.14) and the solution is found by summing the harmonic components produced by multiplying the forcing terms by the transfer functions,

$$x(t) = H(\omega)c_1 e^{i\omega t} + H(2\omega)c_2 e^{i2\omega t} \ldots etc \tag{2.16}$$

There are different lumped parameter models to choose from. Some have been derived for specific projects and others are from general research. The model chosen for this thesis is from the report, *Stochastic Response of Foundations*, published by Pais and Kausel [19]. In their report they analyze previous data from other researchers that used complex and expensive procedures, such as finite element and boundary element methods, to model soil dynamics and soil-structure interaction. They plot the data presented by various other researchers and curve fit an equation to match the data as accurately as possible. This allows the use of the simple equations, which match the data well, in applications that do not require large complicated soil models, such as this thesis.

The soil model equations presented in Section 2.3 calculate the k and c terms in the transfer function, Equation (2.5), where the mass, M, includes only the mass of the ship. The soil model does not include added mass because the soil added mass values are much less than the ship mass. Once these values are calculated, the soil force and moment terms are added to the hydrodynamic equations of motion for the grounded ship.

2.3 Six Degree of Freedom Soil Model

The soil model used here is presented and verified in Pais and Kausel [19]. The model is for rigid foundations embedded in a half-space and subjected to horizontally propagating shear waves, but is valid and useful for other dynamic problems such as the soil-ship interaction. When seismic waves hit the foundation, which is more rigid than the surrounding soil, the equilibrium and compatibility equations are satisfied by adding the effect of the waves scattered by the foundation and the waves generated by its

vibration to the free field motion. Using the superposition theorem, the total dynamic interaction between the soil and the foundation can be separated into two parts, the Kinematic and Inertial interaction.

The exact solution for the kinematic interaction problem is very complex. Some analytical solutions exist, but only for specific geometries. Analytical solutions were derived for cylindrical or disc shaped foundations. These are the only known geometries to have been solved analytically. Then as the analysis and understanding improved, researchers studied strip foundations, square foundations and then rectangular foundations using finite elements. This thesis assumes the specific geometry of a rectangular shape to model the ship hull form. Finite element methods solve the kinematic interaction accurately, but they are expensive. In most cases, an approximate solution is adequate. A more detailed and complex solution is only required if it improves the design of the structure; and reliable and accurate data on the properties of the soil and dynamic loads must be available. The modeling of the soil-ship interaction does not warrant large complex soil models.

Pais and Kausel [19] combine the stiffness and damping coefficients into a single term that they call the dynamic stiffness, Equation (2.17):

$$K^d = K^s (k + i a_0 c) \tag{2.17}$$

where,

- K^s is the static stiffness
- a_0 is the dimensionless frequency ($a_0 = \omega B/V_s$, where ω = frequency of the motion, rad/sec, B = width of the foundation, ft, V_s = shear wave velocity in the soil, ft/sec)
- k (stiffness) and c (damping) are functions of a_0, ν (Poisson's ratio) and degree of embedment E/B (where E = depth of embedment)

A viscously damped system can be represented conveniently by Equation (2.17) for a class of techniques known as complex response analysis [20]. Consider the single degree of freedom system solved earlier subjected to simple harmonic loading of amplitude F and loading frequency ω. The loading is represented by $F(t) = \overline{F}e^{i\omega t}$ and we assume that $X(t) = \overline{X}e^{i\omega t}$, so the harmonic transfer function for the equation of motion $m\ddot{X} + c\dot{X} + kX = F\cos(\omega t + \gamma)$ is:

$$\frac{\overline{X}}{\overline{F}} = H(\omega) = \frac{1}{k - m\omega^2 + ic\omega} \qquad \text{Equation (2.5)} \qquad (2.18)$$

The stiffness and damping terms in Equation (2.18) are combined into the single equivalent complex stiffness term k^*. The equation of motion for this system is:

$$m\ddot{X} + k^* X = F\cos(\omega t + \gamma)$$

Again assume that $X(t) = \overline{X}e^{i\omega t}$, so the harmonic transfer function for the system is:

$$\frac{\overline{X}}{\overline{F}} = H(\omega) = \frac{1}{k^* - \omega^2 m} \tag{2.19}$$

Comparing equations (2.18) and (2.19):

$$k^* = k + ic\omega \tag{2.20}$$

By the appropriate choice of k^*, the displacement amplitude of equation (2.18) can be made equal to that of equation (2.18).

In the derivation of the stiffness equations, it is assumed that:

- The elastic medium, which supports the ship, is a homogeneous, isotropic, and semi-infinite body.
- The ship is rigid while vibrating.
- The ship maintains full contact with the soil.
- There is no slip between the ship and soil.
- The ship grounds with no heel.
- The soil remains linear elastic.
- The ship grounding length and embedment are symmetric.
- The soil rate dependency is introduced via a damping coefficient by a dashpot in the lumped parameter model.

- The effective added soil mass is much smaller than the mass of the ship and is neglected in this analysis.

- For the purpose of calculating ground reaction, the hull shapes of the ships are modeled as:
    - Rectangular box shape for cargo type ships
    - Wedge shape for warships
    - Cylindrical shape for submarines

The geometry of cargo ships is further simplified by not considering a bulbous bow or the small bilge radius as shown in Figure 2.5. The warship geometry does not account for sonar domes as shown in Figure 2.6.

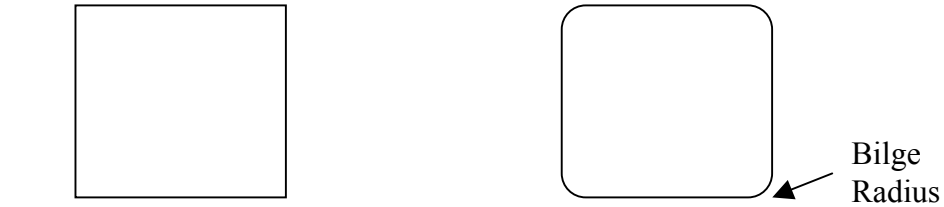

Figure 2.5

Figure 2.6

- To apply the soil model (which describes the forces and moments on a fully rectangular embedded foundation surrounded by soil on all four sides) to the condition of a stranded ship requires the assumption that the difference

between the two situations is minimal. A partially embedded grounded ship, Figure 2.7, has only three sides that are surrounded by soil versus four sides for a foundation or fully embedded grounded ship. This thesis assumes that the effect of this discrepancy is minimal. The soil model assumes that the portion of the grounded ship that is embedded is fully surrounded by soil on all four sides.

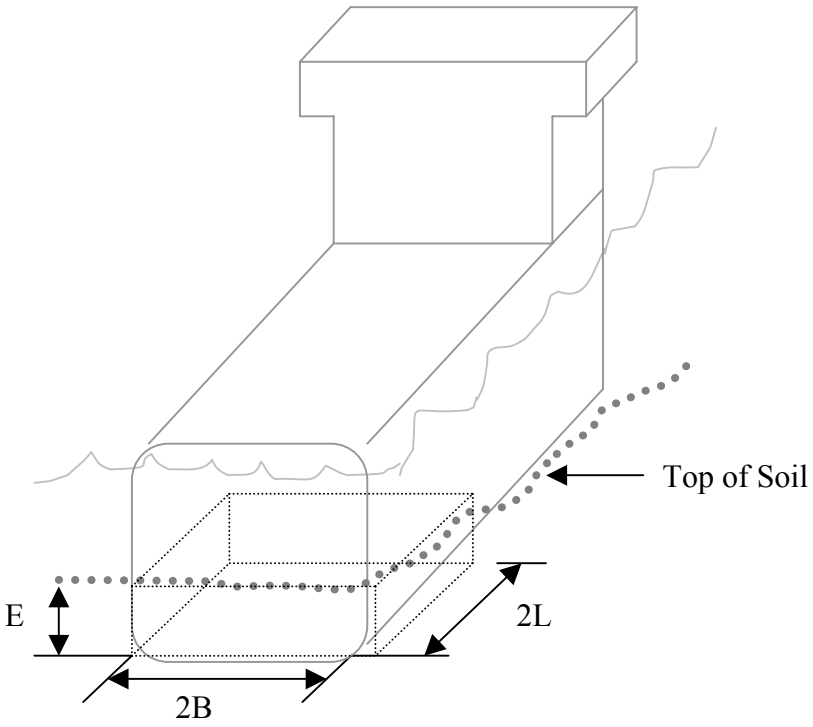

Figure 2.7 Stranded and Embedded Ship Modeled as Rectangular Embedded Foundation

The foundation motion is described in six degrees of freedom; three displacements and three rotations. When the foundation vibrates, it generates waves that carry away energy through the soil. This provides damping in the motion of the foundation and is referred to as either radiation or geometric damping. Damping is modeled using a dashpot in the lumped parameter model. To model this energy loss, the soil model used in numerical methods must include a large region beyond the foundation or use finite or

boundary elements. The data used for curve-fitting is found in this manner. This thesis uses the simple equations to avoid modeling the soil using finite elements or boundary value methods.

The ship hull is approximated as a rectangular embedded foundation. This is a valid approximation because:

- The shape of a large cargo ship hull is approximately a rectangular shape.
- The ship is rigid, meaning its stiffness is several orders of magnitude larger than the soil stiffness.
- The grounded ship is assumed to have uniform distribution of weight.

Figure 2.8 shows the six degrees of freedom for a foundation. This thesis applies this soil model to a grounded ship. Figure 2.9 shows the six degrees of freedom for a grounded ship. Figure 2.10 shows the foundation parameters and Figure 2.11 shows the parameters for the stranded ship. Figure 2.11 assumes the grounded ship is fully embedded. The soil model allows for a partially embedded ship as is shown in Figure 2.7.

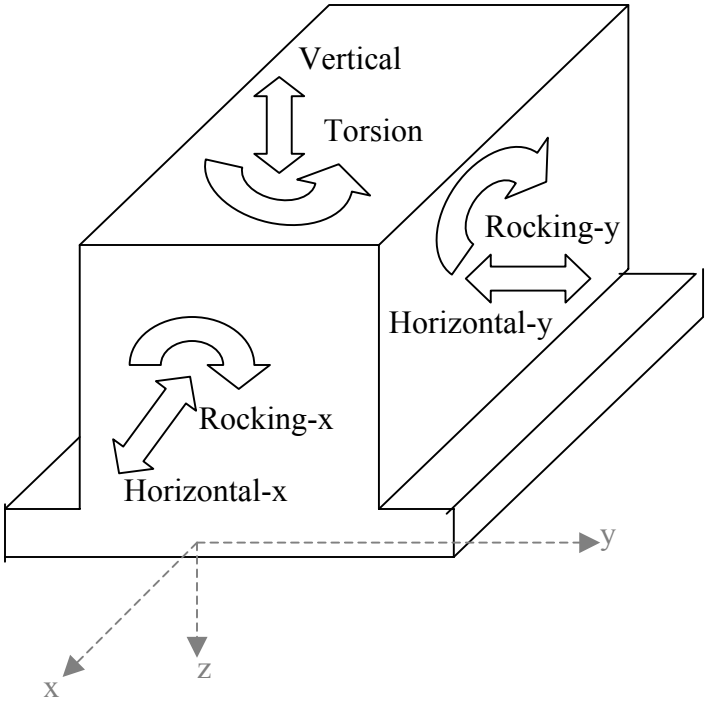

Figure 2.8 6-Degrees-of-Freedom for a Foundation

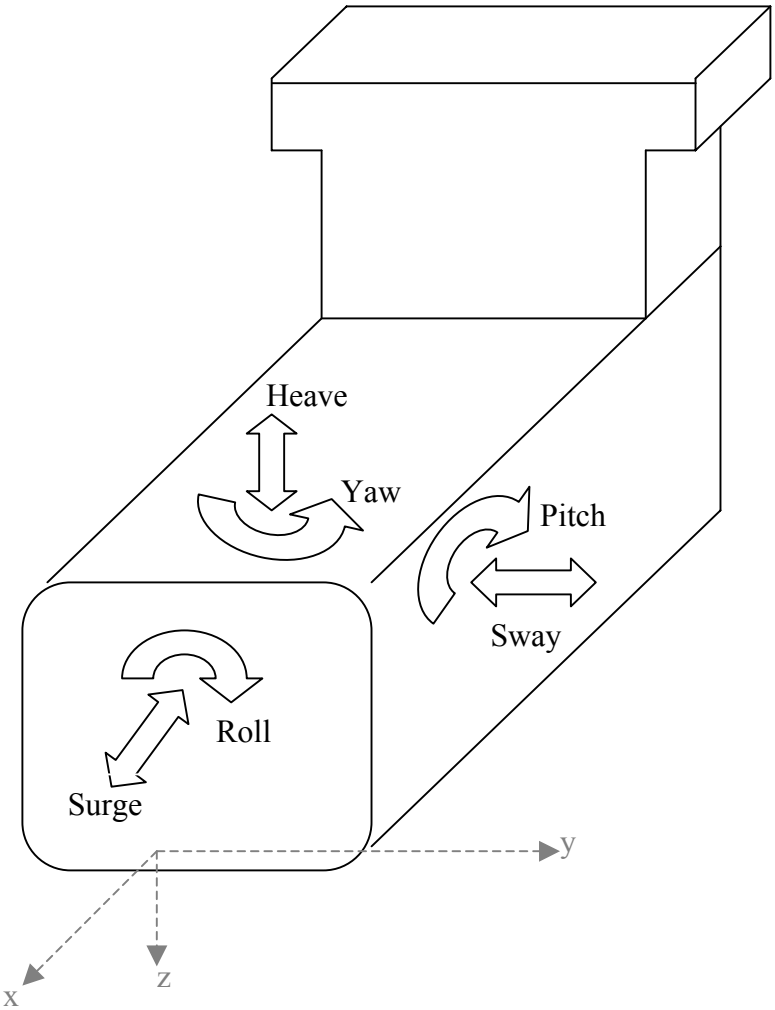

Figure 2.9 6-Degrees-of-Freedom for a Ship

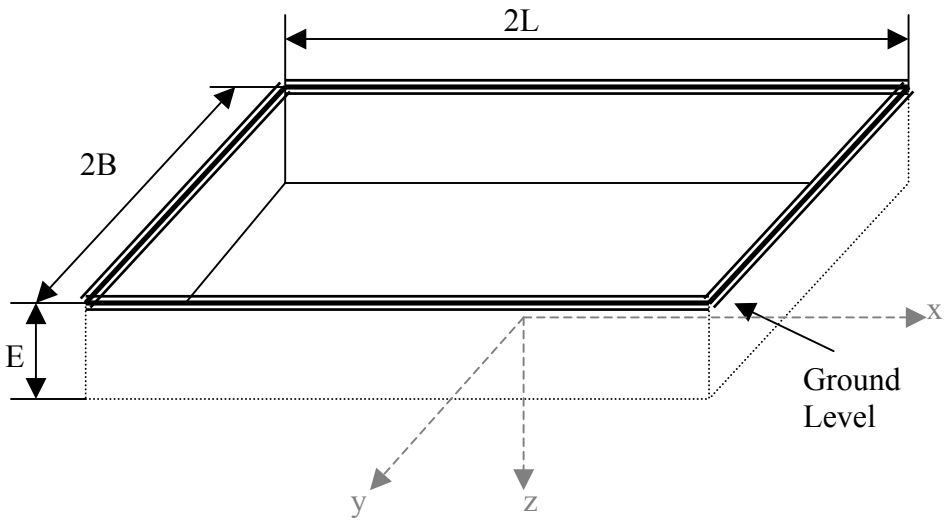

Figure 2.10 Rectangular Embedded Foundation (L>B)

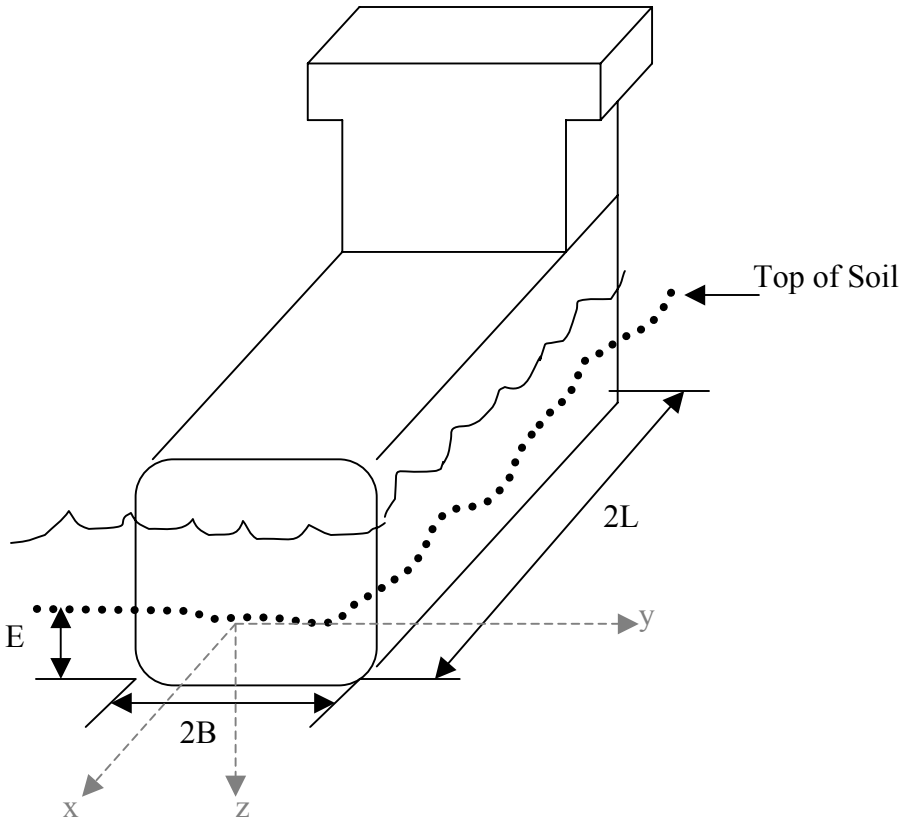

Figure 2.11 Stranded and Fully Embedded Ship

For rectangular foundations there is no axisymmetry, which increases the difficulty of the problem, so there are no analytical solutions available, even for the surface foundation. The ratio of the length to width, L/B, which defines the geometry of the foundation, must be considered. It is assumed that the foundation length is greater then the foundation width, L>B, which is a reasonable assumption because the ship length is greater then the ship width. The dependence on Poisson's ratio, ν, is assumed to be the same for embedded and surface foundations. The influence of Poisson's ratio on the variation of the stiffnesses with frequency is not taken into account. The amount of material damping is assumed to be independent of the value of Poisson's ratio.

To build the model of the embedded rectangular foundation, the static stiffnesses of a surface rectangular foundation are required. Equations (2.21) to (2.26) calculate these static stiffnesses, K^O [19]. The superscripts o, s, and d refer to the stiffnesses for a static surface, static embedded and dynamic embedded foundation, respectively. The coupling stiffnesses are neglected in the equations because their values are very small for a surface foundation. These equations approximate data found by boundary integral methods for a square foundation. The equations compare well with the results for a square foundation calculated by Abascal [21], Dominguez [22], and Wong & Luco [23]. To represent the variation of the static stiffnesses with the shape of the foundation (length-width ratio, L/B) with ν=1/3, the equations approximate data found by Wong et al. [23], Dominguez [22], and Gorbunov-Posanov from [23] for various L's and B's. Table 1 and Table II from [19] in Appendix 1 show the tables of values from these researchers and the values chosen for use in this model. Figures 15-19 from [19] in Appendix 1 show the data from these researchers and the curve-fit that the following equations provide.

Vertical (Heave) $$K_V^O = \frac{[3.1(L/B)^{0.75} + 1.6]GB}{(1-\nu)} \quad (2.21)$$

Horizontal-x (Surge) $$K_{Hx}^O = \frac{[6.8(L/B)^{0.65} + 2.4]GB}{(2-\nu)} \quad (2.22)$$

Horizontal-y (Sway) $$K_{Hy}^O = \frac{K_{Hx}^O(2-\nu) + 0.8(L/B-1)GB}{(2-\nu)} \quad (2.23)$$

Rocking-x (Roll) $$K_{Rx}^O = \frac{[3.2(L/B) + 0.8]GB^3}{(1-\nu)} \quad (2.24)$$

Rocking-y (Pitch) $$K_{Ry}^O = \frac{[3.73(L/B)^{2.4} + 0.27]GB^3}{(1-\nu)} \quad (2.25)$$

Torsion (Yaw) $$K_t^O = [4.25(L/B)^{2.45} + 4.06]GB^3 \quad (2.26)$$

where G is the shear modulus, and is related to Young's Modulus, E, and Poisson's Ratio, ν, by the equation:

$$G = \frac{E}{2(1+\nu)} \quad (2.27)$$

The exponent of (L/B) in equations (2.21) to (2.26) is less than 1 for the vertical and horizontal modes, equal to 1 for rocking around the longitudinal axis, and greater than 1 in the torsional mode and rocking around a transverse axis. These values approach the stiffnesses of a strip foundation as the length/width ratio increases.

With the static stiffnesses for a surface rectangular foundation defined, the equations for an embedded rectangular foundation are developed. The equations assume the stiffnesses depend linearly on the depth of embedment, E. The determination of the stiffnesses of rectangular embedded foundations is a very complex problem and therefore there is very little data available. Dominguez [22] obtained results for square and rectangular, with L/B=2, embedded foundations and Abascal [21] only analyzed the square foundation. In both studies the maximum amount of embedment analyzed was equal to the width of the foundation, E/B=2. Figures 34-36 from [19] in Appendix II show the data from these researchers and the curve fit that the following equations provide. Based on this data the following equations were developed for the stiffnesses as a function of embedment by Pais and Kausel [19]:

Vertical (Heave) $$K_V^S = K_V^O [1.0 + (0.25 + \frac{0.25}{L/B})(E/B)^{0.8}] \quad (2.28)$$

Horizontal-x (Surge) $$K_{Hx}^S = K_{Hx}^O [1.0 + (0.33 + \frac{1.34}{1 + L/B})(E/B)^{0.8}] \quad (2.29)$$

Horizontal-y (Sway) $$K_{Hy}^S = K_{Hy}^O [1.0 + (0.33 + \frac{1.34}{1 + L/B})(E/B)^{0.8}] \quad (2.30)$$

Rocking-x (Roll) $$K_{Rx}^S = K_{Rx}^O [1.0 + E/B + (\frac{1.6}{0.35 + (L/B)})(E/B)^2] \quad (2.31)$$

Rocking-y(Pitch) $$K_{Ry}^S = K_{Ry}^O [1.0 + E/B + (\frac{1.6}{0.35 + (L/B)^4})(E/B)^2] \quad (2.32)$$

Torsion (Yaw) $$K_t^S = K_t^O [1.0 + (1.3 + \frac{1.32}{L/B})(E/B)^{0.9}] \quad (2.33)$$

These equations agree well with Abascal's results. From the plots, it can be seen that the dependence on the depth of embedment is not linear, the exponent (E/B) is less then one, except for rocking where a second-degree parabola gives good agreement. The

asymptotic values for a strip foundation are matched for both rocking around x and for swaying along y. When the foundation is very long, its stiffness in the short direction should approach the stiffness of a strip foundation, which is 2-D. The effect of embedment was assumed to be split evenly between each side, because a strip foundation has only two sides instead of four as shown in Figure 2.11.

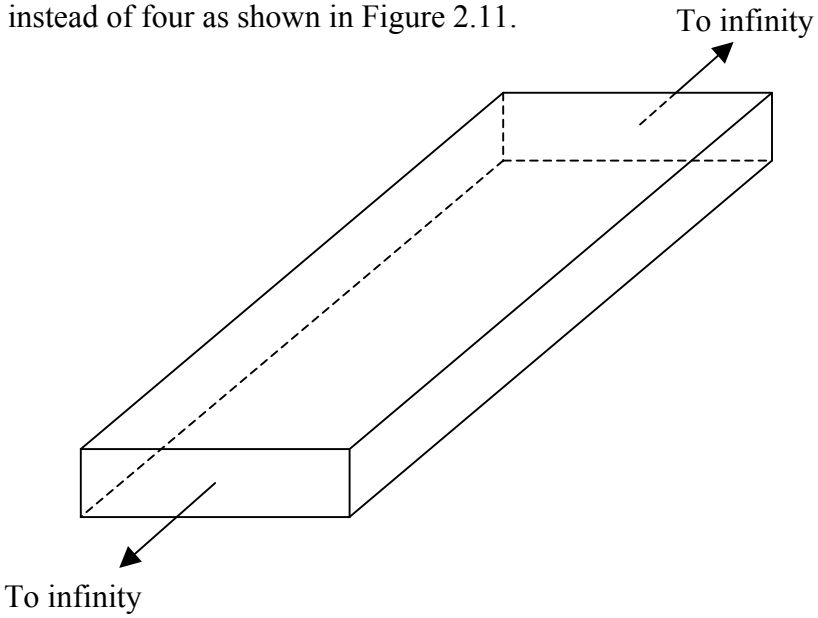

Figure 2.12 Strip Foundation

The decay with the ratio (L/B) is such that the error relative to Dominguez's results is more or less constant. As shown by Dominguez, the height of the center of stiffness is approximately 1/3 of the height of embedment. The coupling stiffness is not as important and can be taken simply as:

Coupling of Horizontal-x (Surge) and Rocking-x (Roll):

$$K^{S}_{HRx} = \frac{1}{3}(E/B)\,K^{S}_{Hx} \tag{2.34}$$

Coupling of Horizontal-y (Sway) and Rocking-y (Pitch):

$$K^{S}_{HRy} = \frac{1}{3}(E/B)\,K^{S}_{Hy} \tag{2.35}$$

Pais and Kausel [19] acknowledge that stiffness in the vertical and rocking modes depends on the value of Poisson's ratio, but for simplicity its influence is not taken into account. So for values of ν that are higher than 0.4 the equations should be used with care especially at high frequencies. The equations produce acceptable results in the high frequency range because the imaginary part of the stiffness is much more important than the real part.

There are two types of damping in the real system: one introduced by the loss of energy through propagation of elastic waves away from the immediate vicinity of the foundation, the other associated with internal energy losses within the soil due to hysteretic and viscous effects. The equivalent damping corresponding to the elastic-wave propagation is called geometric damping or radiation damping. The lumped damping parameter for any particular foundation-soil system includes both the effects of geometric and internal damping.

Now the dynamic stiffness of embedded foundations can be derived. Dominguez [22] and Abascal [21] only present data showing the variation of the stiffnesses in the low frequency range (a_0<1.5 from Dominguez and a_0<2.0 from Abascal, where a_0 refers to the dimensionless frequency by the equation, where V_s is the soil shear wave velocity:

$$a_o = \frac{\omega B}{V_S} \tag{2.36}$$

which corresponds to frequencies less than 0.33 rad/sec and 0.44 rad/sec for a 50ft wide ship grounded in clay (mud); or 2.62 rad/sec and 3.5 rad/sec for a 50ft wide ship grounded in hard rock. This is well within the frequency range of ocean wave energy.

It is assumed that the variation of the stiffnesses with frequency is the same for surface and embedded foundations, because of the lack of better data. Figures 20-33 from [19] in Appendix III show the data from these researchers and the curve fit that the following equations provide. Below are the equations for the dynamic stiffnesses. A coefficient α is used to represent the ratio between the celerity of pressure waves and shear waves.

Note: $L \geq B$; $a_o = \frac{\omega B}{V_S}$; $\alpha = \frac{V_P}{V_S} = \sqrt{\frac{2(1-\nu)}{1-2\nu}}$; $\alpha \leq 2.45$ (2.37)

Vertical (Heave) $\overline{K}_V^d = K_V^S (k + i a_o c)$ (2.38)

$$k = 1.0 - \frac{d a_o^2}{b + a_o^2} \qquad c = \frac{4[\alpha L/B + \frac{E}{B}(1 + L/B)]}{K_V^S}$$

$$d = 0.4 + \frac{0.2}{L/B} \qquad b = \frac{10.0}{1 + 3(L/B - 1)}$$

Horizontal-x (Surge) $\overline{K}_{Hx}^d = K_{Hx}^S (k + i a_o c)$ (2.39)

$$k = 1.0 \qquad c = \frac{4[L/B + E/B(\alpha + L/B)]}{K_{Hx}^S}$$

Horizontal-y (Sway) $\overline{K}_{Hy}^d = K_{Hy}^S (k + i a_o c)$ (2.40)

$$k = 1.0 \qquad c = \frac{4[L/B + E/B(1 + \alpha L/B)]}{K_{Hy}^S}$$

Rocking-x (Roll) $\overline{K}_{Rx}^{d} = K_{Rx}^{S}(k + ia_o c)$ (2.41)

$$k = 1.0 - \frac{d a_o^2}{b + a_o^2} \qquad d = 0.55 + 0.1\sqrt{L/B - 1}$$

$$b = 2.4 - \frac{0.4}{(L/B)^3}$$

$$c = \frac{4[\frac{1}{3}(E/B) + \frac{1}{3}(E/B)^3 + \frac{\alpha}{3}(L/B)(E/B)^3 + (E/B)(L/B) + \frac{\alpha}{3}(L/B)]}{K_{Rx}^{S}} \bullet \frac{a_o^2}{f + a_o^2} + D\frac{f}{f + a_o^2}$$

$$f = 2.2 - \frac{0.4}{(L/B)^3} \qquad D = \frac{\frac{4}{3}(\alpha\frac{L}{B} + 1)(E/B)^3}{K_{Rx}^{S}}$$

Rocking-y (Pitch) $\overline{K}_{Ry}^{d} = K_{Ry}^{S}(k + ia_o c)$ (2.42)

$$k = 1.0 - \frac{0.55 a_o^2}{b + a_o^2} \qquad b = 0.6 + \frac{1.4}{(L/B)^3}$$

$$c = \frac{4[\frac{1}{3}(L/B)^3(E/B) + \frac{\alpha}{3}(E/B)^3(L/B) + \frac{1}{3}(E/B)^3 + (E/B)(L/B)^2 + \frac{\alpha}{3}(L/B)^3]}{K_{Ry}^{S}} \bullet \frac{a_o^2}{f + a_o^2} + D\frac{f}{f + a_o^2}$$

$$f = \frac{1.8}{1.0 + 1.75(L/B - 1)} \qquad D = \frac{\frac{4}{3}(L/B + \alpha)(E/B)^3}{K_{Ry}^{S}}$$

Torsion (Yaw) $$\overline{K}_t^d = K_t^S (k + i a_o c) \tag{2.43}$$

$$k = 1.0 - \frac{d a_o^2}{b + a_o^2} \qquad d = 0.33 - 0.03\sqrt{L/B - 1}$$

$$b = \frac{0.8}{1 + 0.33(L/B - 1)}$$

$$c = \frac{4[(L/B)(E/B) + \frac{\alpha}{3}(L/B)^3 (E/B) + (L/B)^2 (E/B) + \frac{1}{3}(L/B)^3 + \frac{1}{3}(L/B)]}{K_t^S} \bullet \frac{a_o^2}{f + a_o^2}$$

$$f = \frac{1.4}{1 + 3(L/B - 1)^{0.7}}$$

Coupling

Coupling of Horizontal-x (Surge) and Rocking-x (Roll):

$$\overline{K}_{HRx}^d = \frac{1}{3}(E/B)\,\overline{K}_{Hx}^d \tag{2.44}$$

Coupling of Horizontal-y (Sway) and Rocking-y (Pitch):

$$\overline{K}_{HRy}^d = \frac{1}{3}(E/B)\,\overline{K}_{Hy}^d \tag{2.45}$$

The asymptotic values of the coefficient c are obtained by computing geometrical inertias and areas. The rocking modes exhibit a non-zero value of c in the static case. This value is chosen in such a way that it is related to the translation of the sidewalls during rotation of the foundation, and it agrees well with Abascal's results.

The soil model also requires assumptions in its development. The assumption that the soil is a homogeneous, isotropic, elastic body is not exact. Often a soil stratum is layered and may have a hard stratum of soil or rock at a shallow depth below the grounded ship. The amplitudes of vibration at resonance increase by the presence of the underlying rigid layer. This indicates that radiation of energy from the grounded ship is impeded by the presence of the rigid layer and that part of this elastic-wave energy is reflected back to the grounded ship. Further studies need to be conducted on the damping related to vibrations of grounded ships supported by layered media as well as of grounded ships supported by soils, which vary in stiffness with depth or confining pressure. During the vibration of foundations, there is a mass of soil under the foundation, which vibrates along with the foundation.

Since it is assumed that the ship maintains contact with the soil without slip or separation, all friction and suction effects depend on internal soil properties and response. Separation is when a partial gap forms between the side-wall-basemat and the adjacent soil of an embedded foundation for large seismic excitation because tension is not sustained in soil. In the grounded ship case, separation may occur after the ship rocks back and forth causing a gap between the embedded ship structure and the surrounding soil. This is a non-linear effect that can be approximated. In Wolf and Weber [24], they analyze the effects of soil separation. For the case of separation occurring between a circular cavity and the adjacent thin layer, the effect was minimal on the spring coefficient, but the effect halved the damping coefficient for horizontal and vertical motions when compared to the linear case. For the torsional and rocking degrees of freedom, the spring coefficients are halved and the damping coefficients are reduced

somewhat less. Separation effects similar to these are also discussed in Gazetas [25]. Because of the complexity of these separation effects they are neglected in this analysis, but may require consideration in future work.

Chapter 3 Grounded Ship Motions

3.1 Overview of Chapter

This chapter provides an overview of the method used to compute the dynamic response of a grounded ship in regular waves. The method derived is based on a linear theory of ship motions [26].

The first section of this chapter provides a description of the coordinate systems used to describe the motions of the waves and the ship in regular waves. This section also defines the nomenclature used throughout this work.

The second section covers the derivation of the equations of motion in six degrees of freedom: surge, sway, heave, roll, pitch, and yaw. The equations of motion are based on Newton's Second Law (**F** = m**a**), and are written in an inertial coordinate system. The derivation of the equations of motions for a vessel in regular waves is adapted from Lloyd [27]. The main difference between this derivation, and similar derivations for seakeeping is the inclusion of the ground reaction forces, and the assumption that the ship has zero forward speed.

Following the equations of motion, there is an explanation of strip theory and how it is used to compute the sectional and overall hydrodynamic forces on the grounded vessel. The complete derivation of the hydrodynamic problem is mathematically intense and lengthy. Only a summary of this solution method solution is provided.

The section on strip theory follows the derivation as described in the *Principles of Naval Architecture, Volume 3* [28]. Strip theory was chosen over other methods for predicting ship motions because it has been proven to be a successful and practical tool for the calculation of wave induced motions in the early design stages. Strip theory

provides reasonably accurate results with minimal computational effort relative to other methods [26].

The final two sections of this chapter describe how information from the previous sections is used to provide realistic results. Section 3.9 shows how motions and dynamic loads are calculated. Section 3.10 explains how spectral analysis is used to predict ship motions and loads in a realistic seaway.

3.2 Frames of Reference

The following right-handed coordinate systems are used to describe the grounded ship motions. Figure 3.1 corresponds with this description.

- (E x y z) is fixed to the earth at E with the x-axis in the direction of advance of the incident waves, the E x y plane is at the calm water level, and the z-axis is positive downwards. This system is used to define the incident waves.
- (O x_1 x_2 x_3) is also fixed to the earth at O, but is rotated through the heading angle, μ, so that O x_1 coincides with the mean heading of the ship. O and E are in the same location. The O x_1 x_2 plane is at the calm water level, and the x_3-axis is positive downwards.
- The mean position of the center of gravity of the ship, G_o, lies vertically above *O* and is taken as the origin of the axis system G_o x_1 x_2 x_3.
- Another right handed set of axes G x_{b1} x_{b2} x_{b3} is fixed in the ship and is used to define locations within the structure of the ship. The G x_{b1} x_{b3} plane corresponds with the ship's centerline plane, and is a plane of port and starboard symmetry. The positive x_{b1} axis points to the bow, the positive x_{b2} axis points to starboard,

and the positive x_{b3} axis points vertically downwards. The point, G, is located at (0, 0, 0) in this system. When the ship is not in motion, the coordinate systems $G_o\, x_1\, x_2\, x_3$ and $G\, x_{b1}\, x_{b2}\, x_{b3}$ are coincident.

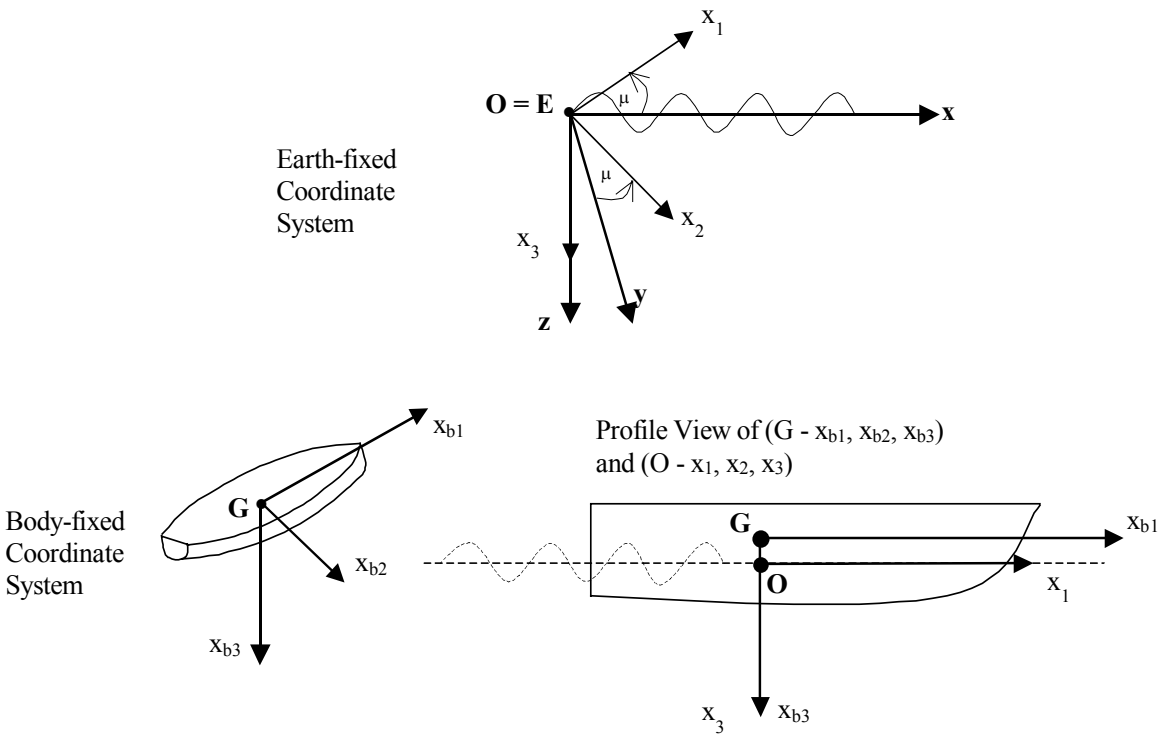

Figure 3.1 Frames of Reference

At any instant of time, ship motions are measured as displacements of the ship's center of gravity, G, relative to the origin, G_o. The six degrees of freedom include three translations: surge (x_1), sway (x_2) and heave (x_3); and three rotations: roll (x_4), pitch (x_5) and yaw (x_6), as shown in Figure 3.2.

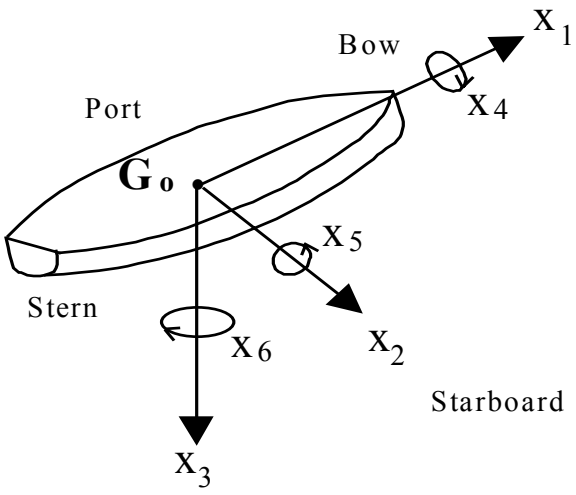

Figure 3.2 Six-degrees-of-freedom of a ship

3.3 Waves

Figure 3.3 shows a regular wave as a function of distance, x, along the wave at a fixed instant in time, Figure 3.3a, and as a time record of the water level observed at one location along the wave, Figure 3.3b:

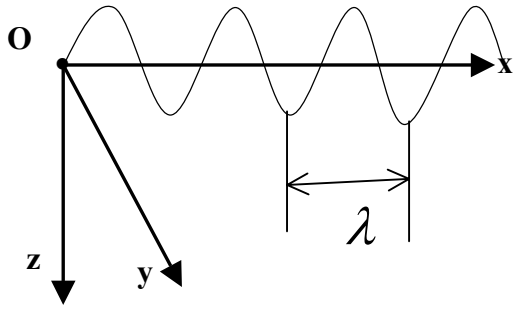

Figure 3.3a Regular Wave Definition in Earth Axis system (O x y z)

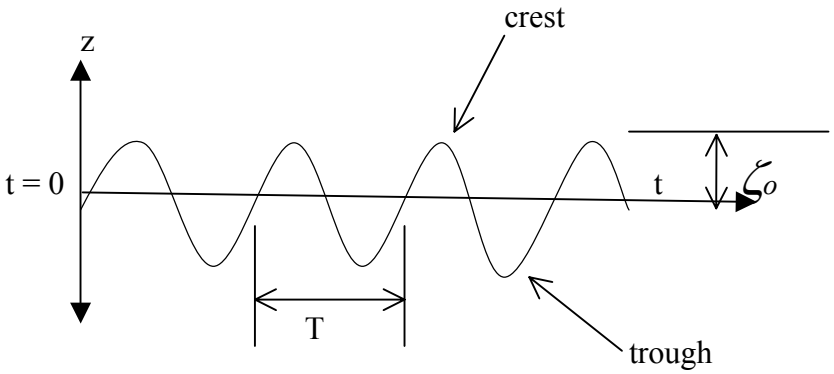

Figure 3.3b Regular Wave Definition as function of time

Assuming that the wave is sinusoidal, wave characteristics are described using equations (3.1) through (3.8).

$$k\lambda = 2\pi \text{ or } k = \tfrac{2\pi}{\lambda} \tag{3.1}$$

$$\omega T = 2\pi \text{ or } \omega = \tfrac{2\pi}{T} \tag{3.2}$$

where k is the wave number (rad/m), ω is the circular wave frequency (rad/s), λ is the wave length and T is the wave period.

The wave form moves one wave length during one period so that its speed or phase velocity, c, is given by:

$$c = \tfrac{\lambda}{T} = \tfrac{\omega}{k} \tag{3.3}$$

Given the above, the wave depression at any point *x* is:

$$\zeta = \zeta_o \sin(kx - \omega t) \quad \text{where } \zeta_o \text{ is the wave amplitude} \tag{3.4}$$

Where the time *t* is measured from an arbitrary datum. Transforming to the axis system aligned with the ship's heading we find that the wave depression at any point is:

$$\zeta = \zeta_o \sin(kx_1 \cos\mu - kx_2 \sin\mu - \omega t) \tag{3.5}$$

3.4 Equations of Motion

3.4.1 Assumptions

In deriving the equations of motion, the following assumptions are made:

a) The equilibrium condition for the ship is known.

b) The ship is aground, thus it has zero forward speed.

c) The waves are regular (sinusoidal).

d) The heading of the ship has a constant angle, μ, measured in a counter-clockwise direction from the wave direction of travel.

e) There are no transient effects due to initial conditions; linear dynamic motions and loads are harmonically oscillating with the same frequency as the wave excitation.

f) The motions are small relative to the inertial reference frame. This is necessary to linearize the problem. This assumption is valid for a stable ship with small incident wave amplitude, but it is not valid in near-resonant conditions.

g) See assumptions made in the previous section regarding soil reaction.

3.4.2 General Equations for Ship Motions in Regular Waves

Starting with Newton's Second Law, **F** = m**a**, applied in the inertial coordinate system, the equations of motion are derived for six degrees of freedom. The equations of motions are linearized with forces and moments defined in the body axis system and displacements in the inertial system.

As described by Lloyd [27], the ship may be regarded as a large number of very small masses, δm. Figure 3.4 below shows one of these masses located at (x_{b1}, x_{b2}, x_{b3}). The ship has linear accelerations $\ddot{x}_1, \ddot{x}_2, \ddot{x}_3$ (ft / sec^2) and angular accelerations $\ddot{x}_4, \ddot{x}_5, \ddot{x}_6$ (rad / sec^2)

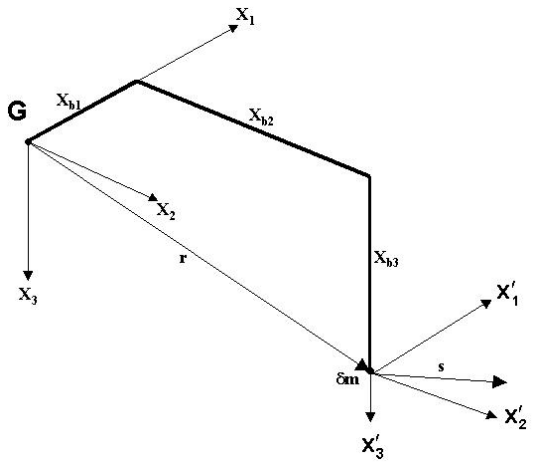

Figure 3.4 Accelerations experienced by the mass δm

The forces and moments required to sustain the linear and angular accelerations of the whole ship are obtained by allowing δm to approach zero, and integrating over the volume of the ship.

3.4.3 Center of Gravity and Mass Moments of Inertia

The center of gravity is defined as:

$$\int x_{b1} dm = \int x_{b2} dm = \int x_{b3} dm = 0 \tag{3.6}$$

where m is the total mass of the ship. I_{44}, I_{55}, and I_{66} are the moments of inertia of the ship defined by:

$$I_{44} = \int {x_{b2}}^2 dm + \int {x_{b3}}^2 dm \quad \text{about the } x_{b1} \text{ axis} \tag{3.7}$$

$$I_{55} = \int {x_{b1}}^2 dm + \int {x_{b3}}^2 dm \quad \text{about the } x_{b2} \text{ axis} \tag{3.8}$$

$$I_{66} = \int {x_{b1}}^2 dm + \int {x_{b2}}^2 dm \quad \text{about the } x_{b3} \text{ axis} \tag{3.9}$$

The products of the moments of inertia are defined by

$$I_{54} = I_{45} = \int x_{b1} x_{b2} dm \tag{3.10}$$

$$I_{64} = I_{46} = \int x_{b1} x_{b3} dm \tag{3.11}$$

$$I_{65} = I_{56} = \int x_{b2} x_{b3} dm \tag{3.12}$$

3.4.4 Linear displacements

For an incremental mass, δm, located at (x_{b1}, x_{b2}, x_{b3}) in the ship, the linearized displacement vector relative to the inertial system, $G_o\ x_1\ x_2\ x_3$, is:

$$\vec{s} = x_1'\mathbf{i} + x_2'\mathbf{j} + x_3'\mathbf{k} = x_1\mathbf{i} + x_2\mathbf{j} + x_3\mathbf{k} + \vec{\Phi} \times \vec{r} \tag{3.13}$$

Note: The $'$ (prime symbol) is used to denote the displacement of a point on the ship.

The angular displacement of G $x_{b1}\ x_{b2}\ x_{b3}$ relative to $G_o\ x_1\ x_2\ x_3$ is :

$$\vec{\Phi} = x_4\mathbf{i} + x_5\mathbf{j} + x_6\mathbf{k} \tag{3.14}$$

The mean position vector is

$$\vec{r} = x_{b1}\mathbf{i} + x_{b2}\mathbf{j} + x_{b3}\mathbf{k} \tag{3.15}$$

The cross product of the angular displacement and the mean position vectors gives:

$$\vec{\Phi} \times \vec{r} = \begin{vmatrix} \mathbf{i} & \mathbf{j} & \mathbf{k} \\ x_4 & x_5 & x_6 \\ x_{b1} & x_{b2} & x_{b3} \end{vmatrix} = (x_{b3}x_5 - x_{b2}x_6)\mathbf{i} - (x_{b3}x_4 - x_{b1}x_6)\mathbf{j} + (x_{b2}x_4 - x_{b1}x_5)\mathbf{k} \tag{3.16}$$

The displacement and accelerations may then be restated as:

$$\vec{s} = x_1'\mathbf{i} + x_2'\mathbf{j} + x_3'\mathbf{k} \tag{3.17}$$

$$x_1' = x_1 + x_{b3}x_5 - x_{b2}x_6 \tag{3.18}$$

$$x_2' = x_2 - x_{b3}x_4 + x_{b1}x_6 \tag{3.19}$$

$$x_3' = x_3 + x_{b2}x_4 - x_{b1}x_5 \tag{3.20}$$

$$\ddot{\vec{s}} = \ddot{x}_1'\mathbf{i} + \ddot{x}_2'\mathbf{j} + \ddot{x}_3'\mathbf{k} \tag{3.21}$$

$$\ddot{x}_1' = \ddot{x}_1 + x_{b3}\ddot{x}_5 - x_{b2}\ddot{x}_6 \tag{3.22}$$

$$\ddot{x}_2' = \ddot{x}_2 - x_{b3}\ddot{x}_4 + x_{b1}\ddot{x}_6 \tag{3.23}$$

$$\ddot{x}_3' = \ddot{x}_3 + x_{b2}\ddot{x}_4 - x_{b1}\ddot{x}_5 \tag{3.24}$$

Given the above, the following is obtained:

$$\delta\vec{F} = \delta F_1\mathbf{i} + \delta F_2\mathbf{j} + \delta F_3\mathbf{k} = \delta m\ddot{\vec{s}} = \delta m(\ddot{x}_1'\mathbf{i} + \ddot{x}_2'\mathbf{j} + \ddot{x}_3'\mathbf{k}) \tag{3.25}$$

$$\delta F_1 = \delta m\ddot{x}_1' = \delta m(\ddot{x}_1 + x_{b3}\ddot{x}_5 - x_{b2}\ddot{x}_6) \tag{3.26}$$

$$\delta F_2 = \delta m\ddot{x}_2' = \delta m(\ddot{x}_2 - x_{b3}\ddot{x}_4 + x_{b1}\ddot{x}_6) \tag{3.27}$$

$$\delta F_3 = \delta m\ddot{x}_3' = \delta m(\ddot{x}_3 + x_{b2}\ddot{x}_4 - x_{b1}\ddot{x}_5) \tag{3.28}$$

3.4.5 Angular Rotations

Using the above equations for the displacement of the incremental mass δm, the moments to sustain the angular accelerations are obtained below.

$$\delta\vec{\Gamma} = \vec{r} \times \delta\vec{F} = \delta F_4 \mathbf{i} + \delta F_5 \mathbf{j} + \delta F_6 \mathbf{k} = \delta m(\vec{r} \times \ddot{\vec{s}}) \tag{3.29}$$

$$\delta m(\vec{r} \times \ddot{\vec{s}}) = \begin{vmatrix} \mathbf{i} & \mathbf{j} & \mathbf{k} \\ x_{b1} & x_{b2} & x_{b3} \\ \ddot{x}_1' & \ddot{x}_2' & \ddot{x}_3' \end{vmatrix} = \delta m\left[(x_{b2}\ddot{x}_3' - x_{b3}\ddot{x}_2')\mathbf{i} - (x_{b1}\ddot{x}_3' - x_{b3}\ddot{x}_1')\mathbf{j} + (x_{b1}\ddot{x}_2' - x_{b2}\ddot{x}_1')\mathbf{k}\right] \tag{3.30}$$

$$\delta F_4 = \delta m(x_{b2}\ddot{x}_3 + x_{b2}x_{b2}\ddot{x}_4 - x_{b2}x_{b1}\ddot{x}_5 - x_{b3}\ddot{x}_2 + x_{b3}x_{b3}\ddot{x}_4 - x_{b3}x_{b1}\ddot{x}_6) \tag{3.31}$$

$$\delta F_5 = \delta m(x_{b3}\ddot{x}_1 + x_{b3}x_{b3}\ddot{x}_5 - x_{b3}x_{b2}\ddot{x}_6 - x_{b1}\ddot{x}_3 + x_{b1}x_{b1}\ddot{x}_5 - x_{b1}x_{b2}\ddot{x}_4) \tag{3.32}$$

$$\delta F_6 = \delta m(x_{b1}\ddot{x}_2 + x_{b1}x_{b1}\ddot{x}_6 - x_{b1}x_{b3}\ddot{x}_4 - x_{b2}\ddot{x}_1 + x_{b2}x_{b2}\ddot{x}_6 - x_{b2}x_{b3}\ddot{x}_5) \tag{3.33}$$

3.4.6 Forces and Moments

The forces and moments for the ship are obtained by allowing δm to approach zero and integrating over the length of the ship:

$$F_1 = m\ddot{x}_1 + \int x_{b3}dm \cdot \ddot{x}_5 - \int x_{b2}dm \cdot \ddot{x}_6 = m(\ddot{x}_1 + \bar{x}_{b3}\ddot{x}_5 - \bar{x}_{b2}\ddot{x}_6) \tag{3.34}$$

$$F_2 = m\ddot{x}_2 + \int x_{b1}dm \cdot \ddot{x}_6 - \int x_{b3}dm \cdot \ddot{x}_4 = m(\ddot{x}_2 - \bar{x}_{b3}\ddot{x}_4 + \bar{x}_{b1}\ddot{x}_6) \tag{3.35}$$

$$F_3 = m\ddot{x}_3 + \int x_{b2}dm \cdot \ddot{x}_4 - \int x_{b1}dm \cdot \ddot{x}_5 = m(\ddot{x}_3 + \bar{x}_{b2}\ddot{x}_4 - \bar{x}_{b1}\ddot{x}_5) \tag{3.36}$$

$$F_4 = \int x_{b2}dm \cdot \ddot{x}_3 + \int {x_{b2}}^2 dm \cdot \ddot{x}_4 + \int {x_{b3}}^2 dm \cdot \ddot{x}_4 - \int x_{b2}x_{b1}dm \cdot \ddot{x}_5 - \int x_{b3}dm \cdot \ddot{x}_2 - \int x_{b3}x_{b1}dm \cdot \ddot{x}_6$$

$$= m\bar{x}_{b2}\ddot{x}_3 + I_{44}\ddot{x}_4 - I_{45}\ddot{x}_5 - m\bar{x}_{b3}\ddot{x}_2 - I_{46}\ddot{x}_6 = I_{44}\ddot{x}_4 - m\bar{x}_{b3}\ddot{x}_2 - I_{46}\ddot{x}_6 \tag{3.37}$$

$$F_5 = \int x_{b3}dm \cdot \ddot{x}_1 + \int {x_{b3}}^2 dm \cdot \ddot{x}_5 + \int {x_{b1}}^2 dm \cdot \ddot{x}_5 - \int x_{b3}x_{b2}dm \cdot \ddot{x}_6 - \int x_{b1}dm \cdot \ddot{x}_3 - \int x_{b1}x_{b2}dm \cdot \ddot{x}_4$$

$$= m\bar{x}_{b3}\ddot{x}_1 + I_{55}\ddot{x}_5 - I_{56}\ddot{x}_6 - \bar{x}_{b1}\ddot{x}_3 - I_{45}\ddot{x}_4 = I_{55}\ddot{x}_5 + m\bar{x}_{b3}\ddot{x}_1 - m\bar{x}_{b1}\ddot{x}_3 \tag{3.38}$$

$$F_6 = \int x_{b1}dm\cdot\ddot{x}_2 + \int {x_{b1}}^2 dm\cdot\ddot{x}_6 + \int {x_{b2}}^2 dm\cdot\ddot{x}_6 - \int x_{b1}x_{b3}dm\cdot\ddot{x}_4 - \int x_{b2}dm\cdot\ddot{x}_1 - \int x_{b2}x_{b3}dm\cdot\ddot{x}_5$$

$$= m\bar{x}_{b1}\ddot{x}_2 + I_{66}\ddot{x}_6 - I_{64}\ddot{x}_4 - \bar{x}_{b2}\ddot{x}_1 - I_{56}\ddot{x}_5 = I_{66}\ddot{x}_6 + m\bar{x}_{b1}\ddot{x}_2 - I_{64}\ddot{x}_4 \tag{3.39}$$

The bar over the x_{bi}-terms denotes the distance measured between the origin and the center of gravity of the ship. F_1, F_2, and F_3 are the surge, sway, and heave forces and F_4, F_5, and F_6 are the roll, pitch and yaw moments required to sustain the accelerations of the ship.

3.4.7 Inertia Matrix

The following is the inertia matrix, which is derived from the equations of motion:

$$\Delta_{ij} = \begin{bmatrix} m & 0 & 0 & 0 & m\bar{x}_{b3} & 0 \\ 0 & m & 0 & -m\bar{x}_{b3} & 0 & m\bar{x}_{b1} \\ 0 & 0 & m & 0 & -m\bar{x}_{b1} & 0 \\ 0 & -m\bar{x}_{b3} & 0 & I_{44} & 0 & -I_{46} \\ m\bar{x}_{b3} & 0 & -m\bar{x}_{b1} & 0 & I_{55} & 0 \\ 0 & m\bar{x}_{b1} & 0 & -I_{46} & 0 & I_{66} \end{bmatrix} \tag{3.40}$$

Given the following assumptions:

a) the motions are linearized and small with no transient effects,

b) the ship has port/starboard symmetry, and

c) the origin is at the center of gravity,

The inertia matrix reduces to the following:

$$\Delta_{ij} = \begin{bmatrix} m & 0 & 0 & 0 & 0 & 0 \\ 0 & m & 0 & 0 & 0 & 0 \\ 0 & 0 & m & 0 & 0 & 0 \\ 0 & 0 & 0 & I_{44} & 0 & -I_{46} \\ 0 & 0 & 0 & 0 & I_{55} & 0 \\ 0 & 0 & 0 & -I_{46} & 0 & I_{66} \end{bmatrix} \tag{3.41}$$

I_{46}, the roll-yaw product, is the only product of inertia that remains if the origin is the center of gravity. This term vanishes if the ship has fore-and-aft symmetry and is small otherwise.

Finally, the equations of motion reduce to:

$$\begin{aligned} m(\ddot{x}_1) &= \mathbf{F}_1 \\ m(\ddot{x}_2) &= \mathbf{F}_2 \\ m(\ddot{x}_3) &= \mathbf{F}_3 \\ I_{44}\ddot{x}_4 - I_{46}\ddot{x}_6 &= \mathbf{F}_4 \\ I_{55}\ddot{x}_5 &= \mathbf{F}_5 \\ I_{66}\ddot{x}_6 - I_{64}\ddot{x}_4 &= \mathbf{F}_6 \end{aligned} \tag{3.42}$$

3.5 Motions In Regular Waves

3.5.1 Forcing Function

The equations of motions for the grounded ship can also be written in the following form (Euler's Equations):

$$\sum_{j=1}^{6} \Delta_{ij} \cdot \ddot{x}_j(t) = F_i(t) \qquad \text{(i = 1, 2 ... 6)} \tag{3.43}$$

Δ_{ij} denotes the components of the inertia matrix for the ship.

Writing Euler's Equations of Motion with the gravitational, fluid and ground reaction forces acting on the ship results in:

$$\sum_{j=1}^{6} \Delta_{ij} \cdot \ddot{x}_j(t) = F_i(t) = F_{Gi} + F_{Hi} + F_{Groundi} \qquad \text{(i = 1, 2 ... 6)} \tag{3.44}$$

where F_{Gi} is the component of the gravity force acting on the vessel in the i-direction, F_{Hi} is the component of the fluid forces acting in the i-direction and $F_{ground\ i}$ is the component of the ground reaction force acting in the i-direction.

In linear theory, the responses of the vessel are linear with wave amplitude and occur at the frequency at which the ship perceives the incident waves. As a result, the time-dependent responses of the vessel, $x_j(t)$, are sinusoidal at the frequency of encounter (ω_e).

$$x_j(t) = \overline{x_j} e^{i\omega_e t} \tag{3.45}$$

In this case, there is no forward speed, so the frequency of encounter is the wave frequency (ω).

$$\begin{aligned} &\omega_e = \omega - \tfrac{\omega^2}{g} U_0 \cos\mu \\ &\omega_e = \omega \quad (\text{for } U = 0) \\ &\qquad \text{and} \\ &x_j(t) = \overline{x}_j e^{i\omega t} \end{aligned} \tag{3.46}$$

The gravitational forces are due to the weight of the vessel applied at the center of gravity. Since the mean gravitational forces cancel the mean buoyant forces, they are usually combined with the hydrostatic part of the fluid forces to give the net hydrostatic forces.

The hydrostatic and hydrodynamic forces acting on the ship are obtained by integrating the fluid pressure over the underwater portion of the hull. The component of the fluid forces acting in each of the six degrees of freedom are given by:

$$F_{Hi} = \iint_{S'} P n_i \mathrm{ds} \quad (\mathrm{i} = 1,\ 2, \ldots 6) \tag{3.47}$$

where n_i is the generalized unit normal to the hull surface into the hull, P is the fluid pressure, and S is the underwater hull surface area.

The components of the generalized normal are equal to the hull surface normals for the translation modes (i = 1, 2, 3) and equal to the moments of the unit normals for the rotational modes (i = 4, 5, 6).

These may be written as:

$$\begin{aligned} &(n_1, n_2, n_3) = \underline{n} \\ &(n_4, n_5, n_6) = \underline{r} \times \underline{n} \end{aligned} \tag{3.48}$$

where $\underline{n}$ is the unit normal to the hull surface out of the fluid, and $\underline{r} \times \underline{n}$ is the vector from origin to a point on the hull.

3.5.2 Bernoulli's Equation

The pressure on the hull, P, can be found using Bernoulli's equation

$$P = \tfrac{1}{2}\rho U_0^2 - \rho\tfrac{\partial\Phi}{\partial t} - \tfrac{1}{2}\rho(\nabla\Phi \times \nabla\Phi) + \rho g z \tag{3.49}$$

where ρ is density, $\nabla\Phi$ is the total velocity vector representing fluid flow, and U_0 is the forward speed of the ship.

In the Bernoulli equation, the first three terms represent the hydrodynamic contributions of the pressure and the last term represents the hydrostatic contribution. When Bernoulli's equation for the pressure is substituted into Euler's equations of motion, the fluid forces acting on the vessel may be divided into the following hydrostatic and hydrodynamic contributions:

$$F_{Hi} = F_{HSi} + F_{HDi} \tag{3.50}$$

where the hydrostatic force is represented by:

$$F_{HSi} = \rho g \iint_S z n_i ds \tag{3.51}$$

and the hydrodynamic force is represented by:

$$F_{HDi} = \rho \iint_S (\tfrac{1}{2} U_0^2 - \tfrac{\partial\Phi}{\partial t} - \tfrac{1}{2}\nabla\Phi \bullet \nabla\Phi) n_i ds \tag{3.52}$$

3.6 Reaction Forces

3.6.1 Hydrostatic Reaction Forces

Evaluation of the integrals in Equation (3.51) provide the net hydrostatic forces. The values of z must be replaced by the equivalent values in the (x_{b1} x_{b2} x_{b3}) system and the integrals are evaluated over the instantaneous underwater hull surface. Due to linear

theory, the integrals only need to be evaluated on the instantaneous wetted surface up to the calm water level. The contributions from the surface between the calm water level and sinusoidal wave surface are of higher order, and are neglected.

Details of the integral evaluation for the net hydrostatic forces may be found in Newman [29]. The net hydrostatic force takes in to account the mean gravitational forces:

$$\text{(net hydrostatic force)} = F^*_{HSi} = F_{Gi} + F_{HSi} \tag{3.53}$$

For a vessel with port and starboard symmetry, the final results of the net hydrostatic force for each of the six components are:

$$\begin{aligned}
&\text{(surge)} && F^*_{HS1} = 0 \\
&\text{(sway)} && F^*_{HS2} = 0 \\
&\text{(heave)} && F^*_{HS3} = \rho g S x_3 + \rho g S_1 x_5 \\
&\text{(roll)} && F^*_{HS4} = \rho g \nabla \overline{GM_T} x_4 \\
&\text{(pitch)} && F^*_{HS5} = -\rho g S_1 x_3 + \rho g \nabla (\overline{GM_L} + \frac{S\overline{LCF}^2}{\nabla}) x_5 \\
&\text{(yaw)} && F^*_{HS6} = 0
\end{aligned} \tag{3.54}$$

where $\overline{GM_T}$ is the transverse metacentric height, $\overline{GM_L}$ is the longitudinal metacentric height, ∇ is the underwater hull volume, $\overline{LCF}$ is the longitudinal center of flotation, and:

$$\begin{aligned}
&S = \int_L B(x)\, dx \text{ is the waterplane area around the y-axis} \\
&S_1 = \int_L x\, B(x)\, dx \\
&B(x) \text{ is the full breath of the waterplane at } x
\end{aligned} \tag{3.55}$$

The equations for the net hydrostatic force may also be written in a general matrix notation format:

$$F^*_{HSi} = \sum_{i=1}^{6} C_{ij}\ \overline{x}_j e^{i\omega t} \tag{3.56}$$

By comparing equations (3.54) and (3.56), the values of C_{ij} (hydrostatic restoring force coefficients) can be found. These coefficients give the net hydrostatic force acting on the vessel in the *j*th direction due to a unit displacement in the *k*th mode of motion. The hydrostatic restoring force coefficients are:

$$\begin{aligned}
&C_{ij} = 0 \text{ except for the following values} \\
&C_{33} = -\rho g \int B(x)\ dx = \rho g A_w \quad (A_w \text{ is the Area of the Waterplane}) \\
&C_{35} = C_{53} = \rho g \int x\, B(x)\ dx = -\rho g \cdot LCF \cdot A_w \\
&C_{44} = -\rho g \nabla \overline{GM_T} \\
&C_{55} = -\rho g \nabla (\overline{GM_L} + \tfrac{\overline{LCF}^2}{\nabla} S) \approx -\rho g S_{11} \\
&C_{55} = -\rho g S_{11} - \rho g \nabla (\overline{KB} - \overline{KG})
\end{aligned} \tag{3.57}$$

where all integrals are taken over the length of the ship.

The hydrostatic restoring force coefficients are equivalent to the hydrostatic coefficients used in ship stability calculations. For example, C_{33} is the same as the quantity for "tons per inch immersion", which is used by ship engineers to calculate draft changes due to weight additions.

3.6.2 Ground Reaction Forces

The previous section described the force terms for the equations of motion resulting from the hydrostatics of the problem. The ground reaction also provides force and moment terms which must be added to the force balance.

$$F_{Groundi} = K^s\ x_i \tag{3.58}$$

3.6.3 Dynamic Grounding Forces and Hydrodynamic Forces

The ground reaction dynamic stiffnesses, K^d, are developed in Chapter 2 and provided in equations (2.38) to (2.45).

As mentioned previously, the contribution from the hydrodynamic forces (F_{Hj}) are captured in the following terms from Bernoulli's equation for zero forward speed:

$$F_{HDi} = \rho \iint_S (-\tfrac{\partial \Phi}{\partial t} - \tfrac{1}{2} \nabla\Phi \bullet \nabla\Phi) n_i \, ds \tag{3.59}$$

The hydrodynamic forces acting on the vessel can be found by evaluating the above equation, which requires that the total velocity potential for the fluid flow be known. Since it is not possible to obtain the total velocity potential, some assumptions must be made to simplify the problem. The first assumption is that the total velocity potential can be subdivided into a simple summation of the various components:

$$\Phi(x,y,z,t) = [\phi_S(x,y,z)] + \phi_T e^{i\omega t}$$

$$\begin{aligned} \Phi(x,y,z,t) = {} & [\phi_S(x,y,z)] && \text{steady part} \\ & + [\phi_I + \phi_D + \sum_{i=1}^{6} \phi_i \overline{x_i}] e^{i\omega t} && \text{unsteady part} \end{aligned} \tag{3.60}$$

where, ϕ_S is the perturbation potential due to steady translation,

ϕ_T is the unsteady perturbation potential

$$\phi_T = \phi_I + \phi_D + \sum_{i=1}^{6} \phi_i \overline{x_i}$$

ϕ_I is the incident wave potential

ϕ_D is the diffracted wave potential

ϕ_i is the radiation potential due to unit motion in the *i*th direction

ϕ_I, ϕ_D, ϕ_i are all independent of time and depend only on space variables. The steady part of Φ results from the steady forward speed of the vessel. The term $-U_0 x$ is the free-stream velocity. The term ϕ_S is the steady perturbation velocity potential due to the presence of the ship hull. The term $(-U_0 x + \phi_S)$ is the solution to the problem of the ship advancing at constant forward speed in calm water. Since the vessel is assumed to have zero forward speed in the grounded ship condition, the steady part of Φ is only defined by ϕ_S.

The unsteady part contains all time dependent terms, and it is subdivided into the:

- incident wave potential (ϕ_I),
- diffracted wave potential (ϕ_D)
- the radiation potentials (ϕ_i) due to motion in each degree of freedom.

The potentials ϕ_I and ϕ_D result from solving the diffraction problem where incident waves act upon the vessel in its equilibrium position. The diffracted waves result from the scattering of the incident waves as they strike the body. The hydrodynamic forces that result from the incident plus diffracted waves are called the exciting forces (F_{EXi}). The radiation potentials (ϕ_i) are the solution to the radiation problem in which the vessel undergoes prescribed oscillatory motion in each of the six degrees of freedom in calm water. The hydrodynamic forces that result from the radiation problem involve added mass and damping.

In a fully-developed ship motion theory there is an interaction between steady and unsteady components because the unsteady components are dependent on ϕ_S.

Developing a ship motion theory that accounts for the interaction between steady and unsteady components is very difficult. As such, the interactions are usually ignored and the steady component is approximated by the free-stream value ($-U_0 x$), which in the grounded ship case equals zero [28].

The complete derivation of the unsteady forces acting on the ship is described in detail in the work of Salvesen, Tuck, and Faltinsen [26], as well as in *Principles of Naval Architecture, Volume 3* [28]. The following provides a summary of the problem, and the final linearized equations of motion as derived in the above work including ground effects.

The expressions for the different forces are substituted into:

$$\sum_{j=1}^{6} \Delta_{ij} \cdot \ddot{x}_j(t) = F_i(t) = F_{Gi} + F_{Hi} + F_{Groundi} \qquad (\text{i} = 1, 2 \ldots 6) \tag{3.61}$$

where $\ddot{x}_j$ is expressed as $\ddot{x}_j = -\omega^2 \overline{x_j} e^{i\omega t}$

The right hand side of the equations of motion becomes:

$$\begin{aligned} \mathrm{F}_i = F_{Gi} + F_{Hi} + F_{Groundi} &= F_{Gi} + (F_{HSi} + F_{HDi}) + F_{Groundi} \\ &= (F_{Gi} + F_{HSi}) + (F_{EXi} + F_{Ri}) + F_{Groundi} \\ &= (F^*_{HSi} + F_{EXi} + F_{Ri}) + F_{Groundi} \end{aligned} \tag{3.62}$$

Equation (3.63) then becomes:

$$\mathrm{F}_i = \sum_{j=1}^{6} -\omega^2 \Delta_{ij} \overline{x_j} e^{i\omega t} = F^*_{HSi} + F_{EXi} + F_{Ri} + F_{Groundi} \tag{3.63}$$

By replacing F^*_{HSi}, F_{EXi}, F_{Ri} (the net hydrostatic force, the exciting force of incident and diffracted waves and the reactionary force respectively) with their derived

components, moving like terms from the right to the left hand side of the equations, and eliminating the $e^{i\omega t}$, the governing equations are found:

$$\sum_{j=1}^{6}[-\omega^2(\Delta_{ij}+A_{ij})+i\omega B_{ij}+C_{ij}]\overline{x_j}=F_i^I+F_i^D \quad \text{(i = 1, 2, ... 6)} \tag{3.64}$$

The right hand side, $F_i^I + F_i^D$ represents the force due to incident and diffracted waves respectively, A_{ij} is the added mass term, B_{ij} is the damping term and C_{ij} is the stiffness term. The equations are the linearized equations of motion for an unrestrained vessel in sinusoidal waves. There are six coupled linear equations for the six unknown complex amplitudes, $\overline{x_j}$. The terms for the mass matrix (Δ_{ij}) and the restoring force coefficient matrix (C_{ij}) were derived in the previous sections, and are as follows:

$$C_{ij}=C_{ij}^H+K^d \tag{3.65}$$

$$\Delta_{ij}=\begin{bmatrix} m & 0 & 0 & 0 & 0 & 0 \\ 0 & m & 0 & 0 & 0 & 0 \\ 0 & 0 & m & 0 & 0 & 0 \\ 0 & 0 & 0 & I_{44} & 0 & -I_{46} \\ 0 & 0 & 0 & 0 & I_{55} & 0 \\ 0 & 0 & 0 & -I_{46} & 0 & I_{66} \end{bmatrix} \quad \text{mass matrix} \tag{3.66}$$

$$C_{ij}=\begin{bmatrix} 0_1 & 0_1 & 0_3 & 0_3 & 0_3 & 0_3 \\ 0_1 & 0_1 & 0_2 & 0_3 & 0_2 & c_{26} \\ 0_1 & 0_1 & c_{33} & 0_3 & c_{35} & 0_3 \\ 0_1 & 0_1 & 0_2 & c_{44} & 0_2 & c_{46} \\ 0_1 & 0_1 & c_{53} & 0_3 & c_{55} & 0_3 \\ 0_1 & 0_1 & 0_2 & 0_3 & 0_2 & c_{66} \end{bmatrix}+K^d \quad \text{stiffness matrix} \tag{3.67}$$

where: 0_1 = zero by physics; 0_2 = zero by symmetry; 0_3 = zero for small motions

The coefficients for added mass (A_{ij}), damping (B_{ij}), and the exciting force complex amplitudes are found by evaluating the integrals for the components of the

unsteady forces acting on the ship. This requires the solution of the radiation and diffraction problem, which is solved using strip theory.

3.7 Strip Theory

3.7.1 Introduction

To obtain values for the complex motion amplitudes, $\overline{x_j}$, the values for the coefficients $\Delta_{ij}, A_{ij}, B_{ij}, C_{ij}$, and the exciting force amplitudes $\overline{F_i^I}, \overline{F_i^D}$, must be determined. Δ_{ij} and C_{ij} are calculated as described in Sections 3.4.7 and 3.6.3. The Froude-Krylov exciting force, $\overline{F_i^I}$, is found by direct integration of the incident wave potential over the ship hull. To find the remaining variables, $A_{ij}, B_{ij}, \overline{F_i^D}$, the hydrodynamic problem must be solved. This is done using strip theory.

The strip theory used in this work was derived by Salvesen *et al.* [26]. The following is a summary of the strip theory process:

1. The ship is divided ship into a number of transverse sections, typically 20-40. Once divided, the two dimensional hydrodynamic coefficients for added mass, damping, wave excitation and the restoring force, are computed.

2. Once the sectional coefficients are derived, the global coefficients are derived by integrating the sectional coefficients along the length of the vessel.

3. Finally, the equations of motion are solved. Since the vertical plane and horizontal plane motions may be considered independently, the coupled heave

and pitch motions can be computed, and then the coupled sway, roll and yaw motions can be computed.

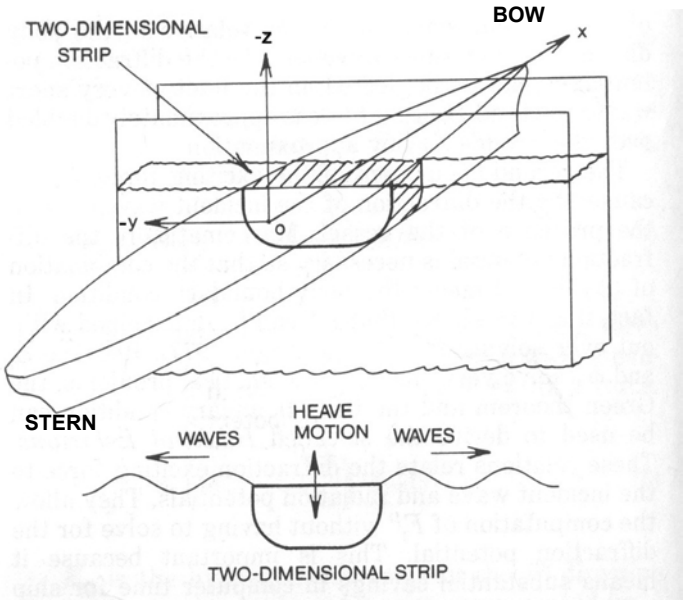

Figure 3.5 Strip Theory [29]

In essence, strip theory breaks down the overall three dimensional hydrodynamic problem into two dimensional problems, which are easier to solve.

3.7.2 Assumptions for Strip Theory

To use strip theory, the following standard assumptions are made:

1. The ship is slender (Length >> Beam or Draft).
2. The hull is rigid so that no flexure of the structure occurs (rigid body motion).
3. No planning hulls.
4. The motions are small.
5. The ship hull sections are wall-sided.

6. The water depth is much greater than the wave length so that deep water wave approximations may be applied.
7. The presence of the hull has no effect on the waves (Froude-Krylov hypothesis).
8. Origin at O is located immediately below the center of gravity, G, in the waterplane.

Although several strip theories for ship motions have been derived since the original strip theory for ship motions derived by Korvin-Korkovsky in 1957, all of them share the basic assumptions listed above [28].

3.7.3 Strip Motions

Assuming forced oscillation in all degrees of freedom except surge results in five degrees of freedom. For small motions, all motions are confined to the plane of a strip. Therefore, strip motions are defined in only three degrees of freedom: sway, heave, and roll. Strips are located at a distance x_{b1} relative to G, and have port/starboard symmetry. Terms marked with a prime indicate local/strip terms.

The motion of a point in the strip on the G x_{b1} axis relative to the G_o x_1 x_2 x_3 reference system is:

$$x_2' = x_2 + x_{b1}x_6 \tag{3.68}$$

$$x_3' = x_3 - x_{b1}x_5 \tag{3.69}$$

$$x_4' = x_4 \tag{3.70}$$

Furthermore, the velocity and acceleration of a point in the strip on the G x_{b1} axis relative to the $G_o\, x_1\, x_2\, x_3$ reference system is:

$$\dot{x}_2' = \frac{Dx_2'}{Dt} = \dot{x}_2 + x_{b1}\dot{x}_6 \tag{3.71}$$

$$\dot{x}_3' = \frac{Dx_3'}{Dt} = \dot{x}_3 - x_{b1}\dot{x}_5 \tag{3.72}$$

$$\dot{x}_4' = \frac{Dx_4'}{Dt} = \dot{x}_4 \tag{3.73}$$

$$\ddot{x}_2' = \frac{D^2x_2'}{Dt^2} = \ddot{x}_2 + x_{b1}\ddot{x}_6 = \ddot{x}_2 + x_{b1}\ddot{x}_6 \tag{3.74}$$

$$\ddot{x}_3' = \frac{D^2x_3'}{D^2t} = \ddot{x}_3 - x_{b1}\ddot{x}_5 = \ddot{x}_3 - x_{b1}\ddot{x}_5 \tag{3.75}$$

$$\ddot{x}_4' = \frac{D^2x_4'}{Dt^2} = \ddot{x}_4 \tag{3.76}$$

3.7.4 Local Coefficients

The excitation required to sustain the strip motions in the three possible degrees of freedom is obtained from the analogous equations for sway, heave and roll for the complete ship [28].

Consider the hydrostatic and hydrodynamic force per unit length in response to in-plane motion in calm water on the incremental slice with center at O:

$$\frac{D}{Dt}(M_2') + b_{22}'\dot{x}_2' + b_{24}'\dot{x}_4' = \frac{\delta F_2}{\delta x_{b1}} \tag{3.77}$$

$$\frac{D}{Dt}(M_3') + b_{33}'\dot{x}_3' + c_{33}'x_3' = \frac{\delta F_3}{\delta x_{b1}} \tag{3.78}$$

$$\frac{D}{Dt}(M'_4) + b'_{42}\dot{x}'_2 + b'_{44}\dot{x}'_4 + c'_{44}x'_4 = \frac{\delta F_4}{\delta x_{b1}} \tag{3.79}$$

where the momentum of water in the plane of the strip is:

$$M'_2 = a'_{22}\dot{x}'_2 + a'_{24}\dot{x}'_4 \tag{3.80}$$

$$M'_3 = a'_{33}\dot{x}'_3 \tag{3.81}$$

$$M'_4 = a'_{44}\dot{x}'_4 + a'_{42}\dot{x}'_2 \tag{3.82}$$

Then the time rate change of momentum per slice is:

$$\frac{D}{DT}(M'_2) = a'_{22}\frac{D\dot{x}'_2}{Dt} + \frac{Da'_{22}}{Dt}\dot{x}'_2 + a'_{24}\frac{D\dot{x}'_4}{Dt} + \frac{Da'_{24}}{Dt}\dot{x}'_4 = a'_{22}\ddot{x}'_2 + a'_{24}\ddot{x}'_4 \tag{3.83}$$

$$\frac{D}{DT}(M'_3) = a'_{33}\frac{D\dot{x}'_3}{Dt} + \frac{Da'_{33}}{Dt}\dot{x}'_3 = a'_{33}\ddot{x}'_3 \tag{3.84}$$

$$\frac{D}{DT}(M'_4) = a'_{44}\frac{D\dot{x}'_4}{Dt} + \frac{Da'_{44}}{Dt}\dot{x}'_4 + a'_{42}\frac{D\dot{x}'_2}{Dt} + \frac{Da'_{42}}{Dt}\dot{x}'_2 = a'_{44}\ddot{x}'_4 + a'_{42}\ddot{x}'_2 \tag{3.85}$$

Substitute equations (3.83-3.85) into the force equations (3.77-3.79) to obtain the excitation force per strip:

$$a'_{22}\ddot{x}'_2 + a'_{24}\ddot{x}'_4 + b'_{22}\dot{x}'_2 + b'_{24}\dot{x}'_4 = \frac{\delta F_2}{\delta x_{b1}} \tag{3.86}$$

$$a'_{33}\ddot{x}'_3 + b'_{33}\dot{x}'_3 + c'_{33}x'_3 = \frac{\delta F_3}{\delta x_{b1}} \tag{3.87}$$

$$a'_{44}\ddot{x}'_4 + a'_{42}\ddot{x}'_2 + b'_{42}\dot{x}'_2 + b'_{44}\dot{x}'_4 + c'_{44}x'_4 = \frac{\delta F_4}{\delta x_{b1}} \tag{3.88}$$

Replace slice motions with system motions:

$$\frac{\delta F_2}{\delta x_{b1}} = a'_{22}(\ddot{x}_2 + x_{b1}\ddot{x}_6) + (b'_{22})(\dot{x}_2 + x_{b1}\dot{x}_6) + a'_{24}\ddot{x}_4 + (b'_{24})\dot{x}_4 \tag{3.89}$$

$$\frac{\delta F_3}{\delta x_{b1}} = a'_{33}(\ddot{x}_3 - x_{b1}\ddot{x}_5) + (b'_{33})(\dot{x}_3 - x_{b1}\dot{x}_5) + c'_{33}(x_3 - x_{b1}x_5) \tag{3.90}$$

$$\frac{\delta F_4}{\delta x_{b1}} = a'_{44}\ddot{x}_4 + a'_{42}(\ddot{x}_2 + x_{b1}\ddot{x}_6) + (b'_{42})(\dot{x}_2 + x_{b1}\dot{x}_6) + (b'_{44})\dot{x}_4 + c'_{44}x'_4 \tag{3.91}$$

Rearrange in the same order as the equations of motion:

$$\frac{\delta F_2}{\delta x_{b1}} = a'_{22}\ddot{x}_2 + b'_{22}\dot{x}_2 + a'_{24}\ddot{x}_4 + b'_{24}\dot{x}_4 + x_{b1}a'_{22}\ddot{x}_6 + x_{b1}b'_{22}\dot{x}_6$$

$$F_2 = \int a'_{22}dx_{b1}\ddot{x}_2 + (\int b'_{22}dx_{b1})\dot{x}_2 + (\int a'_{24}dx_{b1})\ddot{x}_4 + (\int b'_{24}dx_{b1})\dot{x}_4 + \int x_{b1}a'_{22}dx_{b1})\ddot{x}_6 + (\int x_{b1}b'_{22}dx_{b1})\dot{x}_6 \tag{3.92}$$

$$\frac{\delta F_3}{\delta x_{b1}} = a'_{33}\ddot{x}_3 + b'_{33}\dot{x}_3 + c'_{33}x_3 - x_{b1}a'_{33}\ddot{x}_5 + (-x_{b1}b'_{33})\dot{x}_5 + (-x_{b1}c'_{33})x_5$$

$$F_3 = \int a'_{33}dx_{b1}\ddot{x}_3 + (\int b'_{33}dx_{b1})\dot{x}_3 + \int c'_{33}dx_{b1}x_3 - \int x_{b1}a'_{33}dx_{b1}\ddot{x}_5 + (-\int x_{b1}b'_{33}dx_{b1})\dot{x}_5 + (-\int x_{b1}c'_{33}dx_{b1})x_5 \tag{3.93}$$

$$\frac{\delta F_4}{\delta x_{b1}} = a'_{42}\ddot{x}_2 + b'_{42}\dot{x}_2 + a'_{44}\ddot{x}_4 + b'_{44}\dot{x}_4 + c'_{44}x_4 + x_{b1}a'_{42}\ddot{x}_6 + x_{b1}b'_{42}\dot{x}_6$$

$$F_4 = (\int a'_{42}dx_{b1})\ddot{x}_2 + (\int b'_{42}dx_{b1})\dot{x}_2 + (\int a'_{44}dx_{b1})\ddot{x}_4 + (\int b'_{44}dx_{b1})\dot{x}_4 + \int c'_{44}dx_{b1}x_4 + (\int x_{b1}a'_{42}dx_{b1})\ddot{x}_6 + (\int x_{b1}b'_{42}dx_{b1})\dot{x}_6 \tag{3.94}$$

$$F_5 = -\int x_{b1}dF_3$$

$$F_5 = -\int x_{b1} a'_{33} dx_{b1} \ddot{x}_3 - (\int x_{b1} b'_{33} dx_{b1}) \dot{x}_3 - \int x_{b1} c'_{33} dx_{b1} x_3 + \int {x_{b1}}^2 a'_{33} dx_{b1} \ddot{x}_5 - (-\int {x_{b1}}^2 b'_{33} dx_{b1}) \dot{x}_5 - (-\int {x_{b1}}^2 c'_{33} dx_{b1}) x_5 \quad (3.95)$$

$$F_6 = \int x_{b1} dF_2$$

$$F_6 = \int x_{b1} a'_{22} dx_{b1} \ddot{x}_2 + (\int x_{b1} b'_{22} dx_{b1}) \dot{x}_2 + (\int x_{b1} a'_{24} dx_{b1}) \ddot{x}_4 + (\int x_{b1} b'_{24} dx_{b1}) \dot{x}_4 + \int {x_{b1}}^2 a'_{22} dx_{b1} \ddot{x}_6 + (\int {x_{b1}}^2 b'_{22} dx_{b1}) \dot{x}_6 \quad (3.96)$$

3.7.5 Global Coefficients

Comparing equations (3.92) through (3.96) with equations (3.35) and (3.39) provides the hydrodynamic coefficients for the complete hull in terms of the local values. For heave and pitch, the coefficients of the equations of motion are:

Heave (x_3) degree of freedom:

$$(m+a_{33})\ddot{x}_3-(m\bar{x}_{b1}-a_{35})\ddot{x}_5+b_{33}\dot{x}_3+b_{35}\dot{x}_5+c_{33}x_3+c_{35}x_5=\overline{F}_{w30}e^{i\omega_e t} \tag{3.97}$$

$$a_{33}=\int a'_{33}dx_{b1}$$

$$b_{33}=\int b'_{33}dx_{b1}$$

$$c_{33}=\int c'_{33}dx_{b1}=\rho g A_W$$

$$c'_{33}=\rho g B'$$

$$a_{35}=-\int x_{b1}a'_{33}dx_{b1}$$

$$b_{35}=-\int x_{b1}b'_{33}dx_{b1}$$

$$c_{35}=\int x_{b1}c'_{33}dx_{b1}=-\rho g x_{b1LCF}A_W$$

$$x_{b1LCF}=\frac{\int x_{b1}B'dx_{b1}}{A_W}=\frac{\int x_{b1}c'_{33}dx_{b1}}{\rho g A_W}$$

$$\int udv=uv-\int vdu$$

Pitch (x_5) degree of freedom:

$$(I_{55}+a_{55})\ddot{x}_5+m\bar{x}_{b3}\ddot{x}_1-(m\bar{x}_{b1}-a_{53})\ddot{x}_3+b_{55}\dot{x}_5+b_{53}\dot{x}_3+c_{55}x_5+c_{53}x_3=\overline{F}_{w50}e^{i\omega_e t} \qquad (3.98)$$

$$a_{55}=\int {x_{b1}}^2 a'_{33}dx_{b1}$$
$$b_{55}=\int {x_{b1}}^2 b'_{33}dx_{b1}$$
$$c_{55}=\int {x_{b1}}^2 c'_{33}dx_{b1}=\Delta GM_L+\rho g A_W {x_{b1LCF}}^2$$

$$a_{53}=-\int x_{b1}a'_{33}dx_{b1}=a_{35}$$
$$b_{53}=-\int x_{b1}b'_{33}dx_{b1}$$
$$c_{53}=-\int x_{b1}c'_{33}dx=-\rho g A_W x_{b1LCF}$$

3.7.6 Sectional Added Mass and Damping

The calculation of the sectional added mass (the hydrodynamic force in phase with acceleration) and damping (the hydrodynamic force in phase with velocity) coefficients are necessary to determine the global coefficients of the equations of motion. Methods for solving for these coefficients were developed by Ursell (1949), Grim (1959), and others. The techniques used are involved and laborious, requiring the use of a computer for the simplest of solutions. These methods generally begin by examining the properties of a cylinder of infinite length, floating in water of infinite depth and vertically oscillating in small harmonic motion. The oscillating cylinder generates surface waves, which radiate away from the cylinder. The coefficients are then calculated with the usual potential flow assumptions of negligible viscosity and compressibility, no flow separation and no skin friction. Ursell [30] presents a comprehensive treatment of this problem with all necessary references. Readers are referred to the *Principles of Naval Architecture, Volume 3* [28] for further discussion of this material.

Since ship hull sections are generally not circular in shape, conformal mapping is used to extend the results for a circle into solutions for more realistic hull shapes. This is accomplished by defining a mapping function, which can map the ship section to a circular section. Once this mapping is defined, it can be used with Ursell's known solution for a circular cylinder to find the solution for the actual ship section. This method is further extended using *Lewis forms*.

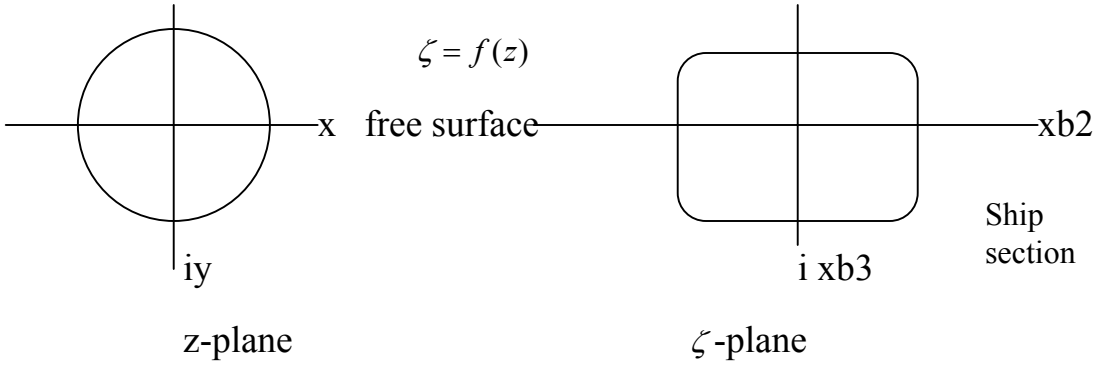

3.7.7 Lewis Forms

Lewis forms define a family of hull forms, which closely resemble ship sections. A representation of the section as a Lewis form in the ζ-plane is based on the sectional beam, draft, and area, and a mapping to a cylinder in the z-plane given by:

$$z = \zeta + \frac{a_1}{\zeta} + \frac{a_3}{\zeta^2} \qquad (3.99)$$

These parameters give satisfactory results for all practical purposes. The half-beam to draft ratio and the sectional area coefficient of the station are expressed in term of the coefficients given by:

$$\lambda' = \frac{Y'}{2T'} = \frac{1 + a_1 + a_3}{1 - a_1 + a_3}$$
$$\sigma' = \frac{A'}{T'Y'} = \frac{\pi}{4} * \frac{1 - a_1^2 - 3a_3^2}{4(1 + a_3^2) - a_1^2} \tag{3.100}$$

where $\underline{Y'}$ is the beam of the section at the waterline, A' is the area of the section, T' is the draft of the section, and σ' is the sectional area coefficient. The Lewis form representation of the stations results in significantly shorter calculations for the sectional added mass and damping. Although, the exact shape of the hull form is not used or needed, in most cases an exact mapping is not necessary [31].

The Lewis form representation of sections has two restrictions. It cannot be used for sections with very small sectional area or for bulbous sections with very large sectional area.

3.7.8 Fine Sections and Bulb Forms

In the case of very fine sections, the minimal sectional area for which a Lewis form exists is given by:

$$\sigma'_{\min} = \frac{3\pi}{32}(2 - \lambda'), \lambda' \le 1$$
$$\sigma'_{\min} = \frac{3\pi}{32}\left(2 - 1/\lambda'\right), \lambda' \le 1 \tag{3.101}$$

Such stations normally occur at the bow or stern of a ship with small block coefficient. Since they are associated with very small areas and beams, the contribution of these sections to the total added mass and damping is minimal. Thus, this problem can

be fixed by increasing the area of the station until the minimum area coefficient is reached.

In the case of bulbous stations, the maximum area coefficient for a Lewis form representation of a station is given by:

$$\sigma'_{\max} = \frac{\pi}{32}(\lambda' + \frac{1}{\lambda'} + 10) \tag{3.102}$$

Since the contribution of the large bulbous sections in the total added mass and damping can be significant, the problem cannot be by-passed. To solve this problem, a family of bulbous section representation was created by the Massachusetts Institute of Technology (MIT) [36] and a procedure was derived for the calculation of added mass and damping of these stations.

Similar to Lewis forms, the representation of a section by an *MIT bulb form* is based on the sectional beam and draft area. The mapping function of an MIT bulb form is given by:

$$z = \zeta + \frac{B\zeta}{\zeta^2 + A} \tag{3.103}$$

The half-beam to draft ratio and the sectional area coefficient of a station are connected to the coefficients of equation 3.103 by:

$$\begin{aligned} \lambda' &= \frac{1 - A^2 + AB + B}{1 - A^2 + AB - B} \\ \sigma' &= \frac{\pi}{4}(1 + A\frac{1 - \lambda'^{\,2}}{2\lambda'}) \end{aligned} \tag{3.104}$$

The MIT bulb forms exist for $\sigma' > \pi/4$ and their maximum area coefficient is given by:

$$\sigma'_{\max} = \frac{\pi}{4}(1 + \frac{1 - \lambda'^{\,2}}{2\lambda'}) \tag{3.105}$$

3.7.9 Excitation Forces in Regular Waves

From Newman [29], the forces and moments applied to the ship by a train of regular waves is described by the following equation:

$$F_i = F_{HSi} + F_{HDi} = F_{Radiationi} + F_{wi} \tag{3.106}$$

where F_{HSi} denotes the hydrostatic forces in the i-direction.

F_{HDi} denotes the hydrodynamic forces in the i-direction.

$F_{Radiationi}$ denotes the forces created by the ship's movement in the i-direction.

F_{wi} denotes the force due to the regular wave.

For a given hull shape at a particular speed and heading in waves of a particular length, the forces and moments F_i are assumed to be functions of the displacement, velocity, and acceleration of the surface depression and the six possible motions. So we may write:

$$\begin{aligned} F_i &= F_i\left[\zeta, \dot{\zeta}, \ddot{\zeta}, (x_i, \dot{x}_i, \ddot{x}_i)\right] \quad (\text{i} = 1,\ 2,\ 3) \\ F_i &= F_i\left[\zeta, \dot{\zeta}, \ddot{\zeta}, (x_i, \dot{x}_i, \ddot{x}_i)\right] \quad (\text{i} = 4,\ 5,\ 6) \end{aligned} \tag{3.107}$$

If the wave amplitude is small compared with the wave and ship lengths the motions will also be small and we may use a Taylor series expansion to obtain linear approximations to the above equations.

$$\begin{aligned} F_i &= a_i \ddot{\zeta} + b_i \dot{\zeta} + c_i + \sum_{j=1}^{6} (a_{ij} \ddot{x}_j - b_{ij} \dot{x}_j - c_{ij} x_j) \quad (\text{i} = 1,3) \\ F_i &= a_i \ddot{\zeta} + b_i \dot{\zeta} + c_i + \sum_{j=1}^{6} (a_{ij} \ddot{x}_j - b_{ij} \dot{x}_j - c_{ij} x_j) \quad (\text{i} = 4,6) \end{aligned} \tag{3.108}$$

The coefficients $a_{i,}$ b_i, and c_i are functions of the wavelength and amplitude, heading angle, ship speed and hull form, and quantify the effect of the wave forces and moments.

The other coefficients $a_{ij,}$ b_{ij}, and c_{ij} quantify the forces and moments required to sustain the motions of the ship.

The linearization of the equations of motion allows the wave excitation to be considered independent of any ship motions and to be expressed as functions of the wave amplitude alone. The following is adapted from Lloyd [27], and provides the derivation for the linear approximation of the excitation force in heave and pitch using Taylor Series expansion.

The wave depression at any point relative to O is:

$$\begin{aligned} \zeta &= \zeta_0 \cos(kx - \omega t) \\ \zeta &= \zeta_0 \cos(kx_1 \cos\mu - kx_2 \sin\mu - \omega t) \end{aligned} \tag{3.109}$$

where $k = \dfrac{\omega^2}{g}$

Since the ship is allowed no motions, the center of gravity remains above O, and

$x_1 = x_{b1}$

The wave depression varies across each strip but we assume the ship to be slender.

To calculate the wave depression with sufficient accuracy, assume

$x_2 = 0$

The wave depression experienced at each strip is then

$$\begin{aligned} &\zeta = \zeta_0 \cos(\omega t - kx_{b1} \cos\mu) = \zeta_0 \cos(\omega t - Q) \\ &\text{where } Q = kx_{b1} \cos\mu \end{aligned} \tag{3.110}$$

The excitation experienced by each strip is related to the pressures, velocities and accelerations in the water beneath the wave surface. These quantities vary by depth and

it is usual to simplify the calculations by taking their values at a mean local draft defined

by $\overline{T}' = \dfrac{A'}{B'}$ (3.111)

The pressure fluctuation at the mean local draft is

$$\tilde{P} = -\rho g \zeta_0 e^{-k\overline{T}'} \cos(\omega t - Q)$$

The vertical velocity of the water at the mean draft is

$$w = -\omega \zeta_0 e^{-k\overline{T}'} \sin(\omega t - Q) \quad (3.112)$$

and the corresponding vertical acceleration is

$$\dot{w} = -\omega^2 \zeta_0 e^{-k\overline{T}'} \cos(\omega t - Q)$$

The horizontal velocity at the mean draft is

$u = -\omega \zeta_0 e^{-k\overline{T}'} \cos(\omega t - Q) = -\omega e^{-k\overline{T}'} \zeta$ (along the O x_1 axis)

The athwartship component of the horizontal velocity is

$$u_2 = \omega \zeta_0 e^{-k\overline{T}'} \cos(\omega t - Q) \sin(\mu) = \omega e^{-k\overline{T}'} \zeta \sin(\mu) \quad (3.113)$$

and the corresponding athwartships component of the horizontal accelertion is

$$\dot{u}_2 = -\omega^2 \zeta_0 e^{-k\overline{T}'} \sin(\omega t - Q) \sin(\mu) = \omega w \sin(\mu)$$

Thus, the vertical excitation due to the force due to the pressure fluctuation plus the rate of change of momentum of the water surrounding the strip and a force associated with the vertical velocity of the water is:

$$\delta F_{w3} = \left(\frac{DM'_{w3}}{Dt} + b'_{33} w - B' \tilde{P}\right) \delta x_{b1}$$

where the vertical momentum is:

$M'_{w3} = a'_{33} w$ (per length of strip) (3.114)

The rate of change of momentum is:

$$\frac{DM'_{w3}}{Dt} = a'_{33} \dot{w}$$

From the previous, the vertical force on each strip and the associated pitch moment about the center of gravity is:

$$\delta F_{w3} = \left(a'_{33}\dot{w} + b'_{33}w - B'\widetilde{P}\right)\delta x_{b1} = [-a'_{33}\omega^2\zeta_0 e^{-k\bar{T}'}\cos(\omega t - Q) + (b'_{33})\omega\zeta_0 e^{-k\bar{T}'}\sin(\omega t - Q) + B'\rho g\zeta_0 e^{-k\bar{T}'}\cos(\omega t - Q)]\delta x_{b1} \tag{3.115}$$

Substituting for P, w and $\dot{w}$ results in the following:

$$\begin{aligned}\delta F_{w3} &= \zeta_0[(B'\rho g - a'_{33}\omega^2)e^{-k\bar{T}'}\cos(\omega t - Q) + (b'_{33})\omega e^{-k\bar{T}'}\sin(\omega t - Q)]\delta x_{b1}\\ \delta F_{w5} &= \zeta_0[(B'\rho g - a'_{33}\omega^2)x_{b1}e^{-k\bar{T}'}\cos(\omega t - Q) + (b'_{33})x_{b1}\omega e^{-k\bar{T}'}\sin(\omega t - Q)]\delta x_{b1}\end{aligned} \tag{3.116}$$

Integrate over the length of the hull to obtain global values for heave. To obtain pitch values multiply heave values by the moment arm x_{b1}, then integrate over the length of the hull.

$$\begin{aligned}F_{w3} &= \zeta_0[\int(B'\rho g - a'_{33}\omega^2)e^{-k\bar{T}'}\cos(\omega t - Q)dx_{b1} + \int(b'_{33})\omega e^{-k\bar{T}'}\sin(\omega t - Q)dx_{b1}]\\ F_{w5} &= \zeta_0[\int(B'\rho g - a'_{33}\omega^2)x_{b1}e^{-k\bar{T}'}\cos(\omega t - Q)dx_{b1} + \int(b'_{33})x_{b1}\omega e^{-k\bar{T}'}\sin(\omega t - Q)dx_{b1}]\end{aligned} \tag{3.117}$$

These may be rewritten as:

$$\begin{aligned}F_{w3} &= \zeta_0\int[P_{C3}\cos(\omega t - Q) + P_{S3}\sin(\omega t - Q)]dx_{b1}\\ F_{w5} &= \zeta_0\int[P_{C5}\cos(\omega t - Q) + P_{S5}\sin(\omega t - Q)]dx_{b1}\end{aligned} \tag{3.118}$$

where $P_{3C} = (c'_{33} - a'_{33}\omega^2)e^{-k\bar{T}'}$

$P_{3S} = (b'_{33})\omega e^{-k\bar{T}'}$

$P_{5C} = (c'_{33} - a'_{33}\omega^2)x_{b1}e^{-k\bar{T}'}$

$P_{5S} = (b'_{33})x_{b1}\omega e^{-k\bar{T}'}$

3.8 Solving the Equations of Motion

3.8.1 General Method

Once the global coefficients for the equations of motion and the excitation forces are calculated, similar terms are grouped together providing an equation of motion, which takes the following form:

$$\left[\Delta_{ij} + A_{ij}\right]\{\ddot{x}\} + [c]\{\dot{x}\} + [k]\{x\} = \{F(t)\}$$

where Δ_{ij} is the inertia matrix and A_{ij} is the added mass matrix
$[c]$ is the damping matrix (3.119)
$[k]$ is the stiffness matrix
$\{F(t)\}$ is the exciting force due to the waves

Since we are assuming that input and system response are both sinusoidal, the equations of motion are rewritten as:

$$[-\omega^2\left[\Delta_{ij} + A_{ij}\right] + i\omega[c] + k]\{\underline{x}\} = \{\underline{F}\} \quad (3.120)$$

The time dependency cancels out of the equations, allowing for analysis in the frequency domain.

The above equation represents five equations with five unknowns. Since the equations are linear, they can be solved using many different techniques, such as back substitution, Cramer's Rule, and direct matrix inversion. Solving the equations of motion in the frequency domain provides the ship motion amplitudes for five degrees of freedom (sway, heave, pitch, roll, yaw).

3.8.2 Heave and Pitch Motions

The following is a solution for the coupled degrees of freedom of heave and pitch. Since there are two equations with two unknowns, the method of back substitution is used.

Rewrite the excitation equations for heave and pitch in the following form:

$$F_{w3} = |F_{w30}|\cos(\omega t + \gamma_3) = |F_{w30}|e^{i(\omega t+\gamma_3)} = \\ |F_{w30}|e^{i\gamma_3}e^{i\omega t} = \overline{F}_{w30}e^{i\omega t} \text{ the real part is implied} \tag{3.121}$$

Since the forcing function is sinusoidal, assume a sinusoidal response:

$$x_3 = |x_{30}|\cos(\omega t + \delta_3) = |x_{30}|e^{i(\omega t+\delta_3)} = \\ |x_{30}|e^{i\delta_3}e^{i\omega t} = \bar{x}_{30}e^{i\omega t} \text{ the real part is implied} \tag{3.122}$$

Thus, the equation for coupled heave motion is written:

$$(m + a_{33})\ddot{x}_3 - (m\bar{x}_{b1} - a_{35})\ddot{x}_5 + b_{33}\dot{x}_3 + b_{35}\dot{x}_5 + c_{33}x_3 + c_{35}x_5 = F_{w3} = \overline{F}_{w30}e^{i\omega_e t} \tag{3.123}$$

The time dependency cancels out, and the heave equation becomes:

$$\left[-\omega_e{}^2(m + a_{33}) + i\omega_e b_{33} + c_{33}\right]\bar{x}_{30} + \left[\omega_e{}^2(m\bar{x}_{b1} - a_{35}) + i\omega_e b_{35} + c_{35}\right]\bar{x}_{50} = \overline{F}_{w30} \tag{3.124}$$

which allows for analysis in the frequency domain.

Similarly, the equation for coupled pitch motion is:

$$(I_{55} + a_{55})\ddot{x}_5 + m\bar{x}_{b3}\ddot{x}_1 - (m\bar{x}_{b1} - a_{53})\ddot{x}_3 + b_{55}\dot{x}_5 + b_{53}\dot{x}_3 + c_{55}x_5 + c_{53}x_3 = F_{w5} = \overline{F}_{w50}e^{i\omega_e t} \tag{3.125}$$

and becomes:

$$\left[-\omega_e{}^2(I_{55} + a_{55}) + i\omega_e b_{55} + c_{55}\right]\bar{x}_{50} + \left[\omega_e{}^2(m\bar{x}_{b1} - a_{53}) + i\omega_e b_{53} + c_{53}\right]\bar{x}_{30} = \overline{F}_{w50} \tag{3.126}$$

These two equations have the form:

$$P\bar{x}_{30} + Q\bar{x}_{50} = F \\ R\bar{x}_{30} + S\bar{x}_{50} = M \tag{3.127}$$

Solving for $\bar{x}_{30}$ and $\bar{x}_{50}$:

$$\bar{x}_{30} = \frac{QM - SF}{QR - PS} \tag{3.128}$$

$$\bar{x}_{50} = \frac{RF - PM}{QR - PS} \tag{3.129}$$

From which pitch and heave response magnitudes and phase angles can be determined.

3.8.3 Relative Motions, Velocities, and Accelerations

Consistent with linear theory, the heave motion at any point along the ship is given by:

$$\bar{\xi} = \bar{x}_3 - \bar{x}_5 x_{b1} \tag{3.130}$$

The vertical velocity and acceleration are found by differentiation to be:

$$\begin{aligned} \dot{\bar{\xi}} &= i\omega\bar{\xi} = i\omega(\bar{x}_3 - \bar{x}_5 x_{b1}) \\ \ddot{\bar{\xi}} &= -\omega^2\bar{\xi} = -\omega^2(\bar{x}_3 - \bar{x}_5 x_{b1}) \end{aligned} \tag{3.131}$$

To find the relative motion between the water surface and the waterline of the ship, subtract the wave amplitude at the desired point from the heave amplitude at that point.

$$\bar{\rho} = \bar{\xi} - \bar{\zeta}(x,t) \quad \text{or} \quad \bar{\rho} = \bar{x}_3 - \bar{x}_5 x_{b1} - \zeta_A e^{i(kx+\omega t)} \tag{3.132}$$

where $\bar{\xi} = \bar{x}_3 - \bar{x}_5 x_{b1}$ and $\bar{\zeta} = \zeta_A e^{i(kx+\omega t)}$

Differentiate $\bar{\rho}$ to find relative velocities and accelerations.

3.9 Structural Design Values

3.9.1 Calm Water Bending Moment

The calm water shear and bending moment is generated from the load curve. The load curve is determined by superimposing the weight distribution (w) and buoyancy distribution (b).

If all loads are distributed, the shear may be expressed as an integral equation:

$$V = \int (b - w)dx = \int p\, dx \tag{3.133}$$

The above integrals are taken from the stern of the ship, to the point at which the shear force is calculated.

The relationship of the bending moment to the shear force is exactly the same as the relationship of the shear force to the load.

$$M = \int V\, dx \tag{3.134}$$

Given the above, at any point on the ship

$$P = \frac{dV}{dx} \text{ and } V = \frac{dM}{dx} \tag{3.135}$$

.

3.9.2 Dynamic Shear Forces and Bending Moments

The calculation of dynamic longitudinal bending moments and shear forces in regular waves is based on strip theory and the linearized equations of motion. As calculated by Salvesen [26], the total dynamic load per unit length operating on a ship section is the sum of the unsteady hydrodynamic forces and the mass inertial forces. In the $G\,x_{b1}x_{b2}x_{b3}$ axis system the dynamic load can be written as:

$$q(x) = \frac{-w(x)}{g}(\underline{\ddot{x}_3} - x_{b1}\underline{\ddot{x}_5}) - \mu(x)\underline{\ddot{x}_3} - N(x)\underline{\dot{x}_3} - \rho g Y(x) + x_{b1}\mu(x)\underline{\ddot{x}_5} +$$

$$x_{b1}N(x)\underline{\dot{x}_5} + \rho g x_{b1} Y(x)\underline{x_5} + \frac{dF_o(x)}{dx}$$

where $w(x)$ = weight per foot for each section (3.136)

$\frac{dF_o(x)}{dx}$ = excitation for per foot

$\underline{x_3}$ = heave amplitude

$\underline{x_5}$ = pitch amplitude

The dynamic shear force is the integral of the dynamic load on the sections, and the dynamic bending moment is the integral of the dynamic shear force.

3.10 Grounded Ship Response

Ocean waves provide a random excitation. By assuming:

- Normal distribution of wave heights,
- Zero mean
- *Ergodic* process: any one sample is typical of the process.
- *Stationary* process: the statistics of the process samples don't change over time.
- Narrow band
- Fully developed seas
- Linear system

It can be shown that the ship motion energy spectrum can be calculated by filtering the encountered wave energy spectrum with the appropriate motion transfer function [27]. This is achieved by multiplying the wave energy spectrum by the square of the motion transfer function, or Response Amplitude Operator (RAO).

$$S_r(\omega) = RAO \cdot S_\zeta(\omega)$$
where $RAO = |H_r(\omega)|^2$
$S_r(\omega)$ is the motion response spectrum.
$S_\zeta(\omega)$ is the wave energy spectrum. (3.137)

In this thesis, the responses of interest are:

$$S_{x_3}(\omega) = S_\zeta(\omega)\left(\frac{x_{3o}}{\zeta_o}\right)^2$$ heave motion spectrum
x_{3o} is the amplitude of heave motion. (3.138)
ζ_o is the the wave amplitude.

$$S_{x_5}(\omega) = S_\zeta(\omega)\left(\frac{x_{5o}}{\zeta_o}\right)^2$$ pitch motion spectrum
x_{5o} is the amplitude of pitch motion. (3.139)
ζ_o is the the wave amplitude.

In predicting the spectra and hence statistical properties of ship responses in a seaway, only the spectrum of the seaway is necessary. Whenever the actual spectrum of the seaway is known, it should be used for predictions. However, the common practice in seakeeping work is to use analytical spectral forms for the seaway. These forms are based on theoretical considerations and fitting of actual seaway spectra and seem to represent real life adequately for seakeeping processes [28].

This work uses a two-parameter spectral family, which according to Bretschneider [32] can represent seaways in all stages of development. The two-parameter family can be used to describe developing or decaying seaways with respectively a higher or a lower circular frequency for the spectral peak than fully developed seaways. A sea spectrum can be generated on the basis of the significant wave height and the circular frequency of the spectral peak.

The wave energy spectrum, $S_\zeta(\omega)$, in equations 3.133 and 3.134 is defined by the Bretschneider wave energy spectrum [32]:

$$S_\zeta(\omega) = \frac{5}{16}\frac{\omega_m^4}{\omega^5}(\bar{H}_{1/3})^2 e^{-1.25\left(\frac{\omega_m}{\omega}\right)^4} \tag{3.140}$$

$\bar{H}_{1/3}$ is the significant wave height or average wave height of the highest one-third waves, and ω_m is the modal frequency. For the purpose of this analysis, the seas are considered to be fully developed, where the modal frequency in equation 3.135 is defined by:

$$\omega_m = 0.4\sqrt{\frac{g}{\bar{H}_{1/3}}} \tag{3.141}$$

g is the acceleration due to gravity.

Chapter 4 Calculation of Static Equilibrium Condition

The program this thesis uses to analyze the motions of and loads on a stranded ship is called the Stranded Ship Motions & Loads Program (SSMLP). It requires, as input, a definition of the equilibrium grounded condition of the ship. This chapter describes the process and equations used to determine this equilibrium condition [8].

The magnitude and location of the static ground reaction is determined by comparing the attitudes and positions of the ship before and after stranding. Four different grounding scenarios are considered:

- stranding on one pinnacle
- stranding on two pinnacles
- stranding on shelf
- stranding on penetrable shelf

One of the following inputs is required to calculate ground reaction:

1. the observed drafts of the vessel in the stranded condition, or
2. the actual depth of water at each grounding location.

Ground reactions are calculated by finding the difference between the total weight of the ship for the current loaded condition and the buoyancy of the vessel as determined by integration of the hull offsets. (Lost Buoyancy Method).

When the observed drafts of the vessel are specified in the stranded condition, hull buoyancy and center of buoyancy are calculated by integration of hull offsets to the defined waterline. The center of gravity is defined by the specified load case. The center of ground reaction is determined by balancing weight, buoyancy, and ground reaction moments. For a ship stranded on one pinnacle, the longitudinal center of ground reaction is required to be within the length of the ground contact. For a ship stranded on two pinnacles, the longitudinal positions of the two grounding points (assumed to be at the center of each pinnacle) are required. Ground reaction at each pinnacle is determined by balancing weight, buoyancy, and ground reaction moments about the other pinnacle. For a ship stranded on a shelf, the forward and after ends of the shelf are specified. The center of ground reaction must be within the grounded length.

When the actual depth of water at each grounding location for one or two pinnacles is specified, an iterative solution is used. For a single pinnacle, the buoyancy is calculated for a trial waterline that passes through the point defined by the water depth at the pinnacle. Weight and buoyancy moments are summed about the center of ground reaction, taken as the center of the pinnacle. The vessel is trimmed and the process is repeated until equilibrium is reached. For two pinnacles, the trimmed waterline is defined by the water depths at the pinnacle locations. No trim iteration is necessary. Specifying water depth at the ends of a shelf defines a waterline in the same way as specifying forward and after drafts.

For ships stranded on a penetrable shelf, the penetration into the shelf is evaluated at each draft and trim iteration. The penetration volume, horizontal area at the mudline, and length are computed. The ground reaction is evaluated based on the soil bearing

capacity, F_q, using Equation (4.14) [33]. The iterative process continues until equilibrium is achieved for longitudinal moments, and for weight versus buoyancy plus ground reaction. The longitudinal and transverse centers of ground reaction are assumed to be at the longitudinal and transverse centers of the penetration volume.

$$F_q = 5AS_u[1+0.2(D/B)][1+0.2(B/L)] \quad (4.14)$$

where,

A = horizontal area at mudline

D = embedment depth

B = equivalent breadth

L = equivalent length

S_u = undrained shear strength, assumed to be $q_u/(N_cK_c)$

q_u = bearing capacity for cohesive soil

N_c, K_c = dimensionless soil and geometry coefficients, taken as 5.1 and 1.05 respectively

This approach is based upon the method presented in the U.S. Navy Salvage Engineer's Handbook [8]. The ratios D/B and B/L are limited to a maximum value of 1.

The ground reaction, for most cases, is assumed to be uniformly distributed along the grounded length of the ship as is shown in Figure 4.1. If the center of ground reaction is at or near the center of grounded length, ground reaction may be assumed to be

distributed symmetrically about this point. If the ship grounds on a uniformly sloping seafloor, the ground reaction is distributed as a right triangle as is shown in Figure 4.2. If the center of ground reaction lies towards one end of the grounded length, the ground reaction distribution is weighted towards that end in an asymmetrical shape.

For ships stranded on pinnacles, ground reaction is assumed to be evenly distributed over the pinnacle length. For ships stranded on a shelf, ground reaction is distributed as a trapezoid if the center of ground reaction falls within the center third of the grounded length. If the center of ground reaction lies outside the center third of the grounded length, ground reaction is distributed as a right triangle. The right angle is fixed at the end of the shelf nearest the center of ground reaction. The height and base length are adjusted so the center of area coincides with the center of ground reaction.

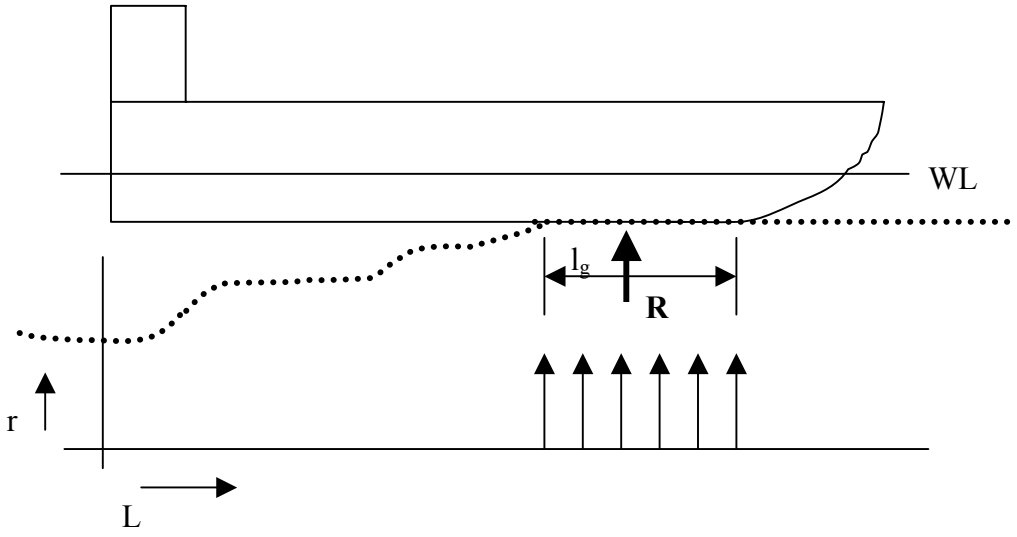

where **R** is the ground reaction and $r = R/l_g$

Figure 4.1 Uniform Ground Reaction Distribution on a stranded ship

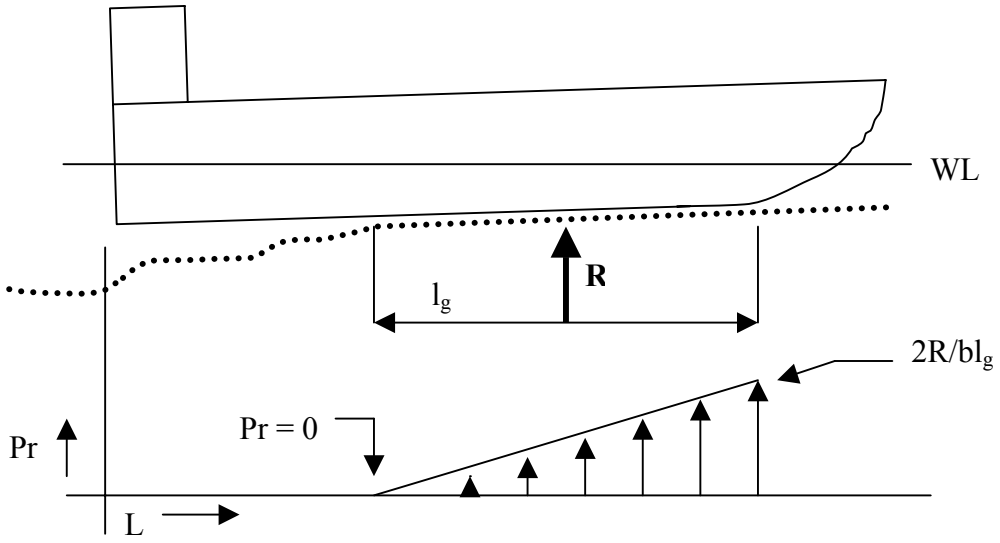

where $P_{max} = 2R/l_g b_{avg}$ r = Pr b

with P_{max} = maximum grounding pressure, lton/ft^2, R = ground reaction, lton, l_g = grounded length, feet, b_{avg} = average breadth of contact area over grounded length, feet, b = breadth of contact area, feet

Figure 4.2 Asymmetric Ground Reaction Distribution on a stranded ship

The ground reaction force is taken into account as a negative weight, which effects the static orientation of the ship in the grounded position.

Ground reaction can be determined by any of the five methods described below. All these methods assume that the ship and supporting ground are perfectly rigid bodies.

1) Residual Buoyancy Distribution Method. The area between the weight curve and the buoyancy curve for the stranded waterline is the total ground reaction. For equilibrium to exist, ground reaction must be distributed in increments over the grounded length so that the combined center of buoyancy and ground reaction

is in vertical line with the center of gravity. The area and buoyancy curves are developed from section areas taken from Bonjean's Curves, which are curves of sectional area slices taken along the length of the ship, or calculated from offsets.

2) Change of Displacement Method. Ground reaction can be estimated by entering the Curves of Form or Hydrostatic Table with the drafts before and after grounding and reading the displacements for the two conditions. Then:

$$R = \Delta_b - \Delta_g \tag{4.3}$$

where,

R = ground reaction

Δ_b = displacement immediately before stranding

Δ_g = displacement after stranding

If the stranded ship is trimmed, a correction to displacement for trim must be made.

3) Change of Draft Forward Method. This method considers the ground reaction as equivalent to a weight removal that causes both parallel rise and change of trim. It is calculated using the following equations as shown in Figure 4.3:

Change of draft forward = change from parallel rise + change forward from trim

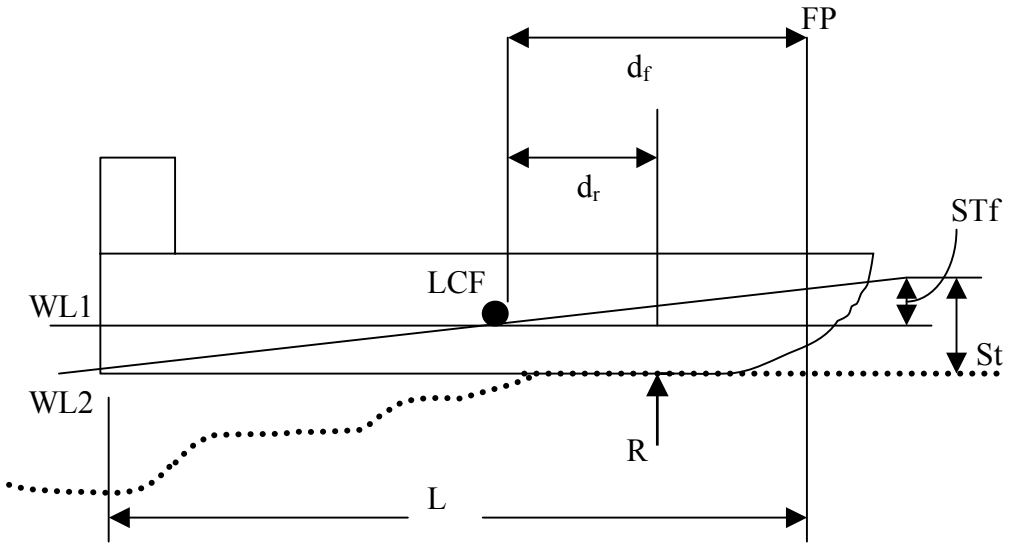

Figure 4.3 Definitions of distances

$$\Delta T_{parallel\ rise} = \frac{R}{TPI}$$

$$\Delta t = \frac{Rd_r}{MT1}, \quad \Delta T_{forward,\,trim} = \frac{d_f}{L}\Delta t$$

$$\Delta T_f = \frac{R}{TPI} + \left[\left(\frac{Rd_r}{MT1}\right)\times\left(\frac{d_f}{L}\right)\right]$$

$$= \frac{R}{TPI} + \frac{R(d_r)(d_f)}{MT1(L)} \tag{4.4}$$

$$\frac{R(L)(MT1) + R(d_r)(d_f)(TPI)}{TPI(MT1)(L)} = \frac{R\left[(L)(MT1) + (d_r)(d_f))TPI)\right]}{TPI(MT1)(L)}$$

$$R = \frac{\Delta T_f(TPI)(MT1)(L)}{(L)(MT1) + (d_r)(d_f)(TPI)}$$

where,

Δt = total change of trim, in.
ΔT_f = change of draft forward = $T_{fb} - T_{fa}$
d_f = distance from the center of flotation to the forward perpendicular
d_r = distance from the center of flotation to the center of ground reaction
R = ground reaction, tons
$MT1$ = moment to trim one inch
TPI = tons per inch immersion

The basic relationship can also be solved for d_r:

$$d_r = \frac{1}{TPI(d_f)} \times \left[\frac{\Delta T_f (MT1)(TPI)L}{R} - L(MT1) \right] \tag{4.5}$$

4) Tons per Inch Immersion Method. An estimate of the ground reaction can be made by multiplying the change in mean draft on stranding by the tons per inch immersion (TPI):

$$R = (T_{mbs} - T_{mas})TPI \tag{4.6}$$

where,

T_{mbs} = mean draft before stranding
T_{mas} = mean draft after stranding

This method only considers the bodily rise of the ship and is a good estimate if the trim has not been changed greatly by the stranding. The mean draft for trim can be corrected if the stranding causes a significant change of trim.

5) Change of Trim Method. Best used when the total trim exceeds one percent of the ship's length, the center of pressure of the ground reaction is known or can be estimated with reasonable accuracy, and change of trim is the dominant effect of stranding. Ground reaction is treated as a force that causes only a change of trim by the equation below:

$$R = \frac{MT1(\Delta t)}{d_r} \tag{4.7}$$

where,

Δt = total change of trim, inches

Tides can change the static condition of the stranded ship. The waterline of a stranded ship rises and falls with the tide. When the tide is highest, the buoyancy of the ship is greatest, and the ground reaction is decreased by the amount of buoyancy regained. When the tide falls, buoyancy decreases and ground reaction increases. For a ship that cannot trim, the change in ground reaction caused by the tide is nearly equal to the change in height of the tide multiplied by TPI. For a ship that can trim with tide changes, the change in ground reaction can be estimated by relating the change in ground reaction to the change in draft at the LCF. For a change of trim, draft is constant at the center of ground reaction. The change of draft at the LCF from trim is found using Equation (4.8):

$$\Delta T_{LCF,trim} = \Delta t(\frac{d_r}{L}) \tag{4.8}$$

where:

Δt = change of trim, in.
d_r = distance from the center of ground reaction, or assumed pivot point, to the center of flotation
L = length between perpendiculars

The total change in draft at the LCF is the sum of the changes caused by trim and the rise or fall of the tide. The change in draft because of tide is simply the change in tide height. The two changes are opposed; a falling tide tends to decrease draft, but the rotation of the ship about the pivot point tends to increase draft at the LCF. A rising tide has the opposite effect. The total change in draft at the LCF is found by the following equation:

$$\Delta T_{LCF} = \Delta h - \left(\frac{d_r}{L} \right) \tag{4.9}$$

where,

Δh = tide change, in.

The change in ground reaction is estimated by multiplying the change in draft at the LCF by TPI as shown below:

$$\Delta R = \left[\Delta h - \Delta t \left(\frac{d_r}{L} \right) \right] TPI = \Delta h \left(TPI \right) - \Delta t \left(\frac{d_r}{L} \right) TPI \tag{4.10}$$

If the change of trim, Δt, is expressed as $\Delta R d_r/MT1$, then the following equations can be used:

$$\Delta R = \Delta h(TPI) - \left(\frac{d_r}{L}\right) TPI \left(\frac{\Delta R d_r}{MT1}\right)$$

$$\Delta h(TPI) = \Delta R + \frac{d_r^2 (TPI) \Delta R}{L(MT1)} = \Delta R \left(1 + \frac{d_r^2 (TPI)}{L(MT1)}\right)$$

$$\Delta R = \frac{\Delta h(TPI)}{\left(1 + \frac{d_r^2 (TPI)}{L(MT1)}\right)} = \frac{\Delta h(TPI)}{\left(\frac{(d_r^2)(TPI) + (L)(MT1)}{L(MT1)}\right)} \qquad (4.11)$$

$$\Delta R = \frac{\Delta h(TPI)(L)(MT1)}{(d_r^2)(TPI) + (L)(MT1)}$$

Using the above equations with Δt expressed as $\Delta R d_r/MT1$, assumes that the ship is trimming about its center of flotation, which it is not. This assumption introduces errors into the ground reaction predictions for different heights of tide.

The center of ground reaction, if the ship is aground over only one segment of its length, can be found by summing moments about a convenient point, for example the LCG. This calculation is shown below (referring to Figure 4.4):

$$Bd_1 = Rd_2 \implies d_2 = Bd_1/R \qquad (4.12)$$

where,

d_1 = distance from LCB to LCG

d_2 = distance from LCG to the center of ground reaction

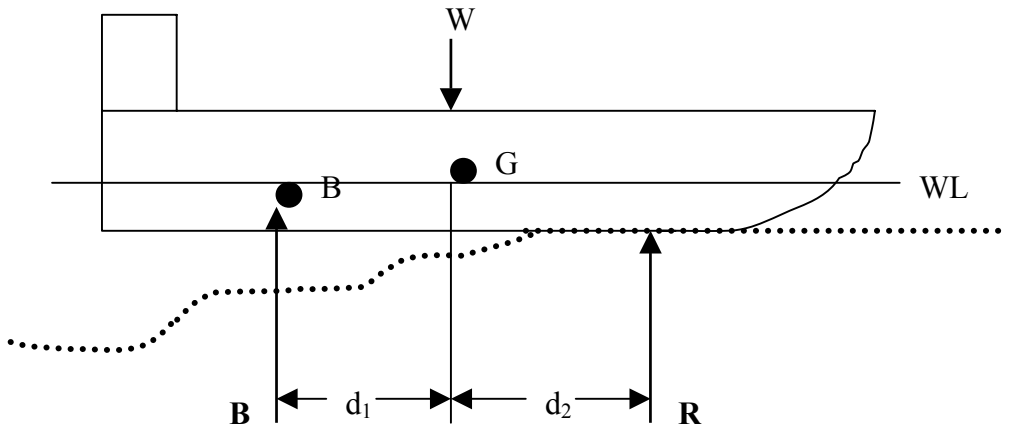

Figure 4.4 Forces on a stranded ship

The centers of gravity and buoyancy are in a vertical line in a floating ship so the LCG can be determined from the pre-stranding LCB adjusted for flooding. The LCB can be determined from the hydrostatic curves of form or tables if the prestranding drafts are known. If the ship was trimmed before grounding, the LCB from even keel hydrostatic data must be corrected by the following equation:

$$BB_1 = BM_L(t)/L \tag{4.13}$$

where:

BB1 = movement of LCB because of trim

BML = longitudinal metacentric radius

t = trim

L = length between perpendiculars

The grounded LCB can be found from the sectional area curve or taken from hydrostatic data for the grounded drafts and corrected for trim. If hydrostatic data are not available, but LCF and MT1 can be estimated, the center of ground reaction can be

estimated by assuming that the ship trims about the LCF, and then use Equation (4.12) where:

d_1 = distance from LCF to the center of ground reaction

d_2 = distance from LCB to LCF

Waves also affect the initial orientation of a stranded ship. Waves move buoyant or partially buoyant objects with their cumulative effects. Near the crest, the buoyancy of a stranded ship is increased and the ground reaction is reduced. Ground reaction distribution and location of the center of pressure are changed; the levering action of the ship disrupts suction and may reduce friction. A stranded ship just inside the breaker line will be battered by short-period water waves. A grounded ship outside the breaker line is exposed to long-period swells and commensurately greater variations in buoyancy over a greater percentage of its length. Wave lengths nearly equal to the ship's length can cause severe hogging or sagging loads.

The grounding of a ship effects its center of gravity. Ground reaction is equivalent to removing an equal weight from the keel, and causes a virtual rise in the center of gravity similar to that caused by the block reaction on a ship in drydock. The following equations calculate the new center of gravity:

$$GG_1 = \frac{R(KG)}{(W - R)} \tag{4.14}$$

The effective height of the grounded ship center of gravity is calculated directly by the following equation:

$$KG_1 = \frac{(KG)(W)}{(W - R)} \tag{4.15}$$

where:

GG_1 = virtual rise of the center of gravity
KG_1 = effective height of the center of gravity when the ship is aground
KG = original height of the center of gravity above the keel
W = weight of the ship
R = ground reaction

The metacentric height, KM, is also affected by grounding. KM for a stranded ship is related to the residual buoyancy of the ship, and can be found from the Curves of Form with poststranding drafts. With a large range of tide, the movement of the metacenter is significant and large negative metacentric heights may develop, Equation (4.16). A stranded ship with a negative metacentric height will tend to list. A stranding off centerline, so that the center of ground reaction is off the centerline, will experience both a loss of displacement and an upsetting moment. If free to incline, the ship will assume a list.

$$GM = KM - KG = KB + BM - KG \tag{4.16}$$

Static loads are based on buoyancy (hull offsets) and weight distribution. The buoyancy distribution is based on hull offsets for all strength calculations. For the stranded ship, the distributed ground reaction is added to buoyancy as an upward force.

The weight distribution is constructed by adding the weight distribution for a specific salvage case to the lightship weight. Shear force and bending moment are changed. The relative magnitude and distribution of ground reaction and buoyancy also vary with the tide and passage of swells. The expression for maximum bending moment for a simply supported beam under uniform load (M = WL/8) can be modified by empirically derived factors [8] to give a first estimate of maximum bending moment for stranded ships on pinnacles as shown in Figure 4.5:

$$M_{\max} = \frac{Rl}{k} \tag{4.17}$$

where,

$M_{\max}$ = maximum bending moment, [length - force]
R = ground reaction [force]
l = length of span = length between perpendiculars or distance between pinnacles [length]
k = factor to account for nonuniformity of force distribution
= 6 for stranded ship supported at both ends
= 7 for stranded ship supported near midships

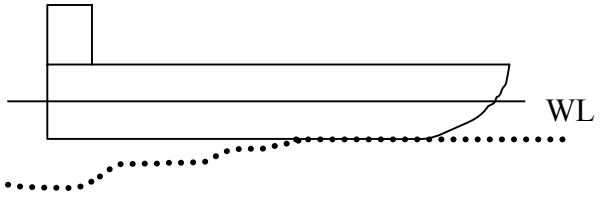

(a) One end aground, other end in deep water

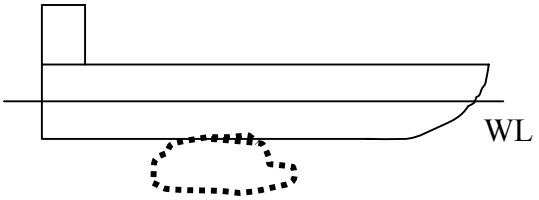

(b) Aground amidships, no support under bow and stern

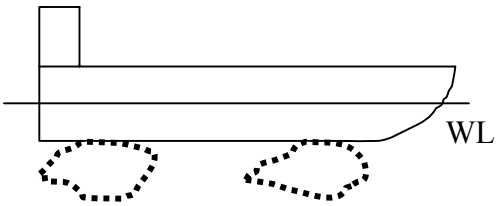

(c) Aground at ends, no support amidships

Figure 4.5 High Bending Moment Strandings

The wave-induced bending moment for stranded ships is not as certain as it is for floating ships. The sum of buoyancy and ground reaction must equal the ship's weight, but the relative proportions change as waves pass along the hull. Large hull deflections indicate high bending moments. A hog or sag greater than 0.001LBP is potentially dangerous. Dynamic effects also become important and must be determined simultaneously in a solution for grounded ship motions.

Hull form characteristics, the forward and aft grounding extreme locations, the water depth at the forward and aft grounding extremes, and the varying tidal heights are used to calculate the bending moments for free floating and stranded cases. The new grounded drafts are used to generate grounded hull form data including local beam, draft and sectional area at station locations. This data also considers grounded trim and are used in the Lewis form strip theory solution.

This thesis uses the static grounded condition as input to the dynamic Stranded Ship Motions & Loads Program with the dynamic soil model. It is calculated based on the above methods and equations using HECSALV. HECSALV is a commercial program that is used in the salvage industry (The U.S. Navy salvage community uses the same program called POSSE).

Chapter 5-Stranded Ship Motions & Loads Program (SSMLP)

The Stranded Ship Motions & Loads Program (SSMLP) calculates the forces and moments on a grounded ship. The preliminary version of this program used for this thesis is written in FORTRAN and solves a two-degree of freedom system for heave and pitch motions. It considers the dynamic effects of regular waves plus the dynamic effects of the soil reaction. It is adapted from a Ship Motions Program by Loukakis [35]. The final version of the program will solve the full six degree of freedom problem. The program requires the following input:

- A description of the immersed grounded hull form by section. This includes local beam, draft and sectional area for a number of stations.
- A complete weight curve including the upward ground reaction.

The program output includes:

- Calm water shear forces and bending moments
- Shear forces and bending moments for the free-floating ship in waves.
- Shear forces and bending moments for the grounded ship in waves.
- Heave and pitch response amplitude operators and phase plots for the grounded ship in waves.

The program uses English units, lb_f, ft, sec. For input-output only:

- angles are in degrees
- frequency is in radians per second
- weight, weight/foot, shearing forces and bending moments are in tons, tons/foot, tons and foot-tons respectively. If the length between perpendiculars is less than 50 feet, the units are pounds, pound/foot, pounds, and foot-pounds respectively.

SSMLP may use Simpson's Rule or the Trapezoidal Rule for integration. These integration methods are performed in subroutines SIMPUN and TRAPIN respectively.

Figure 5.1 is the flowchart for the program. It starts with MAIN calling INPUT and then MAIN calls the subroutines clockwise around the diagram. MAIN contains the body of the program with all the necessary bookkeeping functions.

INPUT reads in the input data, calculates the block coefficient C_B and the LCB, and compares the calculated values with input principal characteristics. These calculations are performed using the function SIMPUN for unequally spaced Simpson's rule integrations. The longitudinal center of gravity LCG and the radius of gyration are calculated from the input weight curve.

BENDSH1 calculates calm water bending moments and shear forces using the weight and buoyancy distributions, Equations (3.133) and (3.134). It also calculates coefficients for the subsequent calculation of wave shearing forces and bending moments in subroutine BENDSH2. The coefficients V1I(I), V2I(I), BM1I(I) and BM2I(I) are calculated for use in BENDSH2. They represent properties of the weight curve, which together with the motions along the hull, are used for the calculation of the dynamic part of the loads in waves.

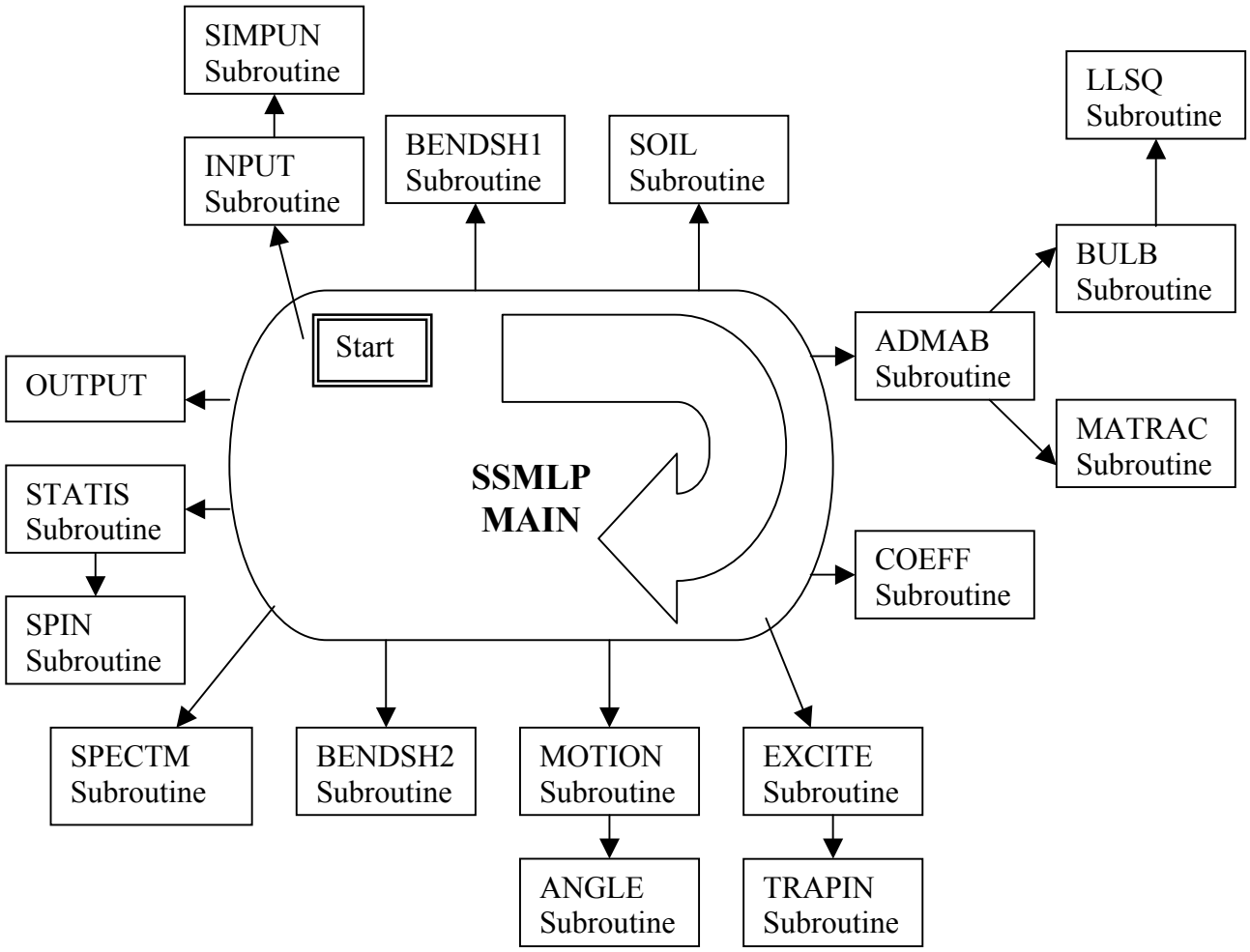

Figure 5.1 Program Flowchart

BENDSH1 also calculates the weight of the hull, the LCG and the radius of gyration based on the weight curve. If the results for weight and LCB are not within specified tolerances (0.1% for the weight and 0.01% of LBP for the LCG) from the input values, the calculation is terminated. This is done to avoid large errors for the calm water results and smaller errors for results in waves.

The SOIL subroutine calculates the dynamic stiffnesses for the soil reaction. These calculations are based on Equations (2.38-2.43). The soil model requires that the length of the embedded section be greater than the embedded beam section. If this is not the

case, the subroutine switches L and B, and calculates the dynamic stiffness value for pitch using the roll equation. Figure 5.2 shows the location of the soil reaction force within the grounded length. Since all forces and moments acting on the ship are calculated about the origin of the body-fixed reference frame - midships, the subroutine transfers the soil reaction force to midships as is shown in Figure 5.2.

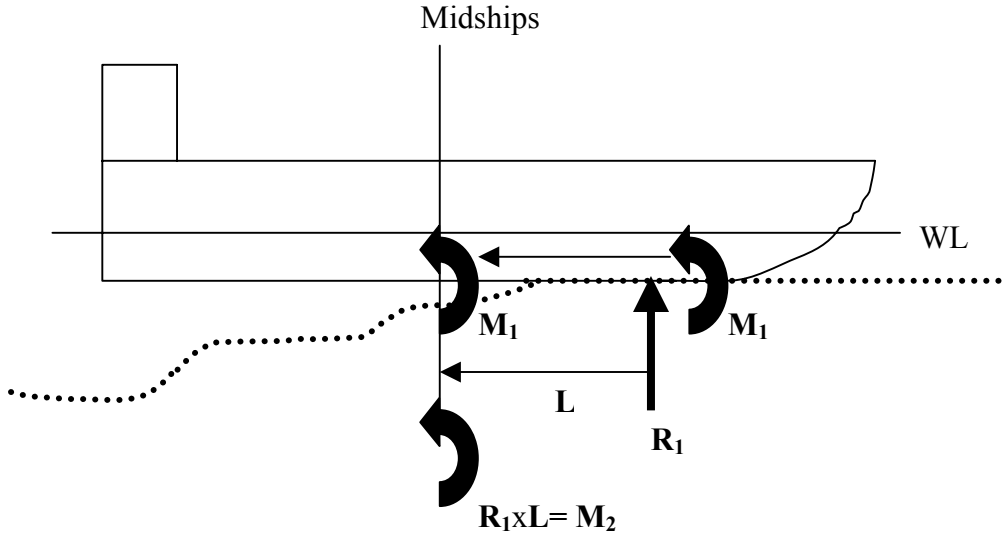

Total Soil Reaction at midships = $M_1 + M_2$

Figure 5.2 Transfer of Soil Reaction force and Moment to Amidships

The hydrodynamic problem consists of determining the added mass and damping for a cylinder of infinite length, floating in water of infinite depth and vertically oscillating in small harmonic motion. Viscous contributions are neglected. SSMLP calculates two degree of freedom hydrodynamic coefficients using the Lewis form mapping described in Section 3.7.7. The Lewis form mapping requires only the local sectional properties of beam, draft and area, which are provided in the program input Equation (3.99). The exact shape of the section need not be known using Lewis forms. A sectional area curve, design waterline and a keel line are adequate for the conformal

description of the hull. The calculated sectional added mass and damping are correct even for high frequencies.

The subroutine ADMAB uses the input beam, draft, and section area at each station to generate a Lewis form. The calculations of added mass and damping coefficients for the two dimensional Lewis form sections at a given encounter frequency are performed by the method of Grim [34], and subroutine MATRAC is used to solve the simultaneous equations.

For large bulbous sections the added mass and damping coefficients are calculated in subroutine BULB, which is a new mapping function defined by Equations (3.103) and (3.104) [36]. The subroutine uses LLSQ for the solution of the simultaneous equations.

The subroutine COEFF computes the coefficients for the equations of motion. The terms are calculated by summing up the sectional terms generated in MAIN, ADMAB, SOIL, and BENDSH1.

Subroutine EXCITE calculates the wave-induced and sectional exciting forces and moments using Equations (3.117) and (3.118). The forces and moments are returned in their real and imaginary parts. It calls subroutine TRAPIN to sum the sectional forces and moments.

Subroutine MOTION solves the equations of motion for heave amidships and pitch using Equations (3.128) and (3.129) as described in Section 3.8.2. The motions are returned to the main program as complex numbers in polar form. MOTION calls function ANGLE, which converts radians to degrees.

Subroutine BENDSH2 calculates the dynamic shear forces and bending moments in regular waves using Equation (3.136). If the entire weight distribution along the length

of the hull is given, the shear forces and bending moments are computed at each hydrodynamic station for RMS, H1/3 and H1/10. The results are returned in the form of amplitudes and phase angles for each frequency. The calculations are performed keeping the hydrodynamic and the inertial effects separate until the final addition to determine the amplitudes and phase angles. The calculation of the inertial part of the shearing forces and bending moments is done by using the coefficients calculated in BENDSH1. The hydrodynamic forces are integrated along the hull by a Hermitian integration with first derivative terms.

Regular wave motion and load results are generated for unit amplitude waves at a series of discrete wave frequencies. These results are then used to build RAO values for each response and frequency using Equation (3.137).

These values are applied to the wave energy spectra at each discrete frequency to calculate the response spectra using Equations (3.138) and (3.139). RMS and significant response values are calculated from the response spectra.

The default values for spectral frequencies are determined based on the modal frequency. The 25 default $\omega/\omega p$ values are 0.6 to 2.5 in multiples of 0.1 then 0.84, 0.94, 1.06, 2.75 and 3.0. The wave spectra values are calculated in SPECTM at specified or default frequencies as a function of input significant wave height and modal frequency.

The program can generate a family of two-parameter sea spectra (which includes the fully developed sea spectra recommended by the 11th ITTC and decaying sea spectra) using Equation (3.140). If the modal frequency is not given, the program assumes a fully developed sea using Equation (3.141).

STATIS calculates the response spectrum, spectral moments, broadness factor, and significant response. The function SPIN is used to perform the spectral integrations.

Chapter 6 Results and Conclusions

6.1 Case Study

A simple grounding case study is performed to exercise and troubleshoot the model, generate preliminary results and assess the hypothesis that the moments and loads of a ship grounded in waves is significantly higher than those predicted by static analysis.

The case study analyzes a box barge with dimensions, length=177ft, beam=59ft, draft=9ft, that is grounded with the first 10ft of the bow aground and the center of ground reaction located 5ft from the forward perpendicular, shown in Figure 6.1. Calculations were solved varying soils and depths of embedment.

6.2 Results

Bending moment plots are generated using RAOs obtained from the ship's performance in a regular seaway using the Bretschneider spectra and the 25 frequencies, ω/ω_p, of 0.6 to 2.5 in multiples of 0.1 and then 0.84, 0.94, 1.06, 2.75 and 3.0. SSMLP calculates the response of the ship and dynamic loads placed on the ship. The bending moment plots, which follow, correspond to the ship's response to the calculated significant wave height (H 1/3).

The Response Amplitude Operator (RAO) plots were developed using SSMLP. To obtain RAOs, SSMLP was set up to obtain the response of the grounded ship in regular waves. Given a range of frequencies and a wave amplitude of 1.0 foot, SSMLP calculates the RAO for each given frequency.

Profile View

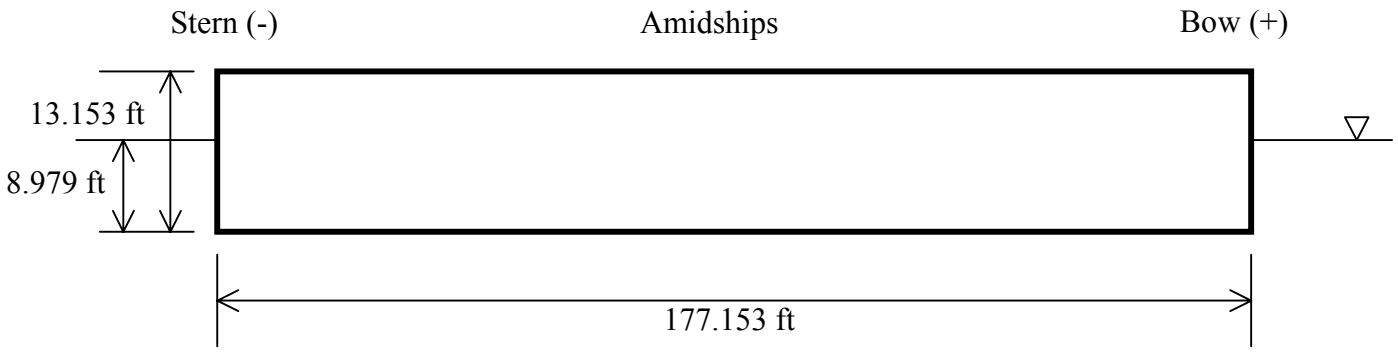

Box barge, free floating, no trim	
Length	177.15 ft
Beam	59.06 ft
Draft	8.98 ft
Displacement	2687 LT

Profile View

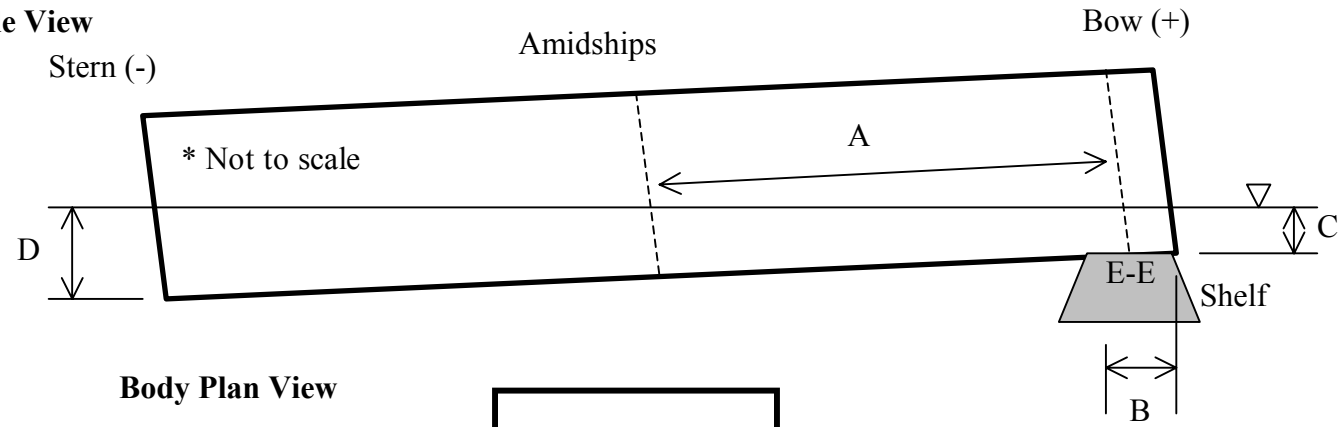

Body Plan View

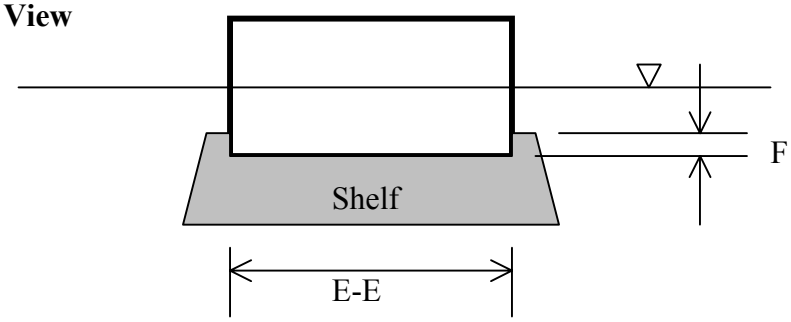

Box barge grounded, trimmed by stern	
A: Distance from Midships to Center of Ground Reaction	83.5 ft
B: Length of embedment	10.0 ft
C: Draft at forward perpendicular	8.45 ft
D: Draft at aft perpendicular	9.28 ft
E-E: Beam of embedded section	59.055 ft
F: Depth of embedment	0 ft - 10 ft
Tons aground (evenly distributed over length B)	45 LT
Soil parameters (see Table 2.1)	various

Figure 6.1 Case Study

6.2.1 Comparison of Bending Moments

The conditions listed in Table 6.1 are analyzed with SSMLP. The bending moments listed are calculated for each soil type listed. The main result is to show that our hypothesis is true, which is that a grounded ship in waves may have significantly higher loads and bending moments than predicted by static analysis. These results also show the difference in bending moments based on the soil type and the effect of embedment depth on each soil type bending moment. Results are also calculated for each soil type at 1ft and 10ft of embedment to compare the effect of embedment.

Table 6.1 Calculated Bending Moments

Soil Types	**Bending Moments**
Sand	Static grounded
Clay	Free floating in waves
Soft Rock	dynamic grounded with embedment depth of 0ft
Hard Rock	dynamic grounded with embedment depth of 10ft

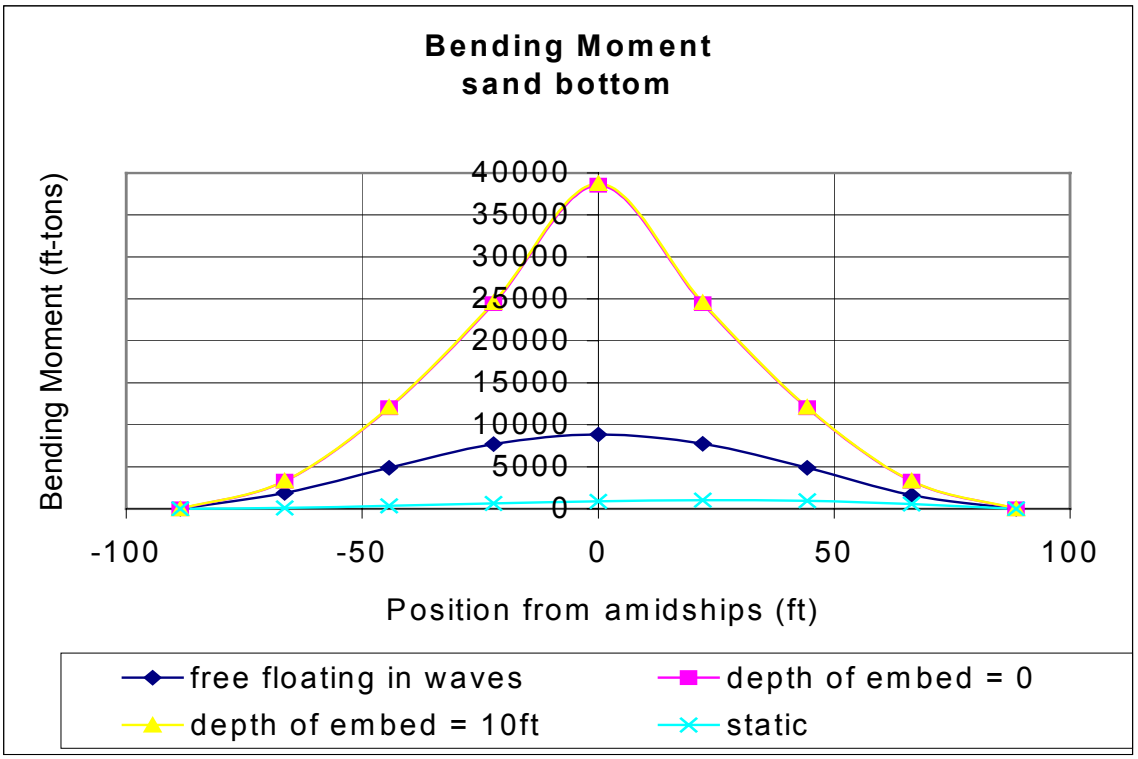

Figure 6.2 Dynamic Bending Moment for free floating in waves and for the static and dynamic Grounded Ship in Sand at embedment depths of 0ft and 10ft

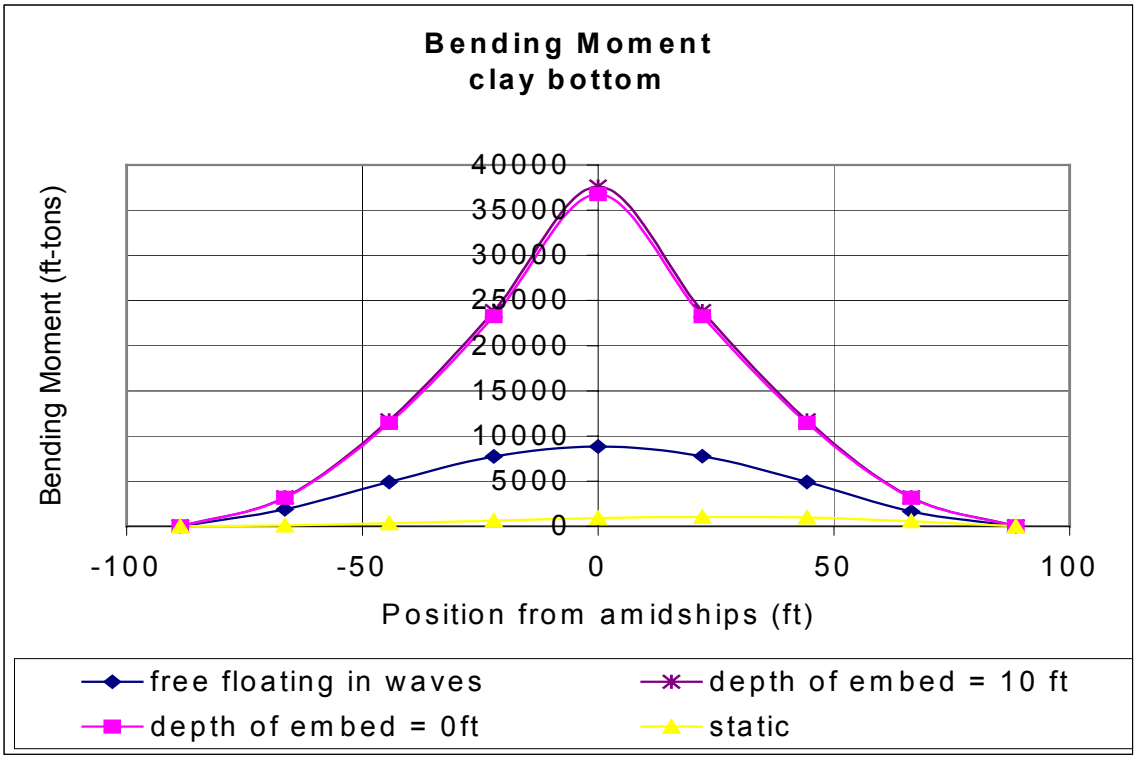

Figure 6.3 Dynamic Bending Moment for free floating in waves and for the static and dynamic Grounded Ship in Clay (Mud) at embedment depths of 0ft and 10ft

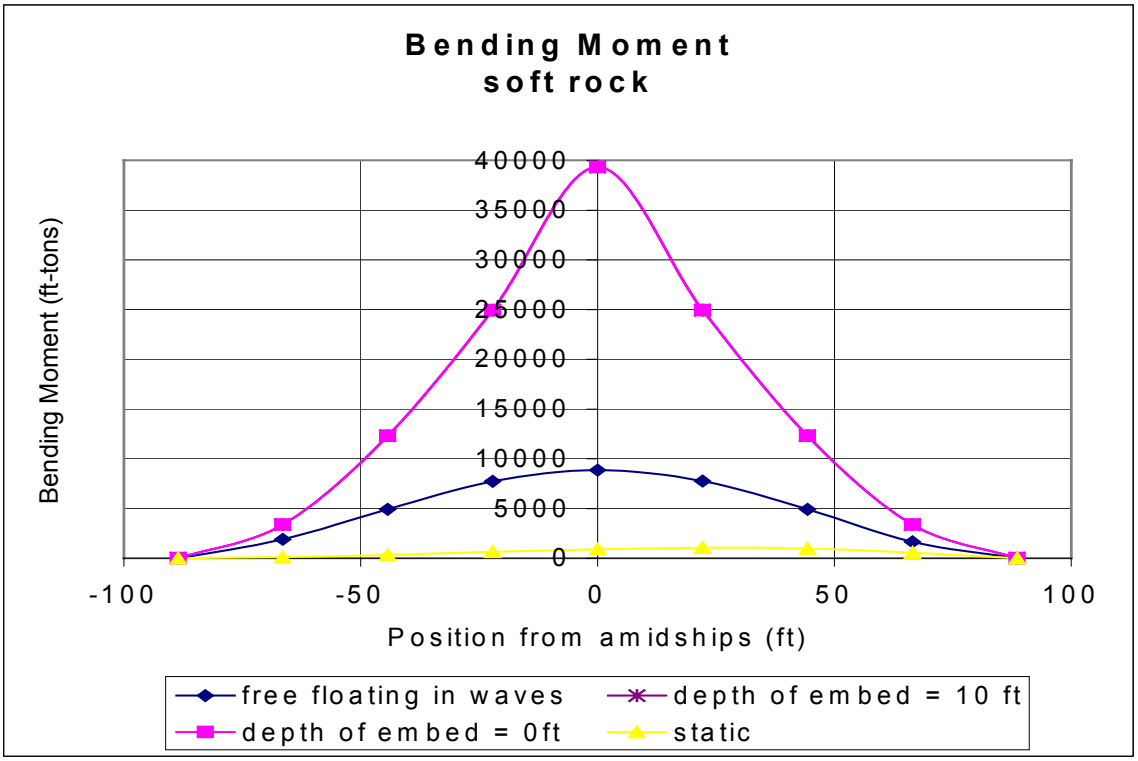

Figure 6.4 Dynamic Bending Moment for free floating in waves and the static and dynamic Grounded Ship in Soft Rock (Coral) at embedment depths of 0ft and 10ft

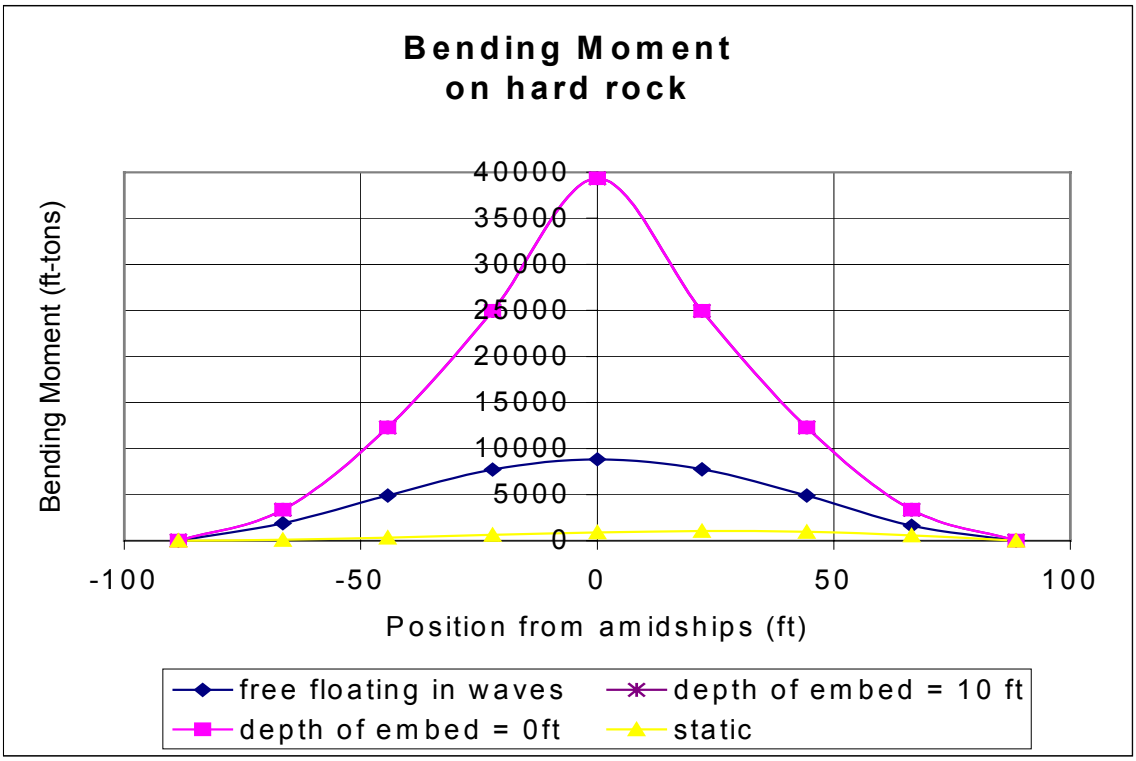

Figure 6.5 Dynamic Bending Moment for free floating in waves and the static and dynamic Grounded Ship in Hard Rock at embedment depths of 0ft and 10ft

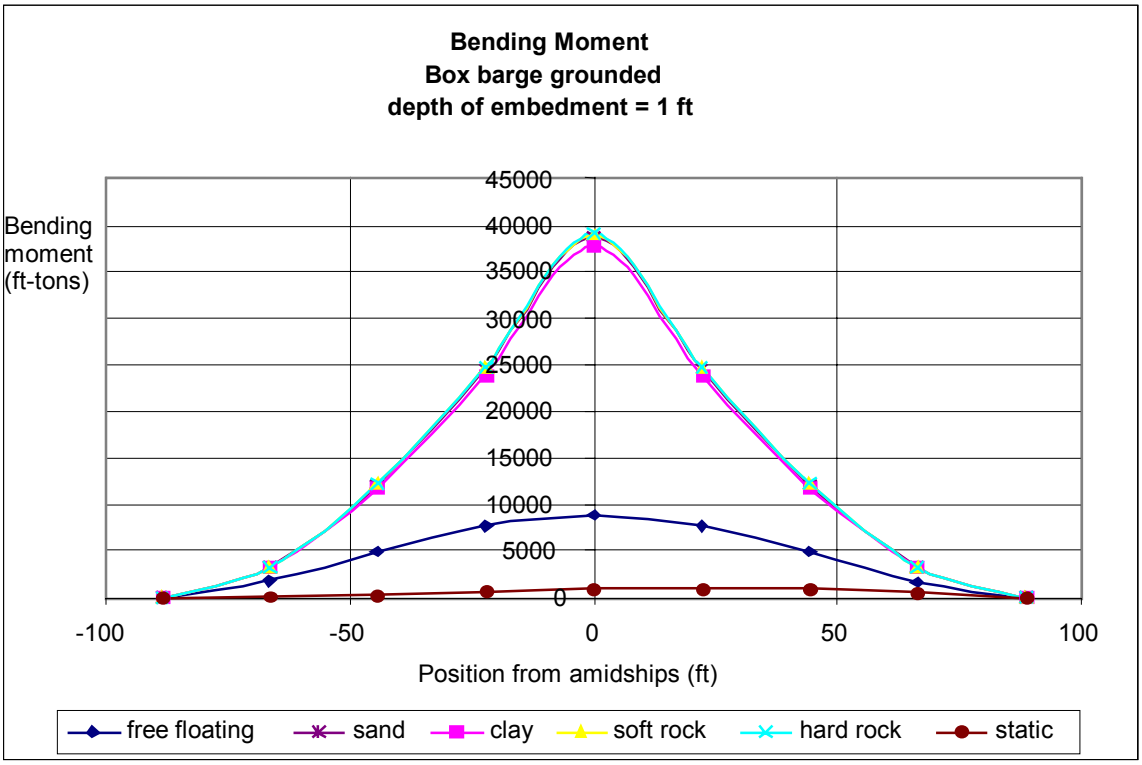

Figure 6.6 Dynamic Bending Moment for free floating in waves and the static and dynamic Grounded Ship in various soils at embedment depth of 1ft

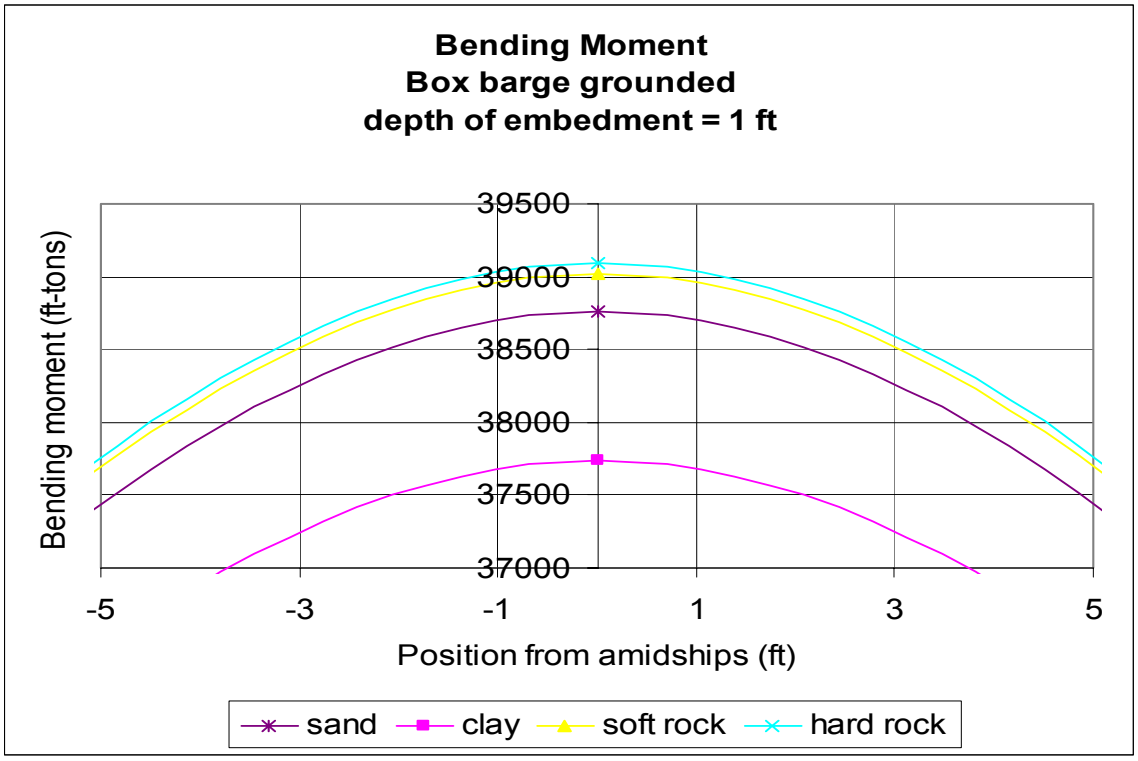

Figure 6.7 Dynamic Bending Moment for the Grounded Ship in various soils at embedment depth of 1ft

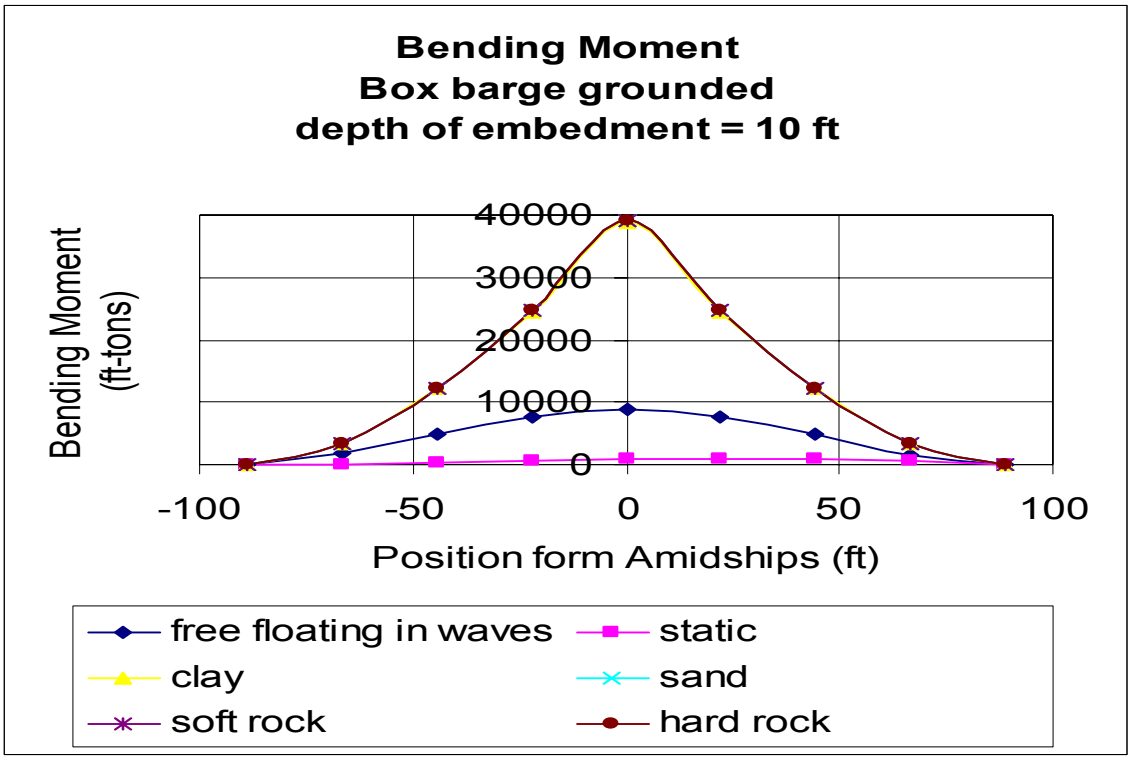

Figure 6.8 Dynamic Bending Moment for free floating in waves and the static and dynamic Grounded Ship in various soils at embedment depth of 10ft

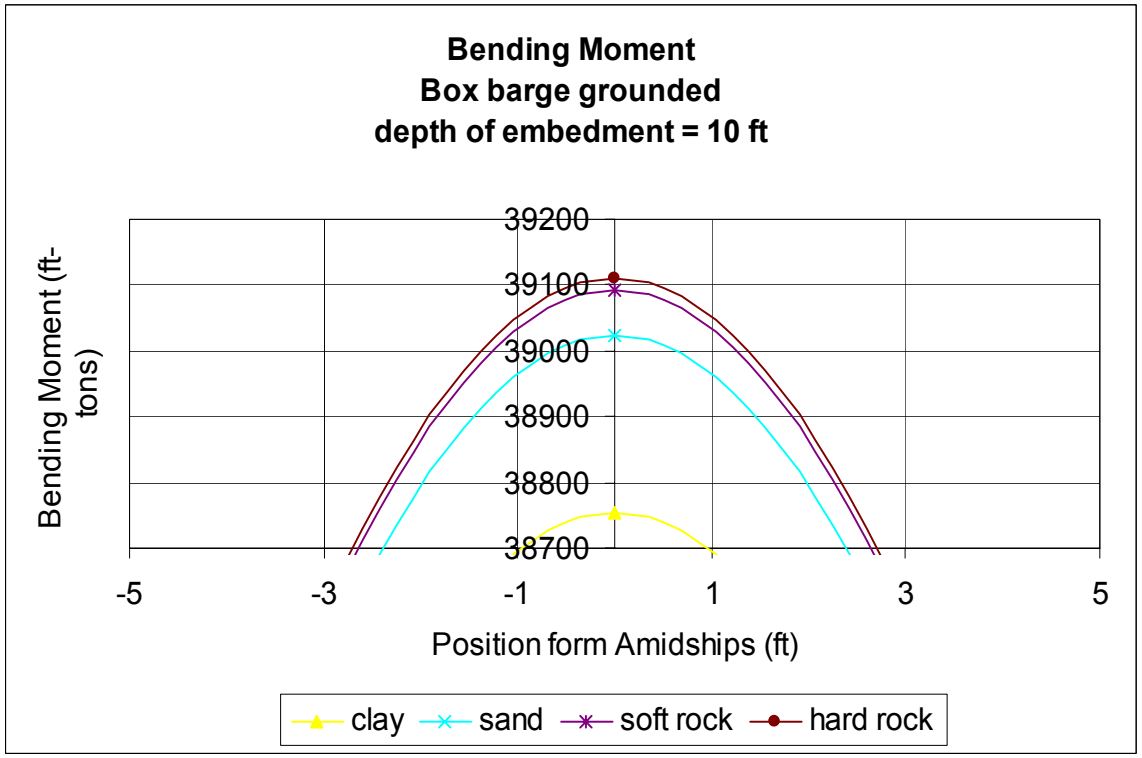

Figure 6.9 Dynamic Bending Moment for the Grounded Ship in various soils at embedment depth of 10ft

6.2.2 Response Amplitude Operators

The heave and pitch response amplitude operators and phase angles are calculated for each soil type for the ship free floating in waves and the ship grounded with embedment depths of 0ft and 10ft. The heave and pitch RAOs are also calculated at embedment depths of 1ft and 10ft for each soil type for comparison.

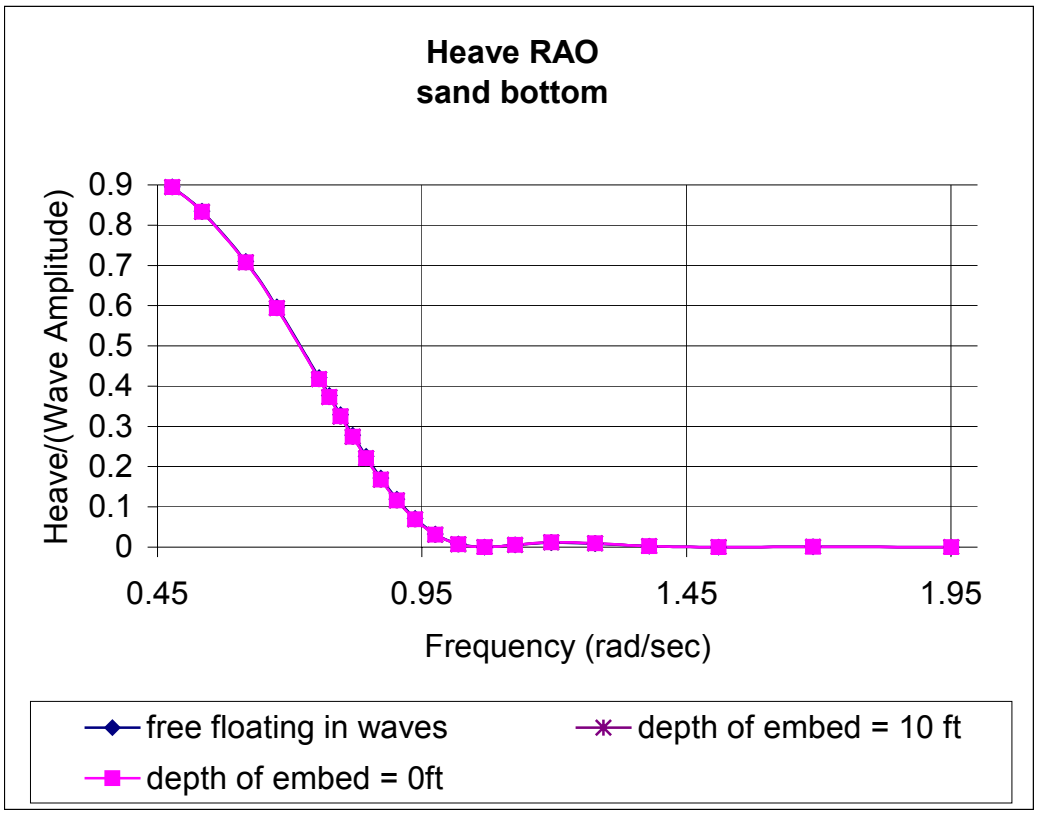

Figure 6.10 Heave RAO for Sand at free floating in waves and the grounded ship with embedment depths of 0ft and 10ft

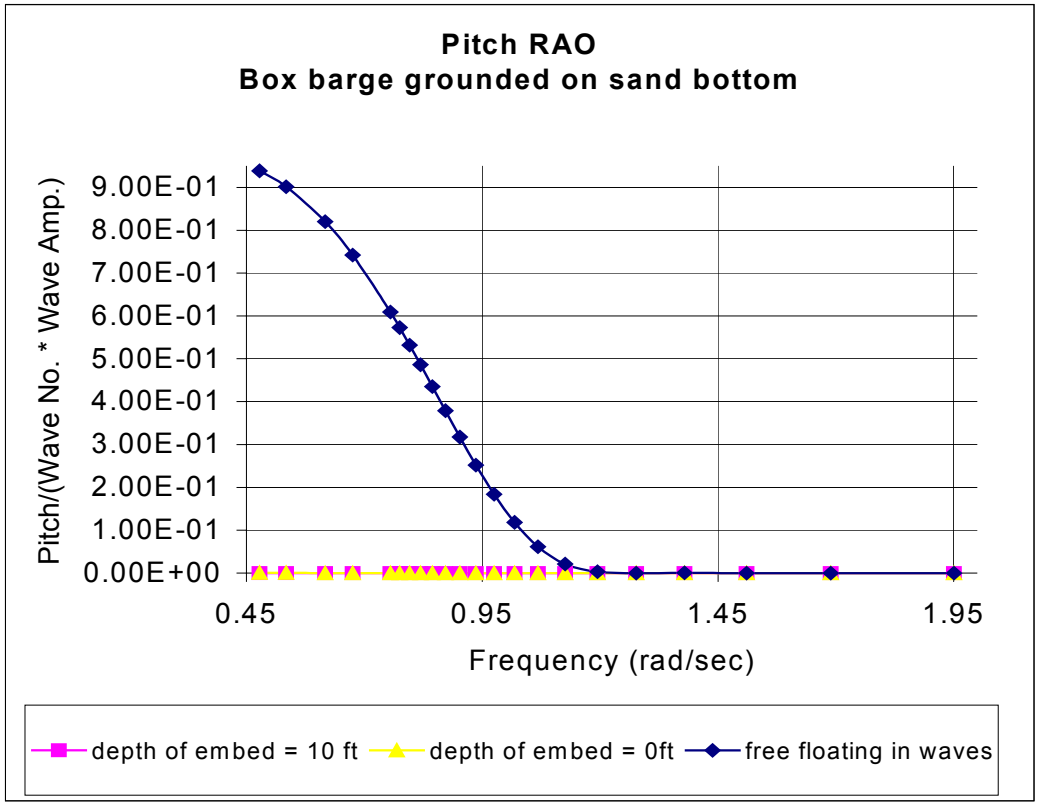

Figure 6.11 Pitch RAO for sand at free floating in waves and embedment depths of 0ft and 10ft

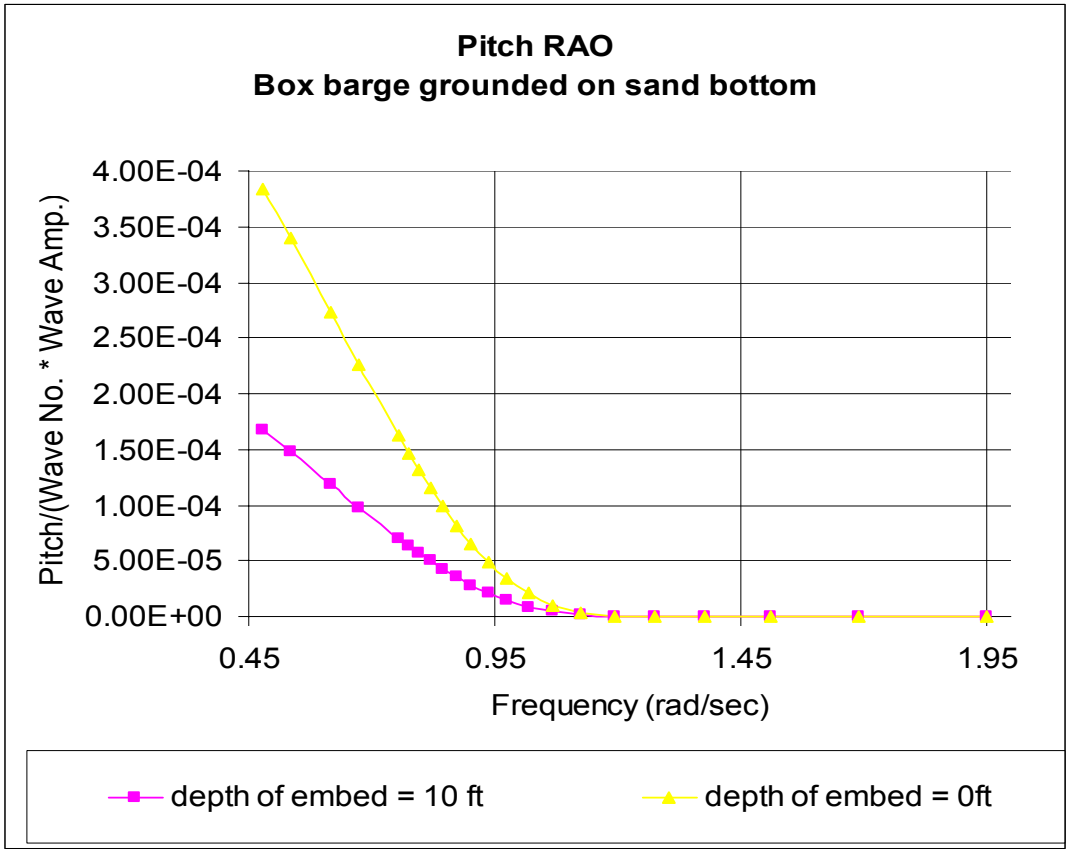

Figure 6.12 Pitch RAO for Sand at embedment depths of 0ft and 10ft

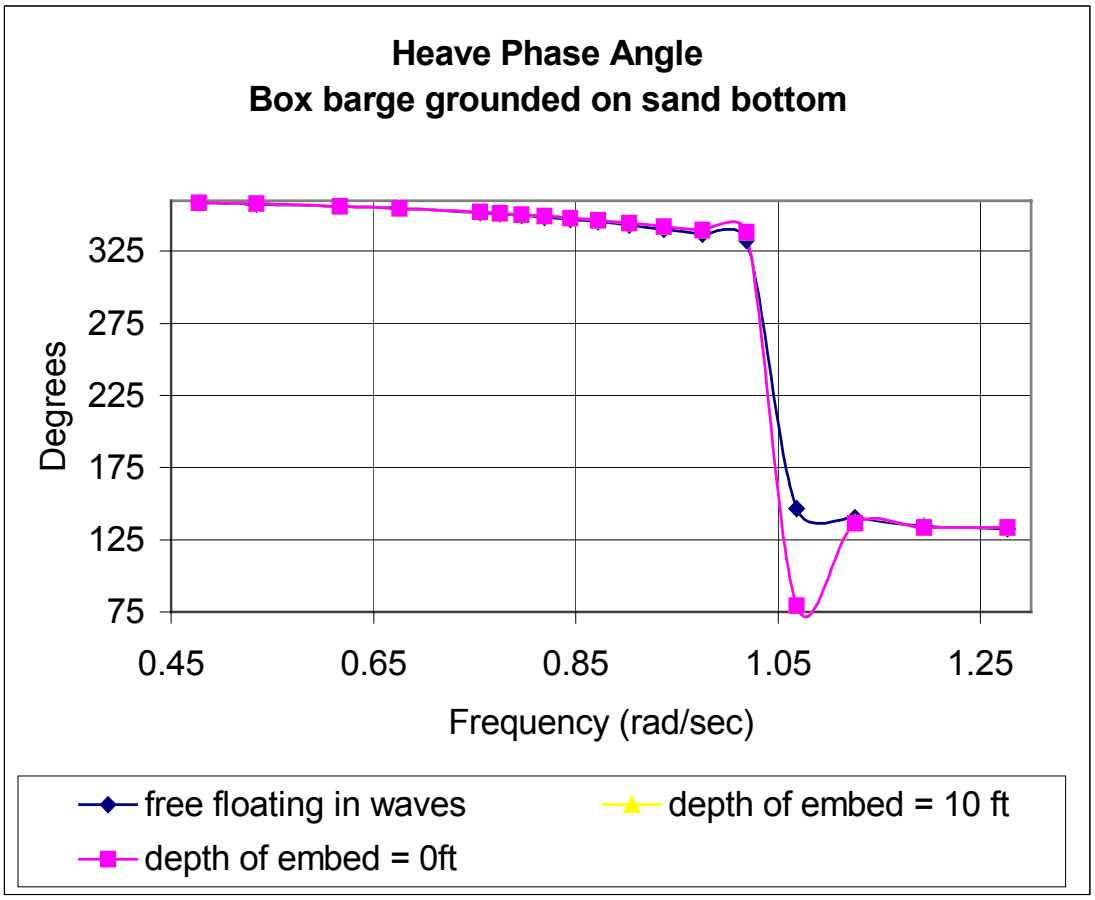

Figure 6.13 Heave Phase Angle for Sand at free floating in waves and at embedment depths of 0ft and 10ft

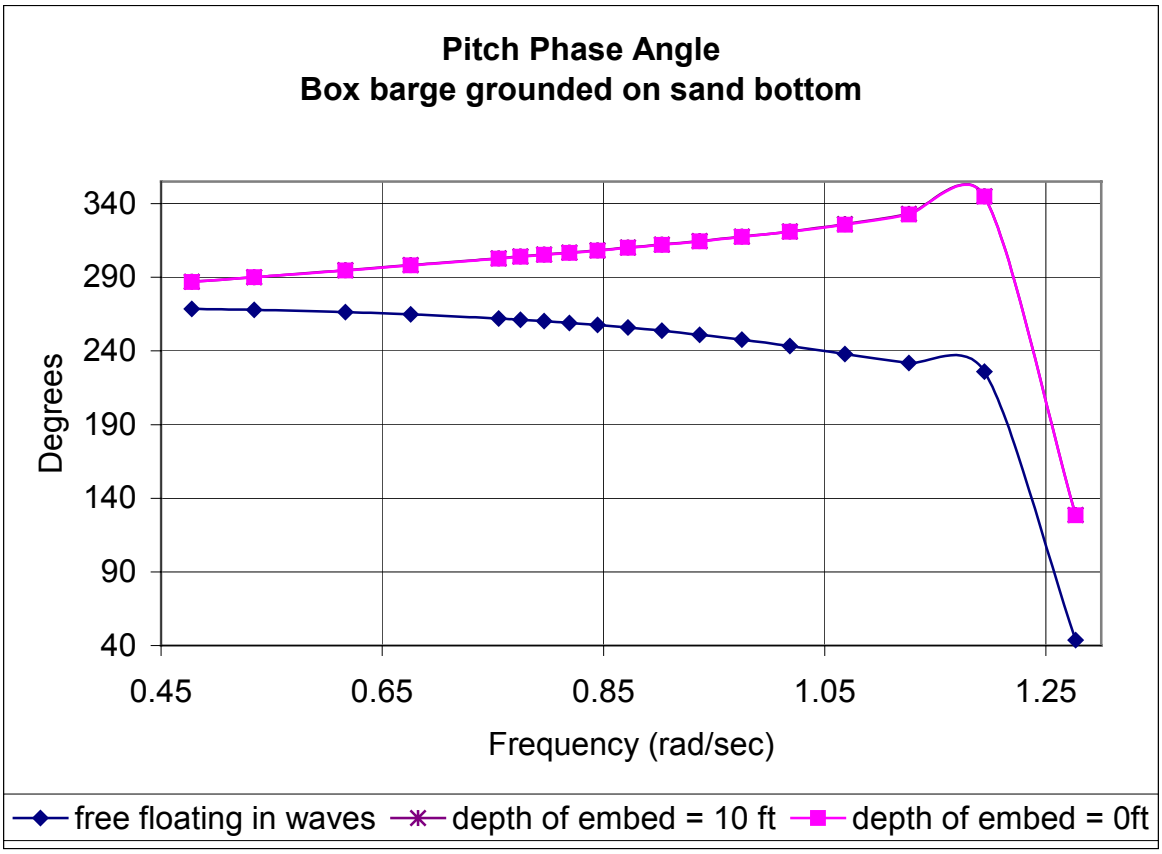

Figure 6.14 Pitch Phase Angle for Sand at free floating in waves and at embedment depths of 0ft and 10ft

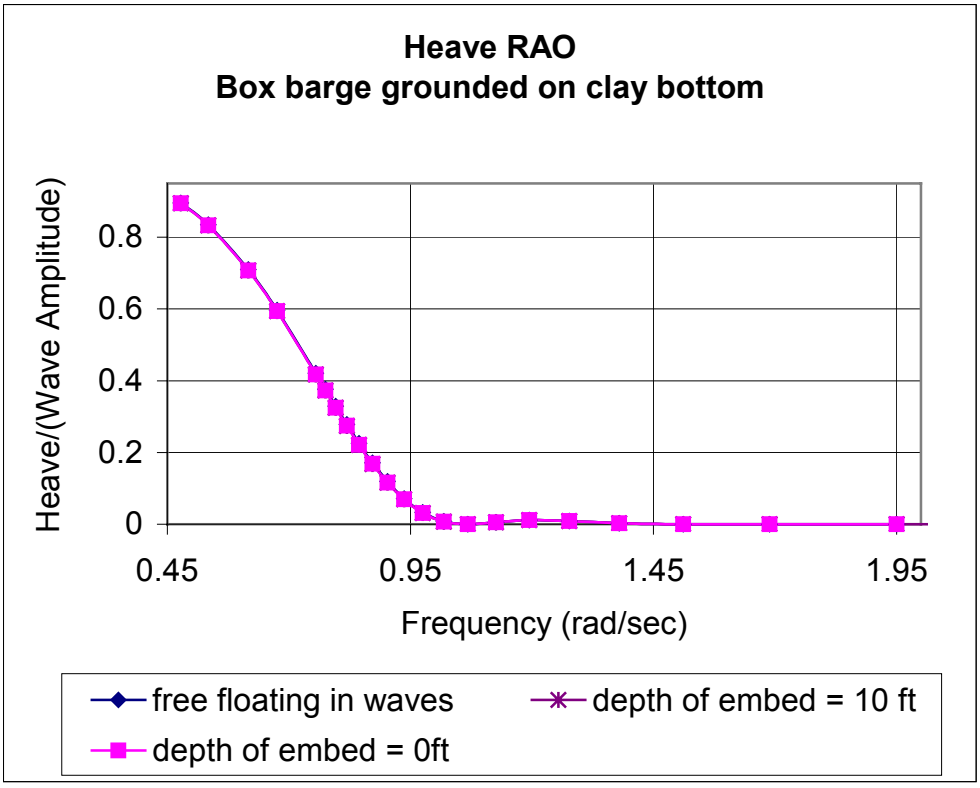

Figure 6.15 Heave RAO for Clay at free floating in waves and the grounded ship with embedment depths of 0ft and 10ft

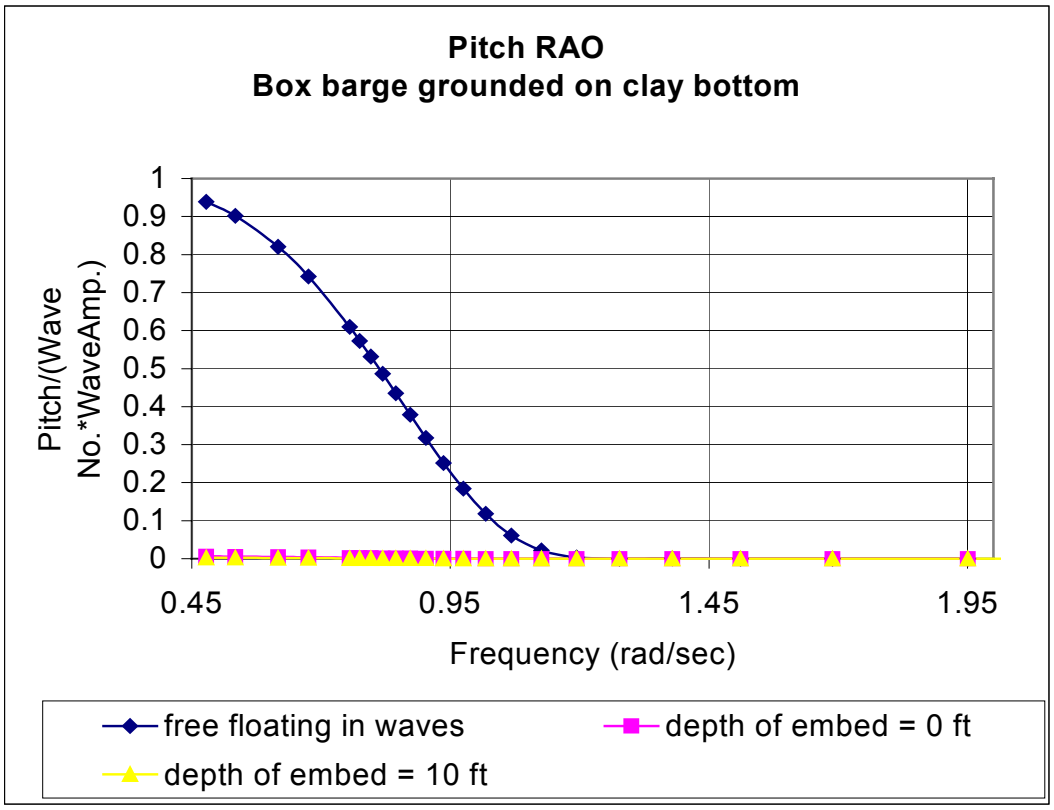

Figure 6.16 Pitch RAO for Clay at free floating in waves and at embedment depths of 0ft and 10ft

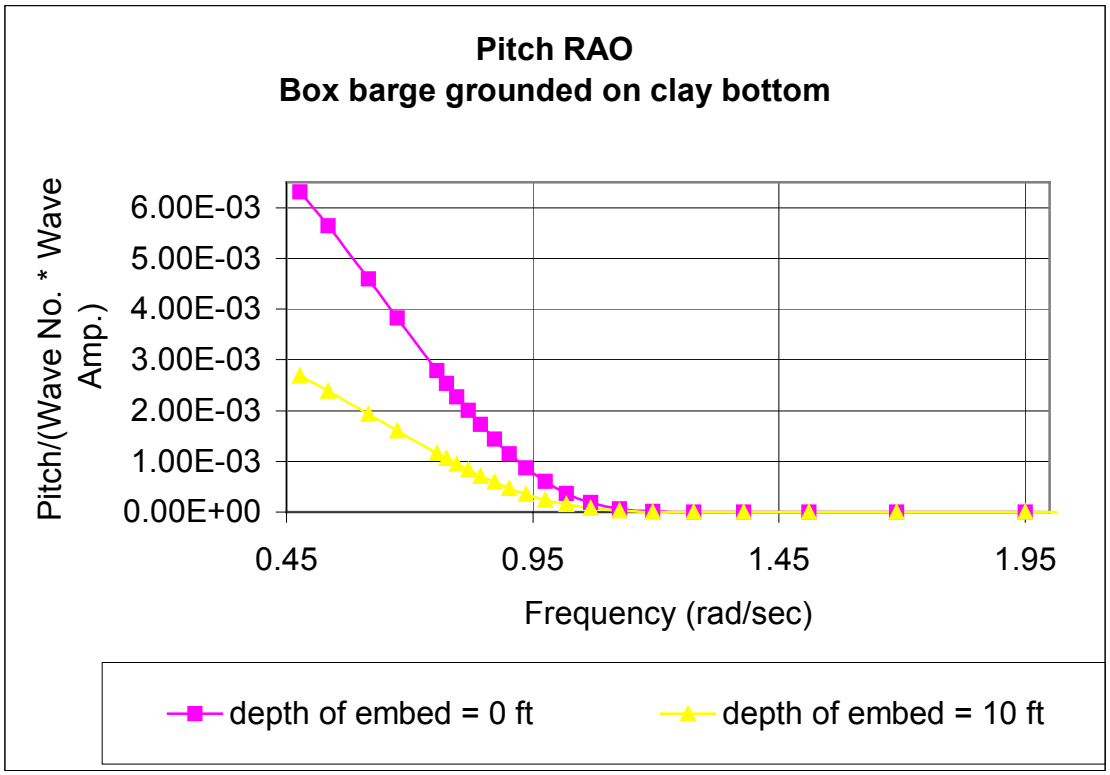

Figure 6.17 Pitch RAO for Clay at embedment depths of 0ft and 10ft

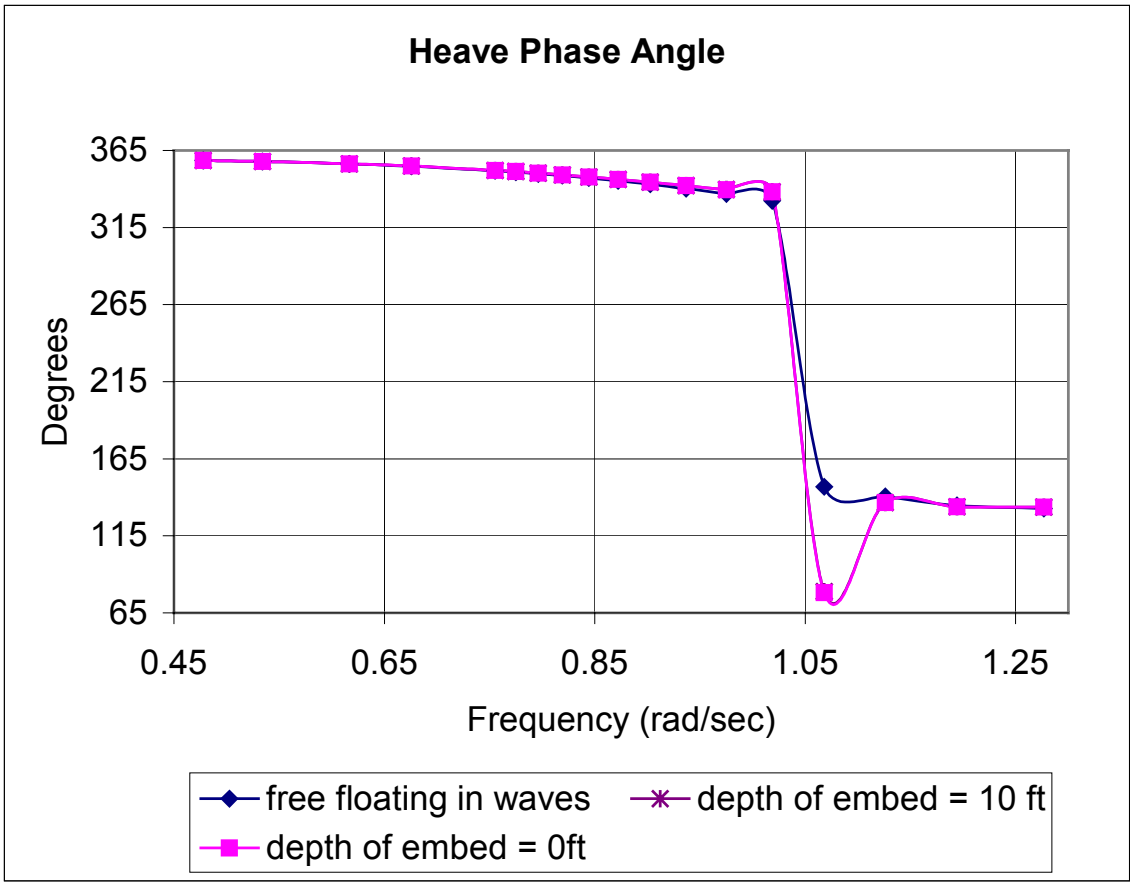

Figure 6.18 Heave Phase Angle for Clay at free floating in waves and embedment depths of 0ft and 10ft

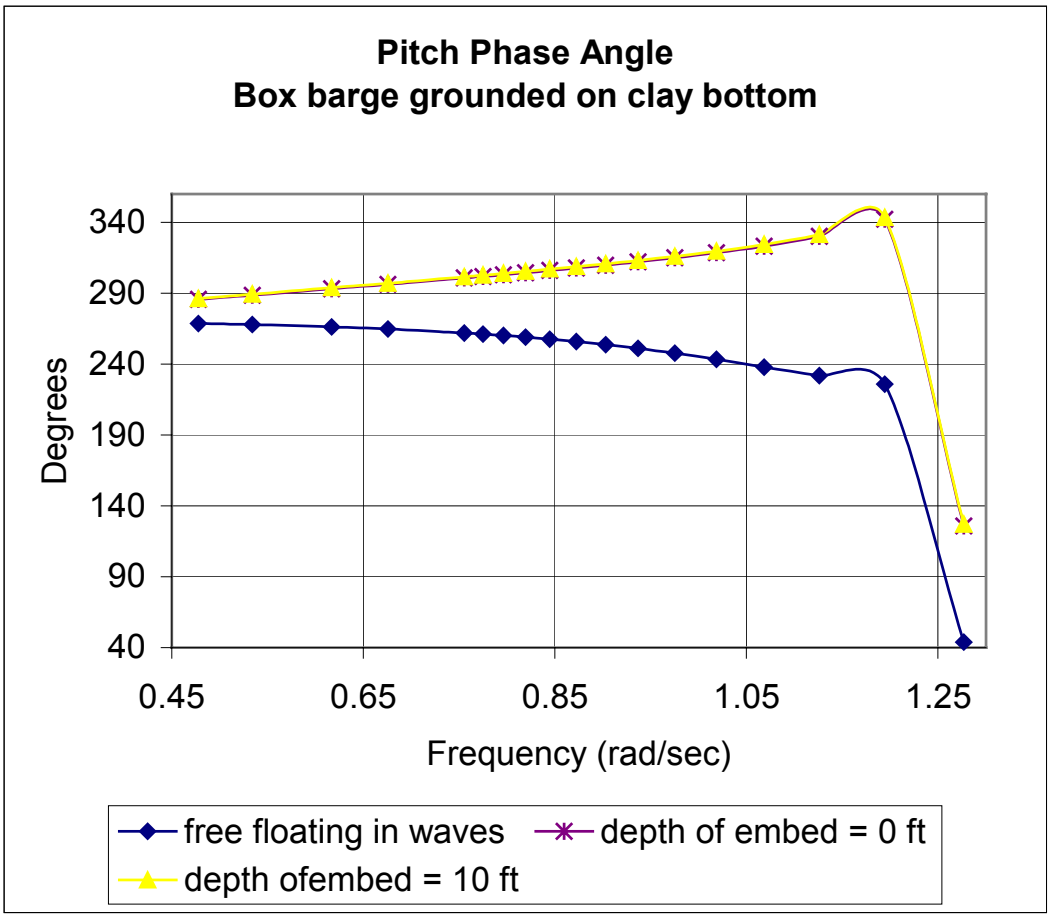

Figure 6.19 Pitch Phase Angle for Clay (Mud) at free floating in waves and embedment depths of 0ft and 10ft

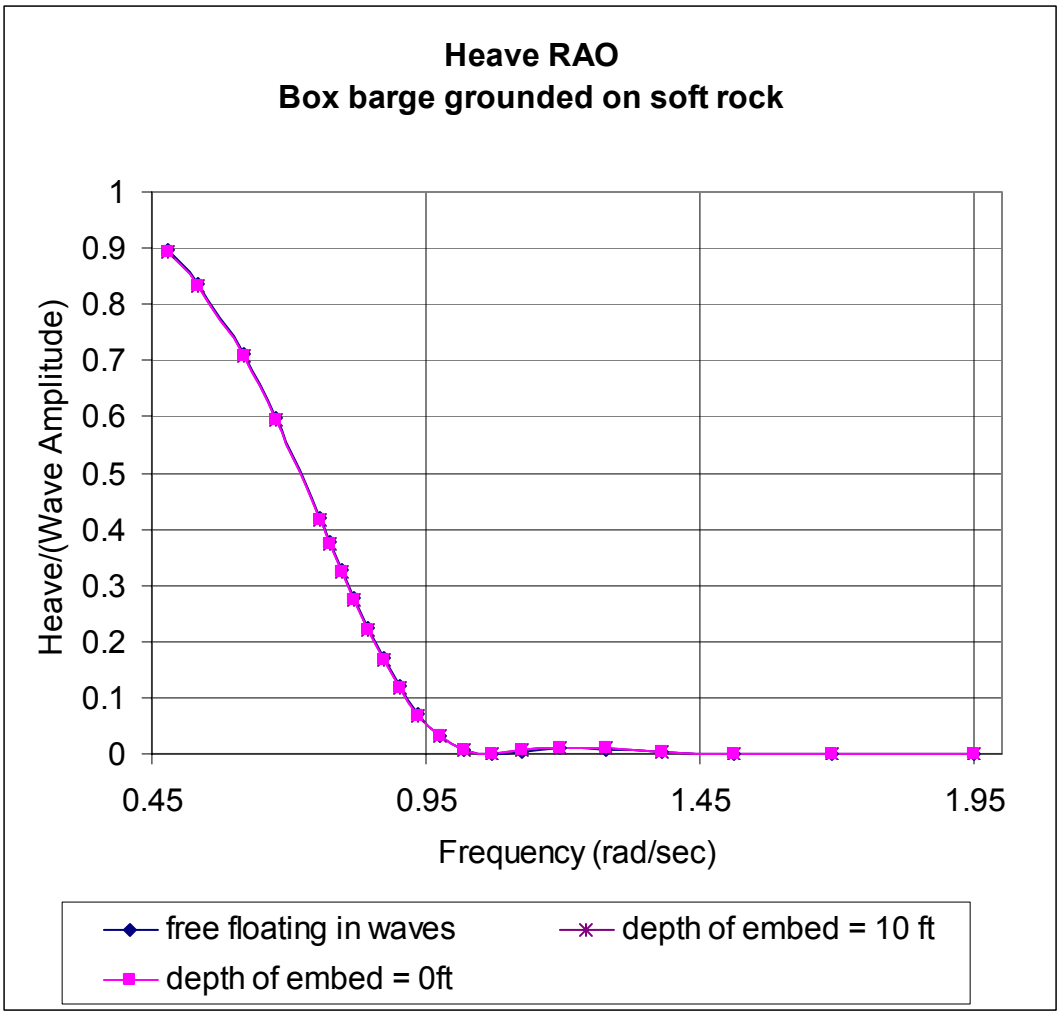

Figure 6.20 Heave RAO for Soft Rock (Coral) at free floating in waves and embedment depths of 0ft and 10ft

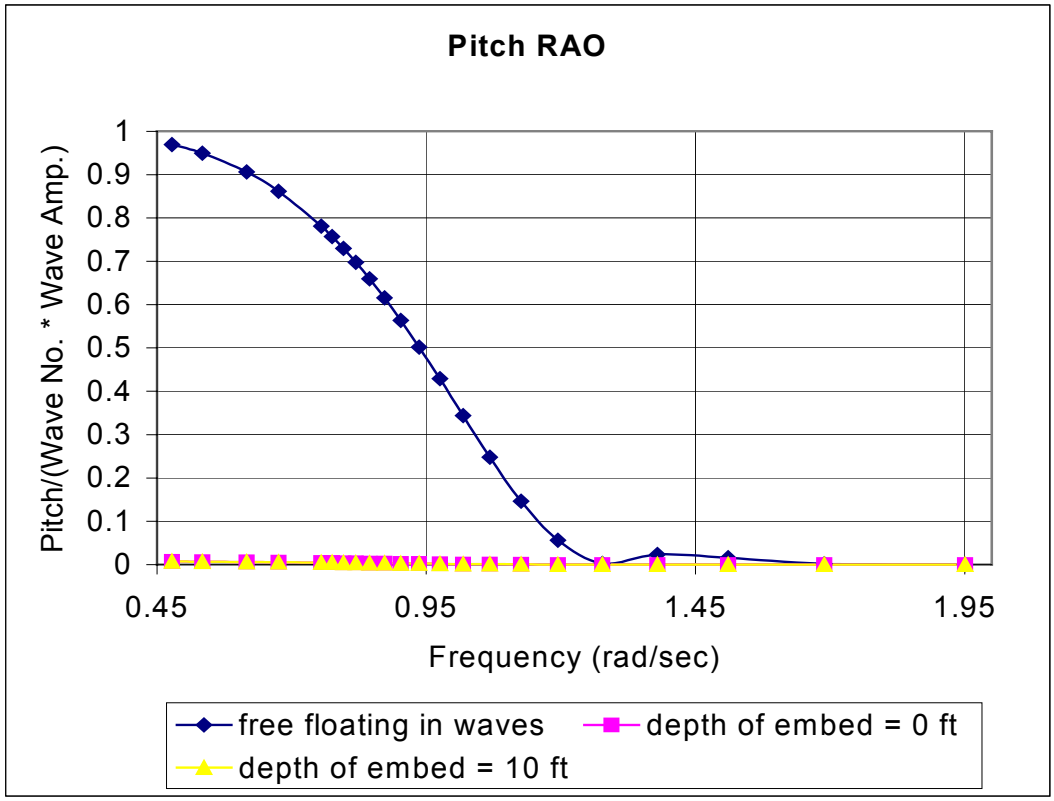

Figure 6.21 Pitch RAO for Soft Rock(Coral) at free floating in waves and embedment depths of 0ft and 10ft

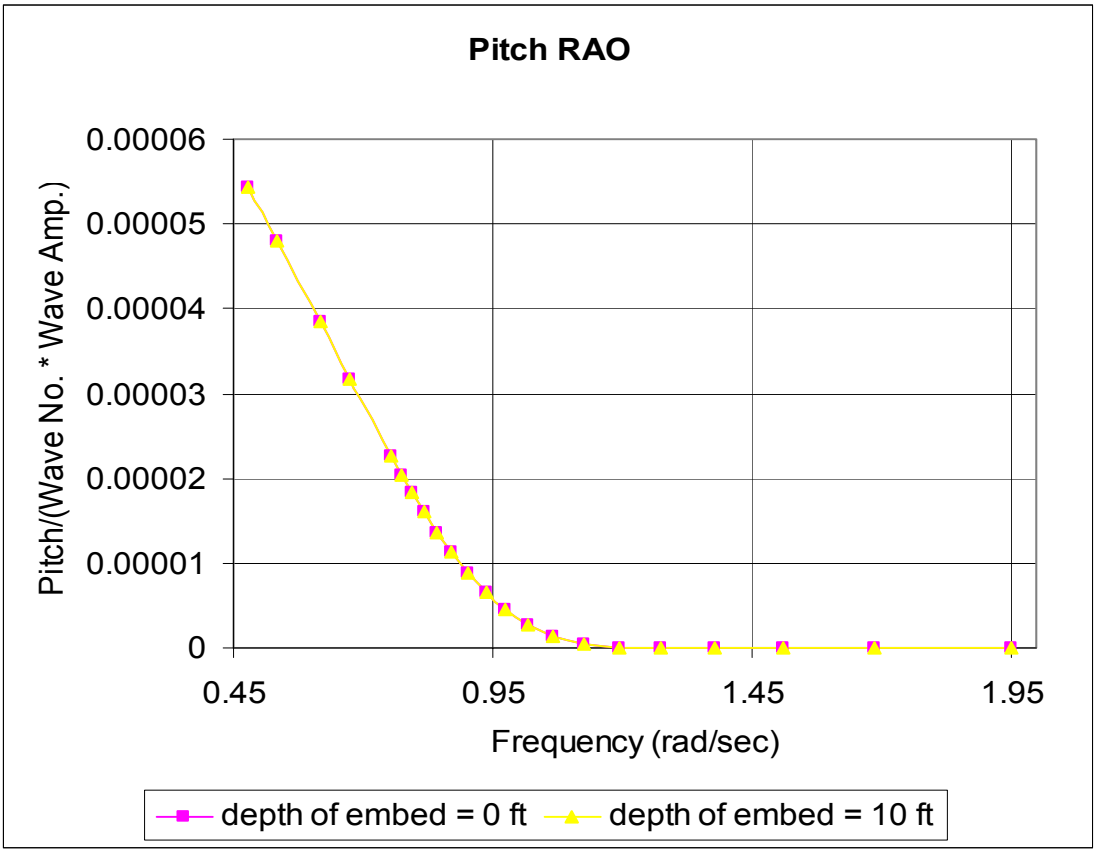

Figure 6.22 Pitch RAO for Soft Rock(Coral) at embedment depths of 0ft and 10ft

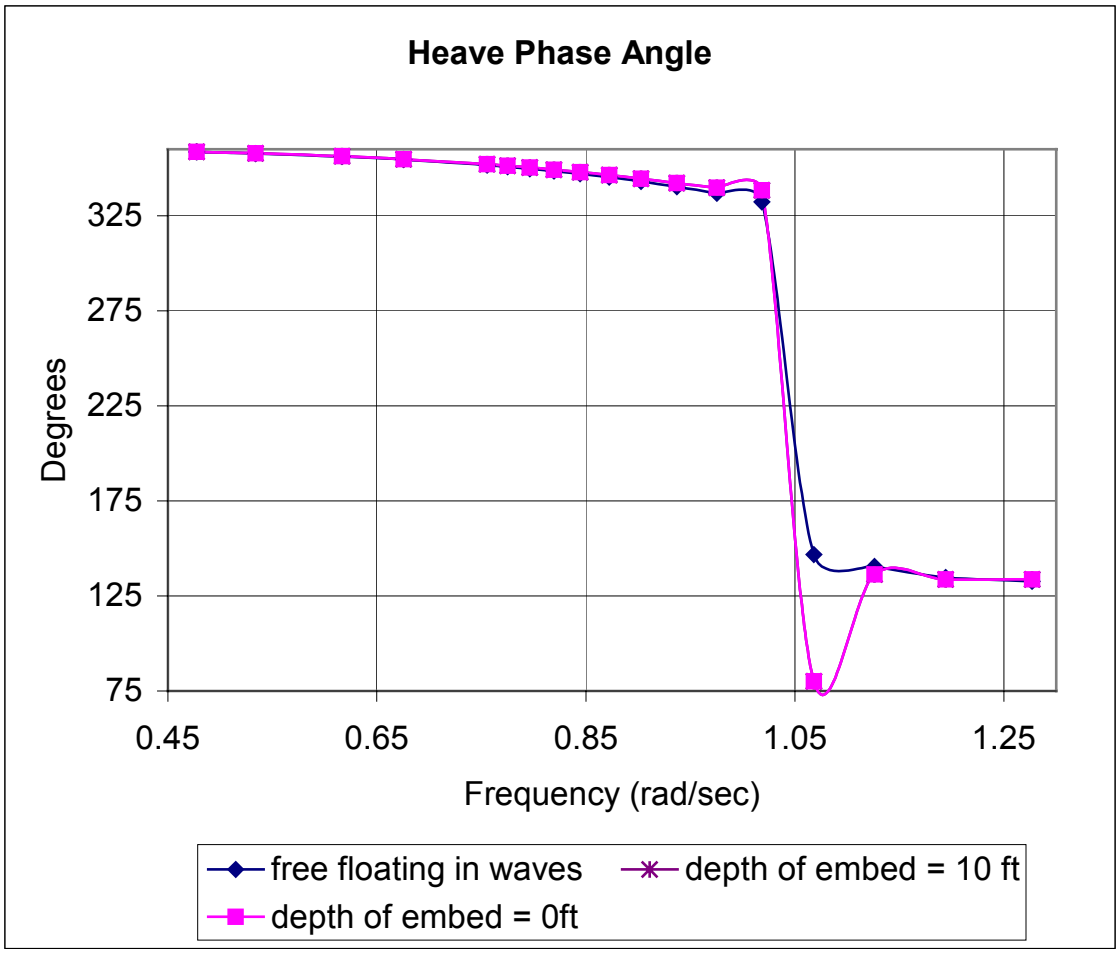

Figure 6.23 Heave Phase Angle for Soft Rock(Coral) at free floating in waves and embedment depths of 0ft and 10ft

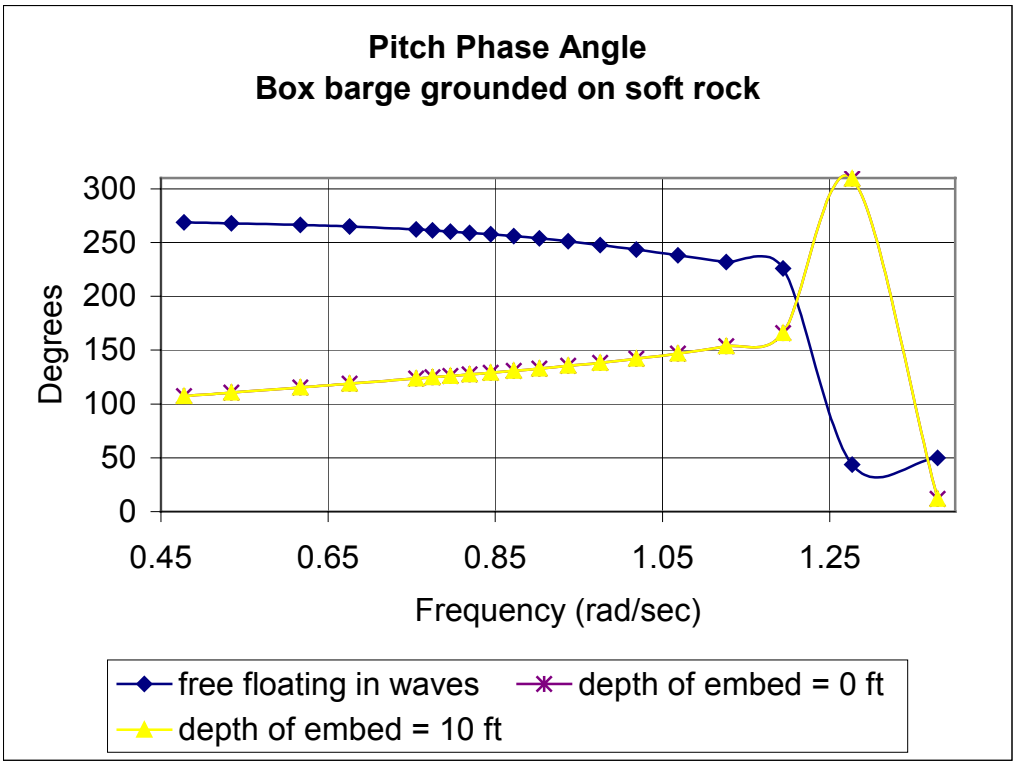

Figure 6.24 Pitch Phase Angle for Soft Rock(Coral) at free floating in waves and embedment depths of 0ft and 10ft

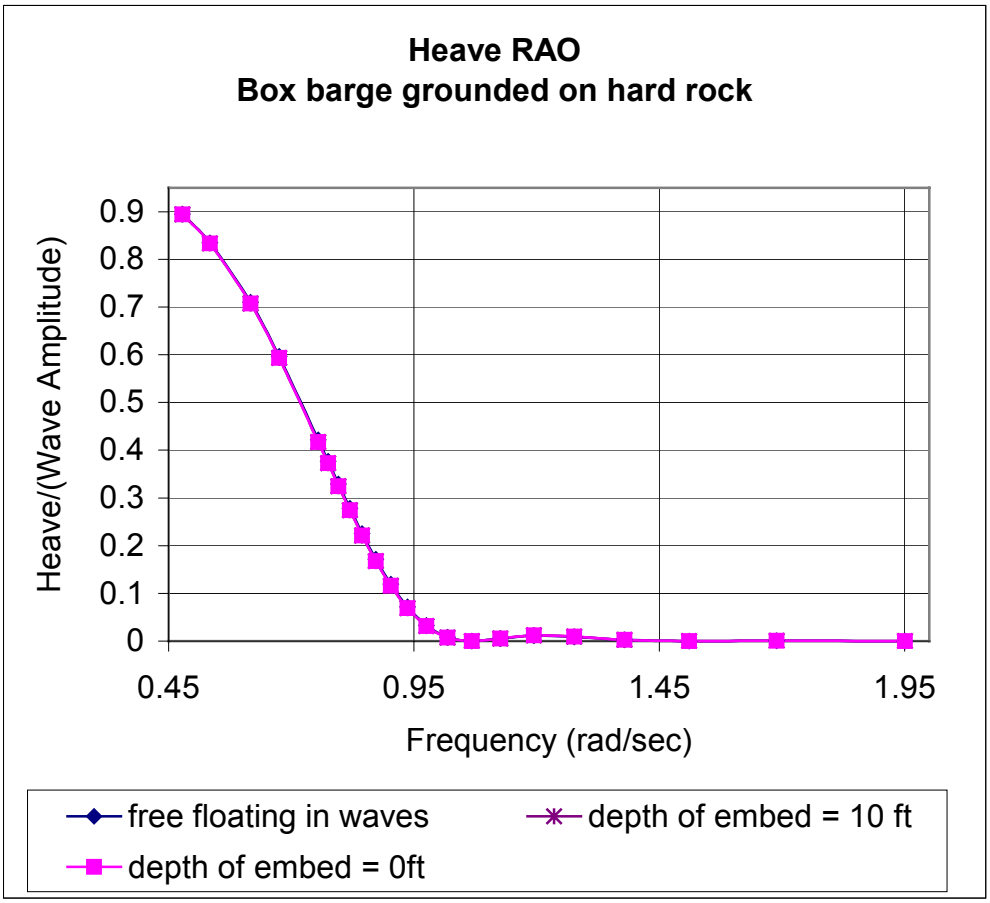

Figure 6.25 Heave RAO for Hard Rock at free floating in waves and embedment depths of 0ft and 10ft

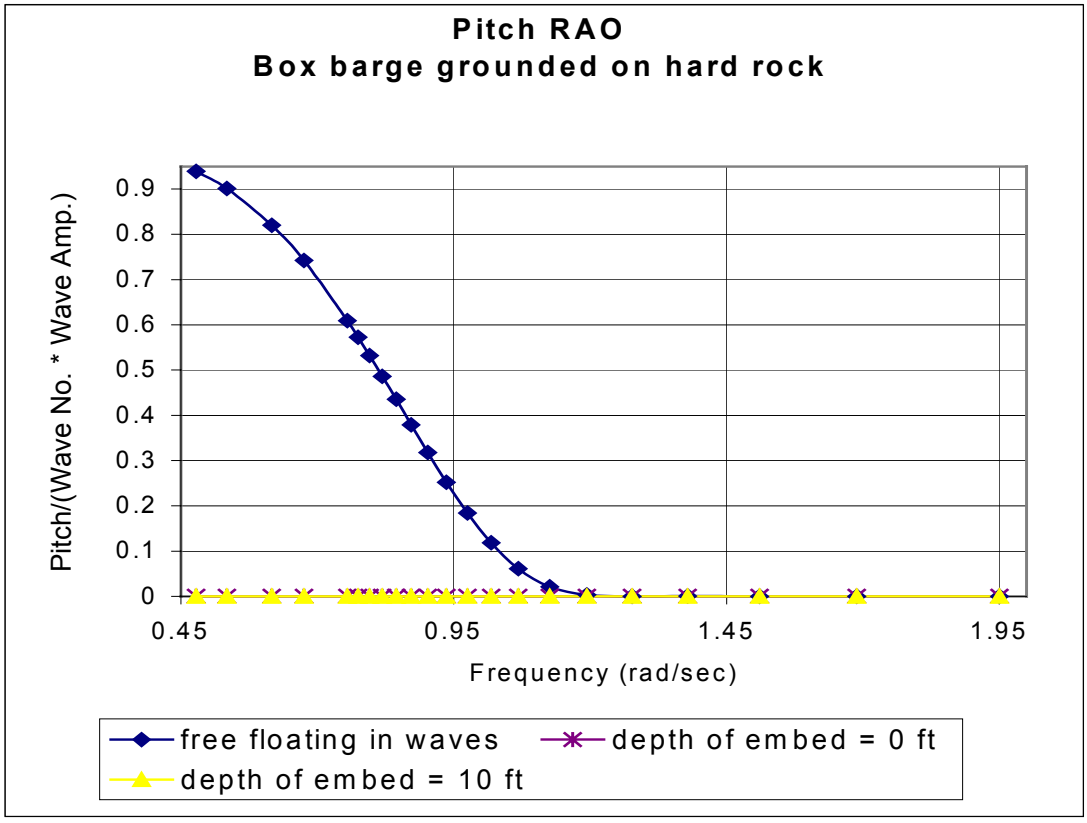

Figure 6.26 Pitch RAO for Hard Rock at free floating in waves and embedment depths of 0ft an 10ft

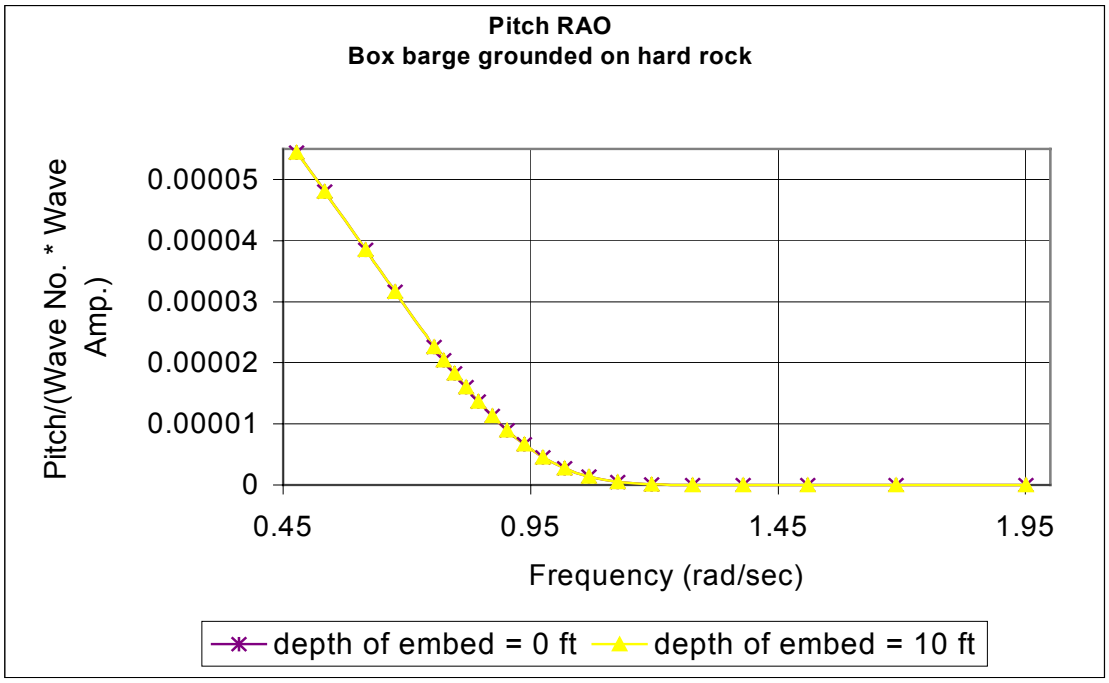

Figure 6.27 Pitch RAO for Hard Rock at embedment depths of 0ft an 10ft

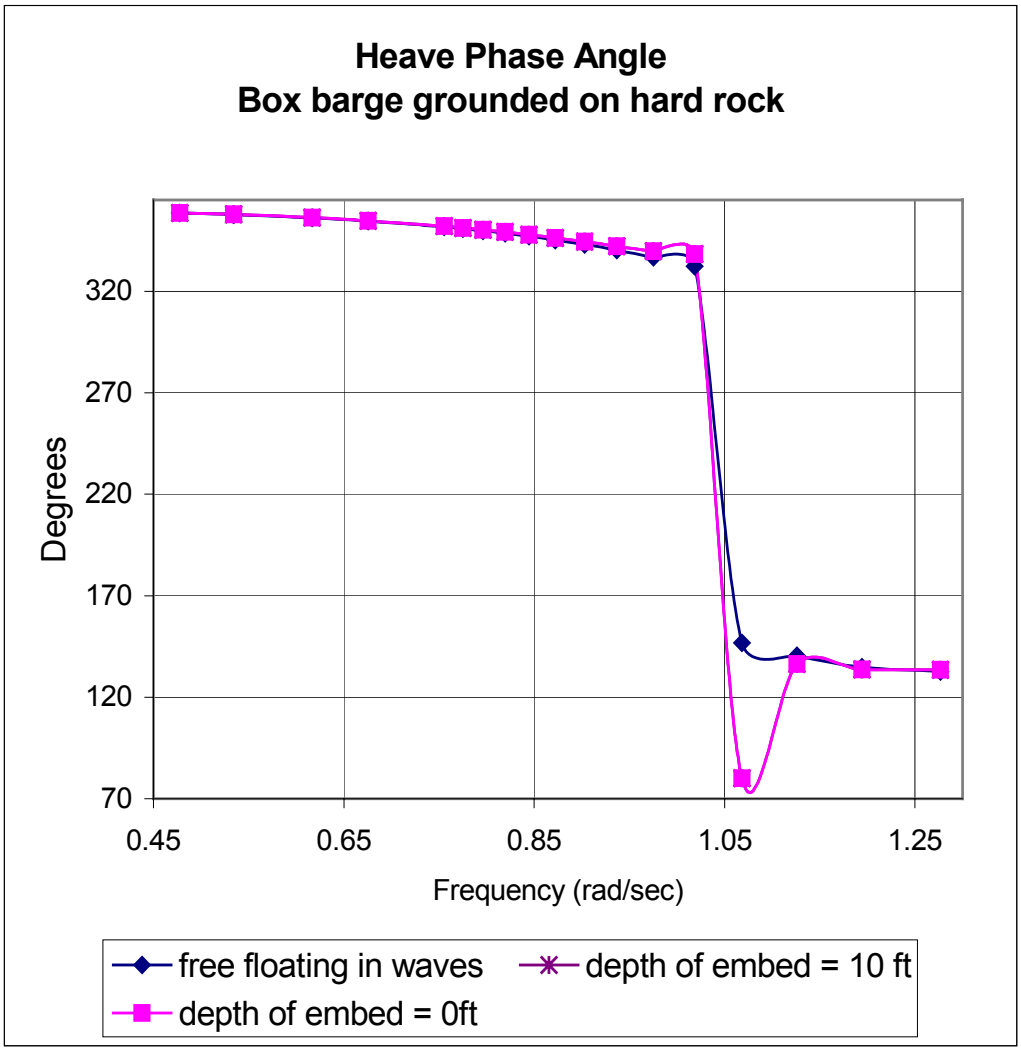

Figure 6.28 Heave Phase angle for Hard Rock at free floating in waves and at embedment depths of 0ft and 10ft

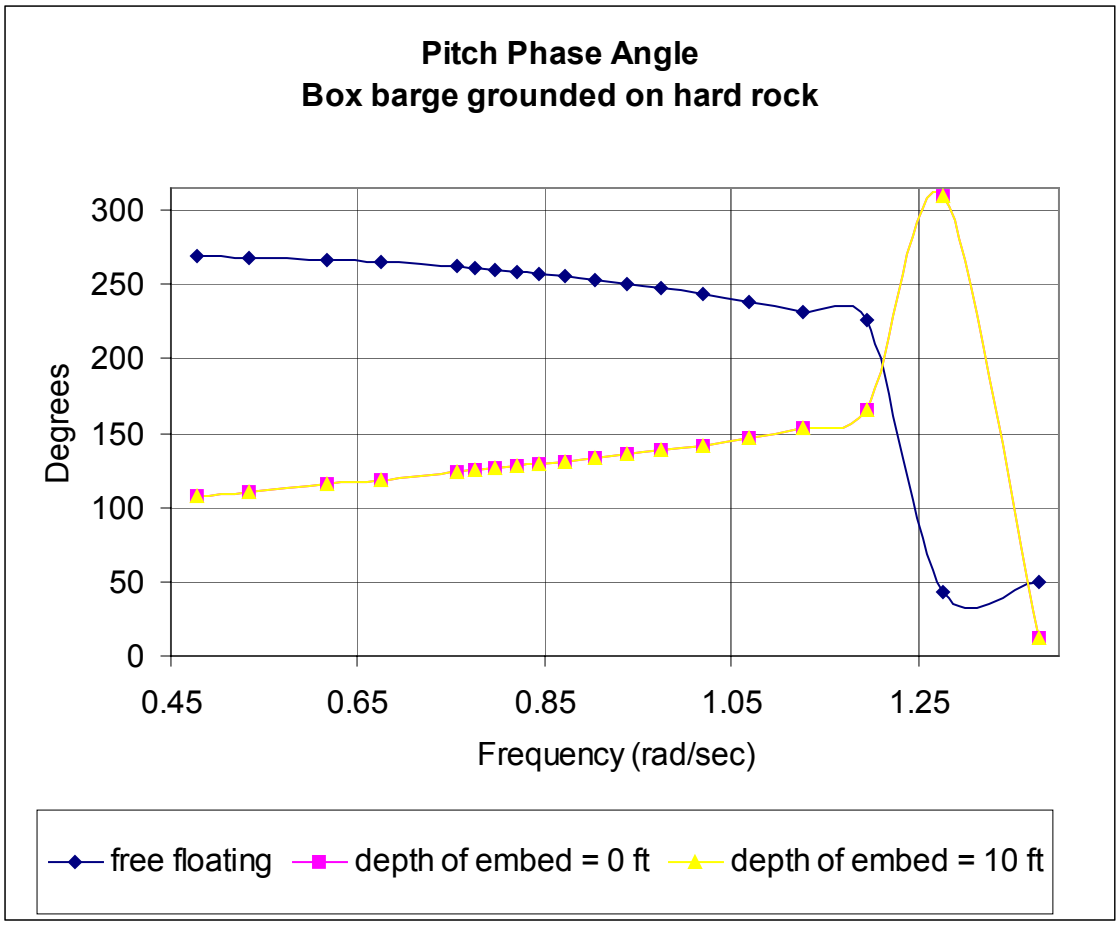

Figure 6.29 Pitch Phase angle for Hard Rock at free floating in waves and at embedment depths of 0ft and 10ft

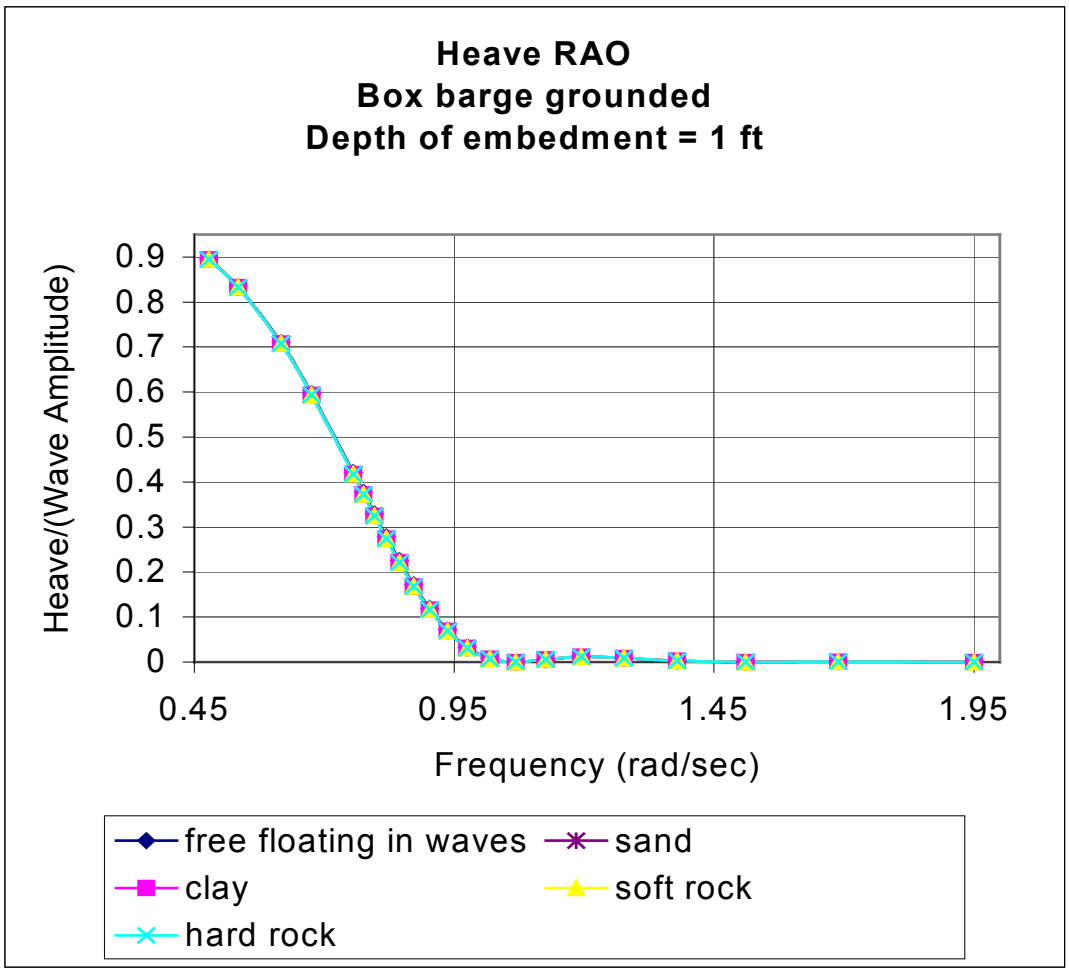

Figure 6.30 Heave RAO for various soils at free floating in waves and at embedment depth of 1ft

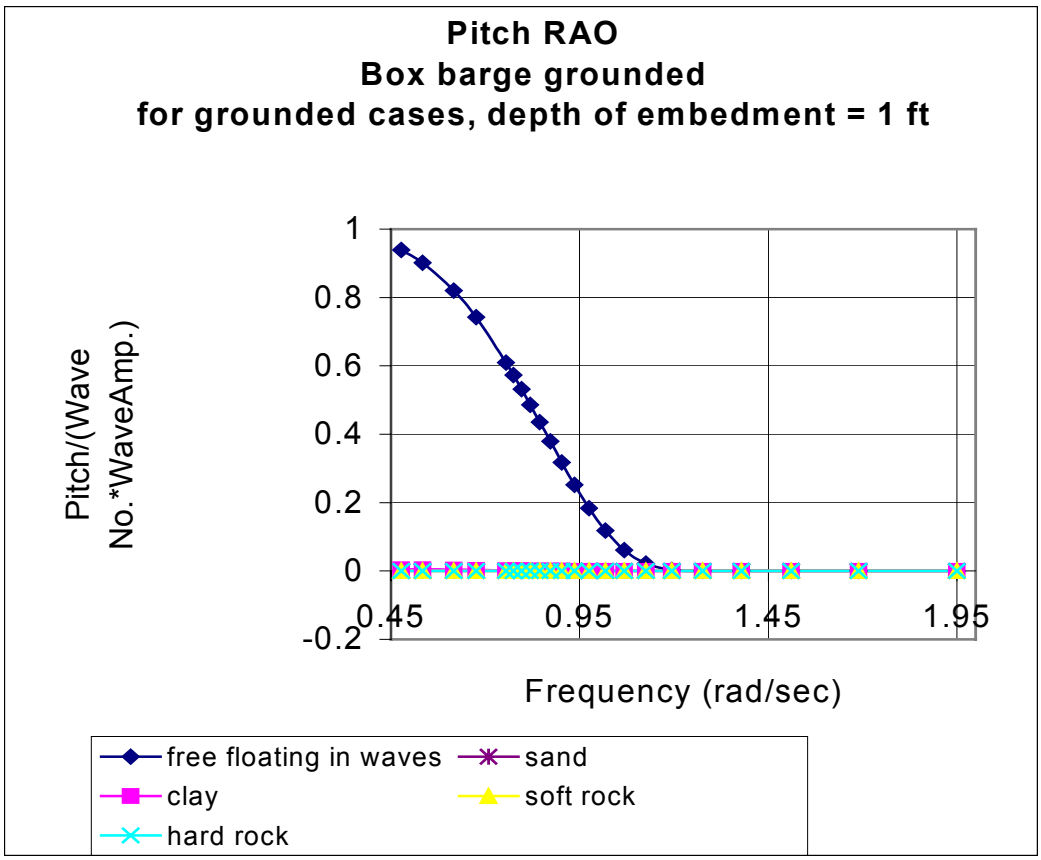

Figure 6.31 Pitch RAO for various soils at free floating in waves and at embedment depth of 1ft

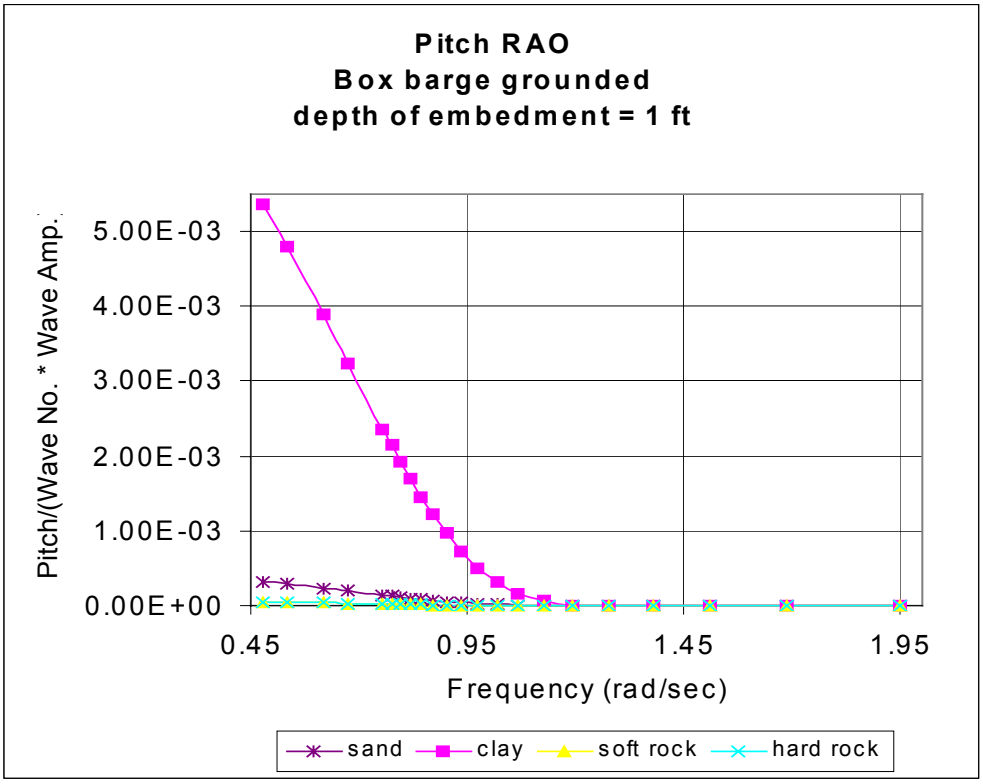

Figure 6.32 Pitch RAO for various soils at embedment depth of 1ft

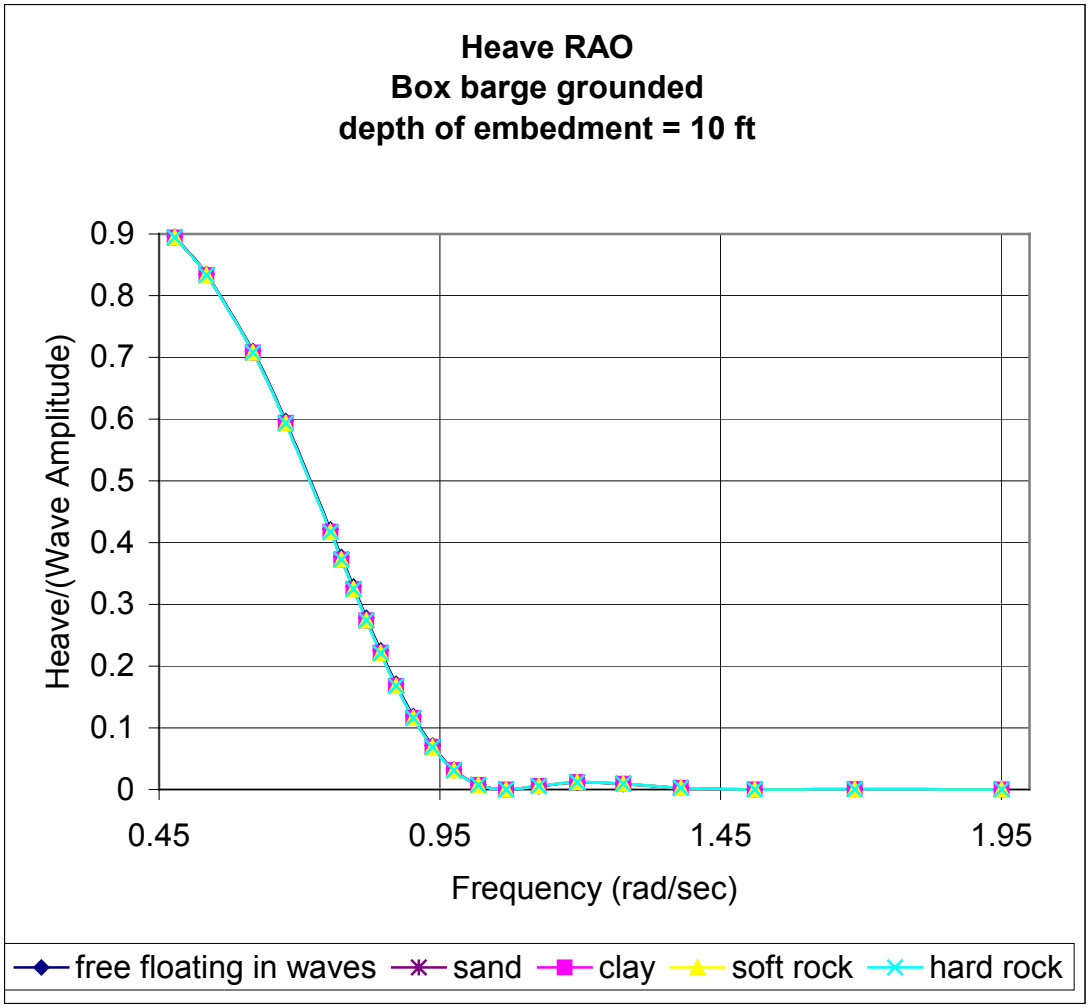

Figure 6.33 Heave RAO for various soils at free floating in waves and at embedment depth of 10ft

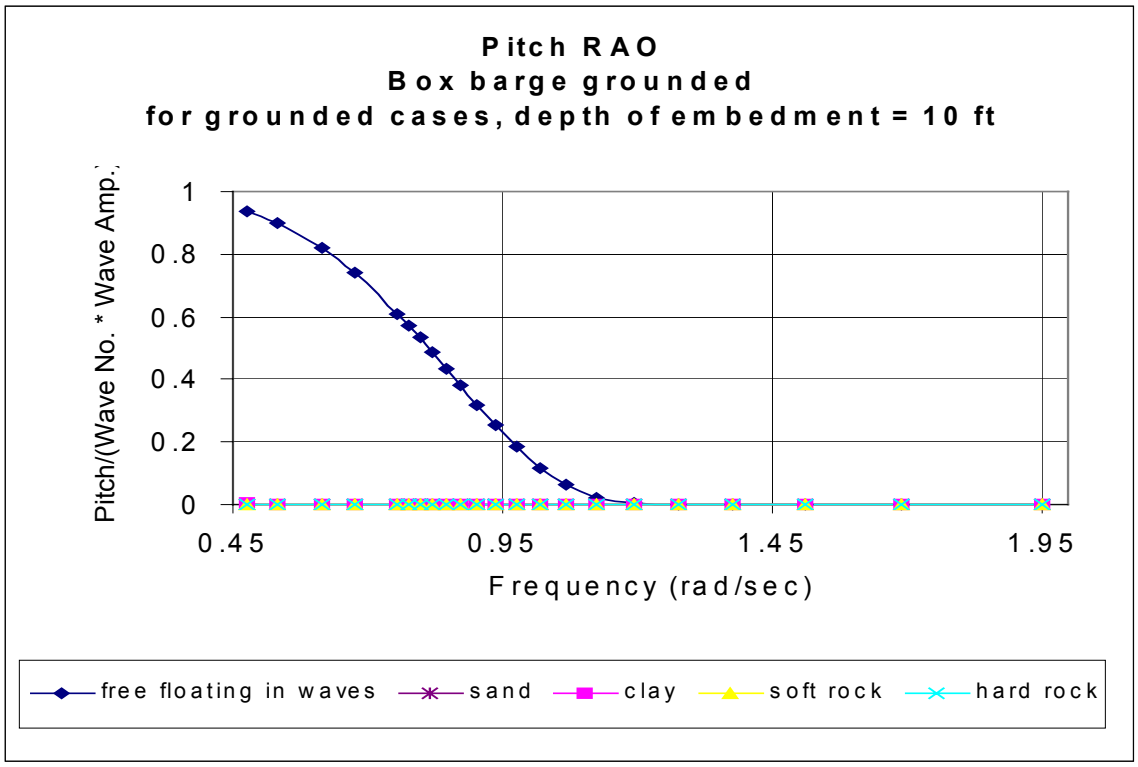

Figure 6.34 Grounded Pitch RAO for various soils at free floating in waves and at embedment depth of 10ft

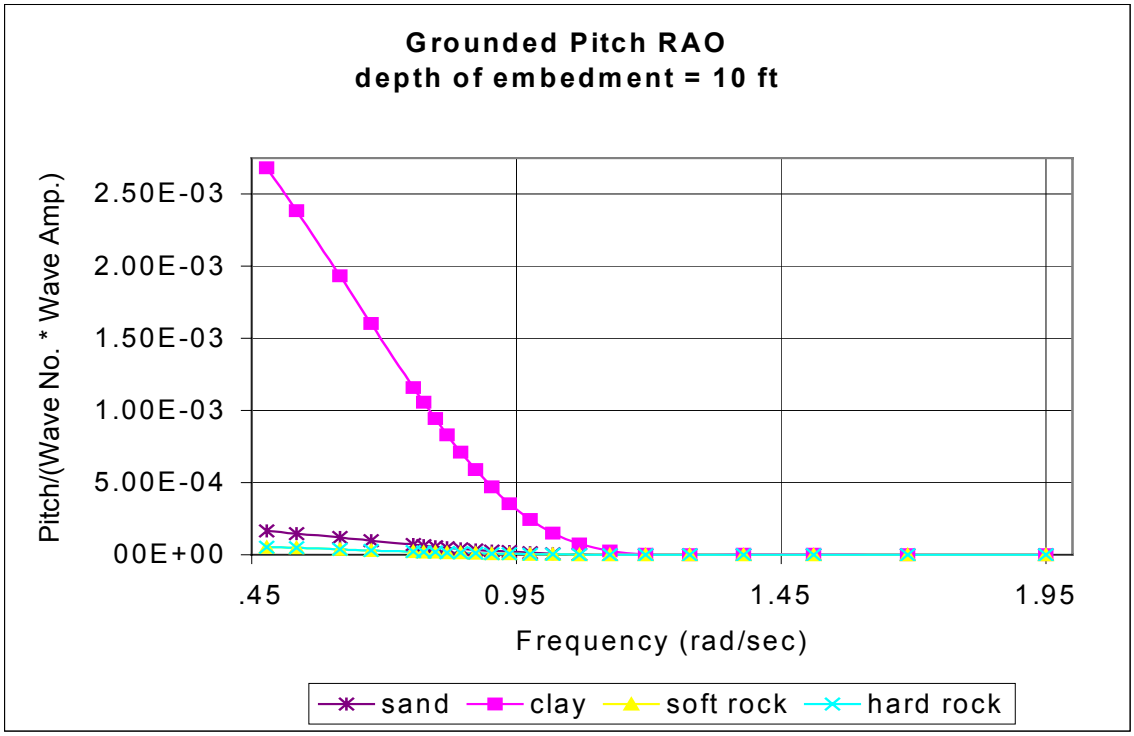

Figure 6.35 Grounded Pitch RAO for various soils at embedment depth of 10ft

6.2.3 Soil Parametric Study

To see how sensitive the soil model is to changes in the soil parameters a parametric study is conducted. The only soil parameter that needs to be varied is the Shear Modulus, G. This is because G is the only independent variable. It is related to the shear wave velocity by the equation

$$G = \rho(Vs)^2 \tag{6.1}$$

The soil density, ρ, does not change much so it does not need to be varied and Poisson's Ration, ν, varies very little for different soil types. To see the effects on the soil model, G is varied logarithmically from 100 ($10^3 lb_f/ft^2$) to 1,000,000 ($10^3 lb_f/ft^2$). The smallest shear modulus is that of clay, which is 1,580 ($10^3 lb_f/ft^2$) and the largest shear modulus is that of hard rock, which is 124,200 ($10^3 lb_f/ft^2$). Table 6.2 shows the logarithmic value of the Shear Modulus, G with the corresponding values of shear wave velocity, Vs.

Table 6.2 Values of G and the corresponding values of Vs

G	Vs
k/ft^2	$k\text{-}sec^2/ft^4$
100	151.61961
1000	479.4633
10000	1516.1961
100000	4794.633
1000000	15161.961

The example grounded ship scenario used to generate the dynamic soil stiffness versus frequency for various shear modulus is the same as is used in the beginning of Section 6.1 with the depth of embedment of 5ft in hard rock.

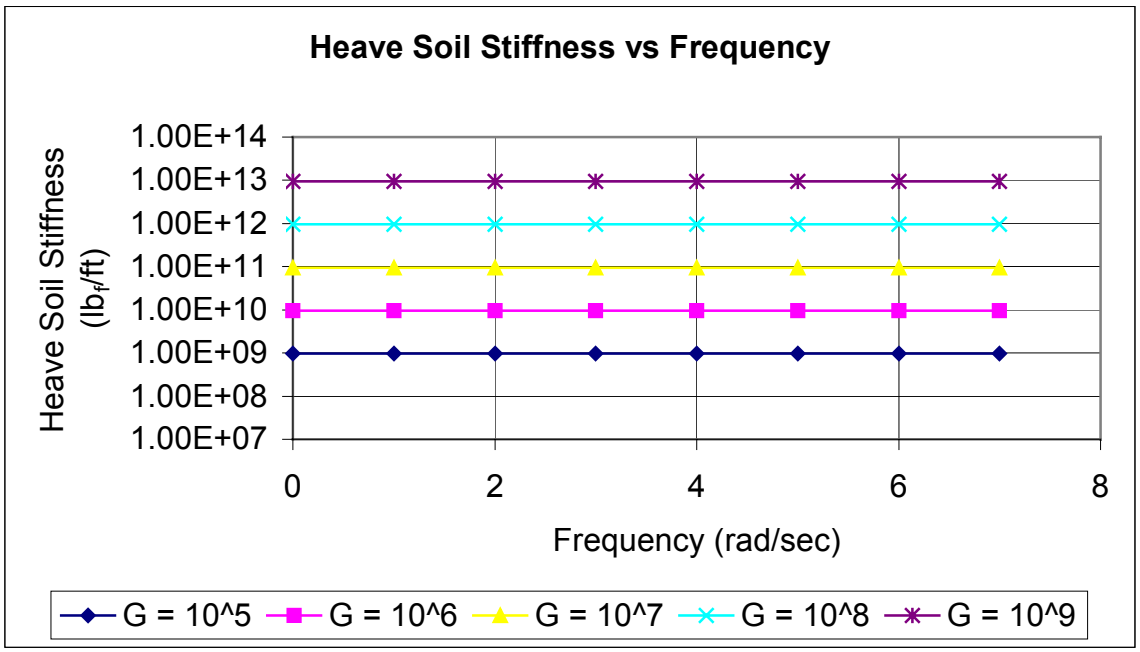

Figure 6.36 Heave Soil Dynamic Stiffness versus frequency with varying Shear Modulus

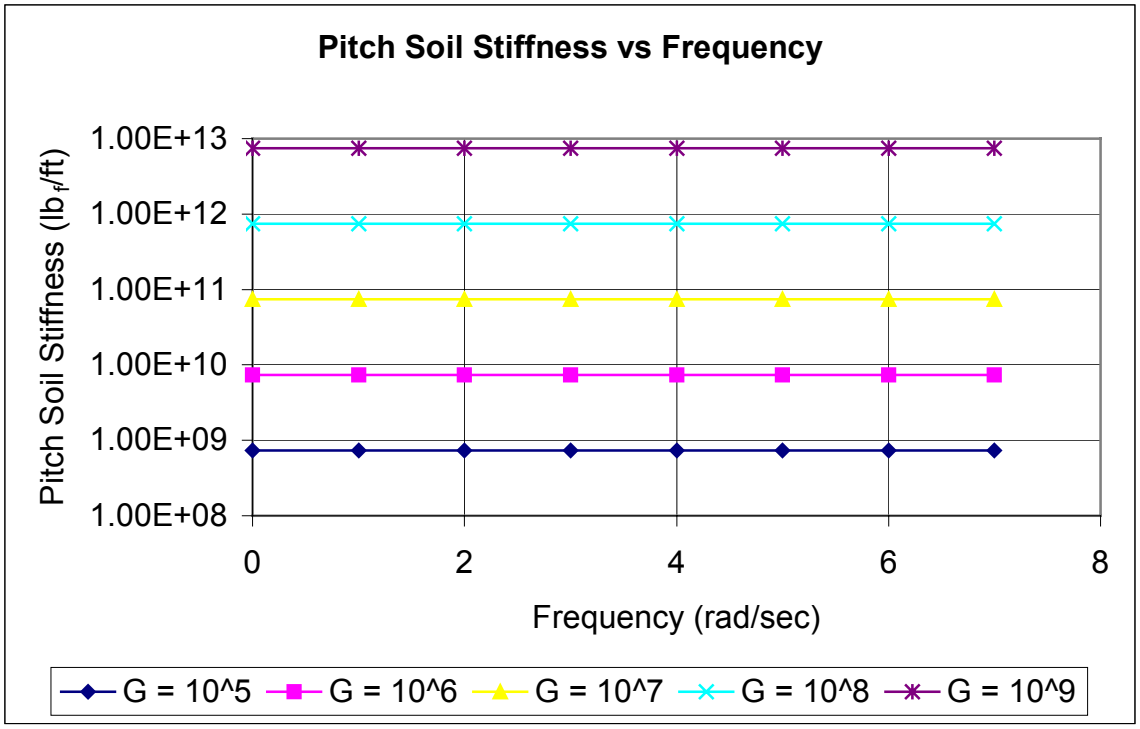

Figure 6.37 Pitch Soil Dynamic Stiffness versus frequency with varying Shear Modulus

The example grounded ship scenario used to generate the dynamic bending moments for various shear modulus is the same as is used in the beginning of Section 6.1 with the depth of embedment of 5ft.

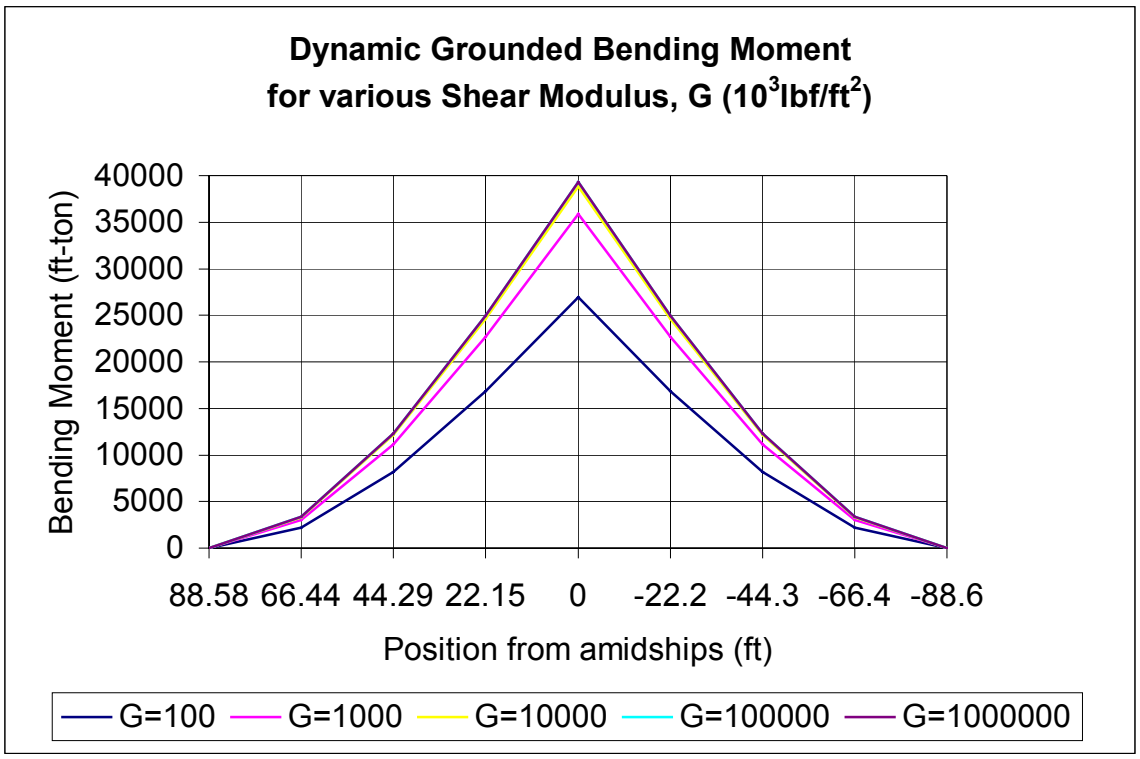

Figure 6.38 Dynamic Grounded Bending Moment with varying Shear Modulus

6.3 Conclusions

Our hypothesis, that a grounded ship in waves may have significantly higher loads and bending moments than predicted by static analysis, is shown to be true in Figures 6.2-6.6. In all these plots for each soil bottom type the dynamic grounded bending moment is significantly higher then the static grounded bending moment by a factor of about 40.

Figures 6.2-6.5 show that the effect of embedment is not great in the two degrees of freedom analyzed here, heave and pitch. This seems logical as the heave and pitch responses do not involve lateral motions, like those experienced in sway and yaw, which would be greatly affected by embedment depth.

Figures 6.6-6.9 shows that the dynamic grounded bending moment is directly influenced by the type of soil bottom, clay(mud), sand, soft rock(coral), and hard rock. Clay (mud) generates the smallest bending moment while hard rock generates the largest bending moment. These figures also show that the depth of embedment has a small influence on the magnitude of the bending moment.

Figure 6.10 for sand, Figure 6.15 for clay, Figure 6.17 for soft rock and Figure 6.25 for hard rock show that the grounded heave RAO is not affected by the soil reaction. Figures 6.11 and 6.12 for sand, Figures 6.17 and 6.18 for clay, show the grounded pitch RAO is influenced by the soil reaction as well as the depth of embedment. Figures 6.22 and 6.23 for soft rock and Figures 6.27 and 6.28 for hard rock show that the grounded pitch RAO is influenced by the soil reaction, but not the depth of embedment.

Figure 6.14 for sand, Figure 6.18 for clay, Figure 6.23 for soft rock and Figure 6.28 show that the grounded heave phase angle is affected by the soil reaction, but not the depth of embedment. Figure 6.15 for sand, Figure 6.19 for clay, Figure 6.24 for soft rock and Figure 6.29 for hard rock show the grounded pitch phase angle is influenced by the soil reaction, but not the depth of embedment.

A comparison of Figure 6.30 with Figure 6.33 shows the grounded heave RAO does not change with the depth of embedment or with the soil properties of grounding bottom. A comparison of Figures 6.31 and 6.32 with Figures 6.34 and 6.35 shows the grounded pitch RAO is affected by the depth of embedment and the soil properties of the grounding bottom. For example the grounded RAO for pitch in clay at an embedment depth of 10ft is about half the grounded pitch RAO in clay at 1ft.

Figures 6.37 and 6.38 show how the dynamic stiffness varies with frequency with different values of shear modulus. Figure 6.38 shows how the bending moment is affected by the shear modulus. The higher shear modulus generates a higher bending moment than a smaller shear modulus value. This figure also shows that the bending moment seems to converge to a maximum value at the higher values of the shear modulus.

6.4 Future Studies

Future studies could analyze the effects of soil-structure interaction for an embedded wedge shape, which could be used to model the hull of a warship. Currently, there have been no studies and are none planned to develop stiffnesses in all six degrees of freedom for an embedded wedge shape. These stiffnesses would be essential to analyze grounded motion and loads of a stranded warship.

Future work could include residual strength left after the hull has suffered some damage from the first phase of grounding, the impact event. The current model assumes the hull of the grounded ship is intact without damage. This would make the model more realistic because the impact event usually causes some structural hull damage.

Future work could include irregular waves that arise from different weather conditions, which would also make the model more realistic since grounded ships tend to experience these waves.

The current Stranded Ship Motions & Loads Program will need to be updated with analysis in all six degrees of freedom. Then coupling effects need to be studied and taken into account as best as possible in the program. Also, the assumption that the grounded portion of the ship is surrounded by soil on all four sides needs to be investigated when surge is taken into account. The soil surge reaction force needs to be reduced to account for the fact that one side of the grounded ship is not surrounded by soil.

Also, the influences of friction from sliding between the ship and soil and separation effects between the ship and soil will need to be investigated.

The deepwater wave equations need to be replaced with shallow water wave equations and an analysis needs to be completed to see if there is any difference.

Some experimental research needs to be done to verify and study some of the effects and interactions the ship's motion has on the soil and vice versa.

Works Cited

[1] Cahill, Richard A. Capt., *Disasters at Sea-Titanic to Exxon Valdez*. Texas and New York: Nautical Books and U.S. Merchant Marine Library Association, 1991.

[2] Bartholomew, C.A., Capt., *Mud, Muscle, and Miracles-Marine Salvage in the United States Navy*. Washington D.C.: Naval Historical Center and Naval Sea Systems Command, 1990.

[3] U.S. Navy Salvage Engineers, *POSSE Technotes*. Washington D.C.: Naval Sea Systems Command, Volume 1, 1997. Volume 1, 1998. Volume 1 No. 2, 1998. Volume 1 No. 1, 1999; Volume 2 No. 1, 2002; Volume 2 No. 2, 2002.

[4] U.S. Navy Salvage Engineers, *U.S. Navy Supervisor of Salvage Case Files*. Washington D.C.: Naval Sea Systems Command.

[5] ATSB Investigation Reports on Groundings retrieved 15 July 2002 from ATSB Marine Safety website:http://www.atsb.gov.au/marine/incident/index.cfm

[6] Schauer, Todd, LT, USGC, "NEW CARISSA Complete Hull Failure in a Stranded Bulk", Case Study 1 retrieved 08 July 2002 from Ship Structure Committee website:http://www.shipstructure.org/case_studies.shtml

[7] ABC News Online (Australian Broadcasting Corporation), "Attempts to Refloat Ship on Barrier Reef Suspended", retrieved 16 July 2002 from ABC News Online website:http://www.abc.net.au/news/2000/11/item20001102130431_1.htm

[8] U.S. Navy Supervisor of Salvage, *U.S. Navy Salvage Engineer' Handbook*. Washington D.C.: Naval Sea Systems Command, 1997.

[9] McCormick, Michael E., On the Motions of Grounded Ships, Johns Hopkins University Technical Report produced under NSWC Carderock Contract N00167-99-M-0226, Baltimore, Maryland, 1999.

[10] McCormick, Michael E. & Patrick J. Hudson, "An Analysis of the Motions of Grounded Ships," *International Journal of Offshore and Polar Engineering*, Vol. II(2),pp. 99-105, 2001.

[11] Reissner, E., "Stationare, axialsymetrische durch eine schuttelnde Masse erregte Schwingungen eines homogenen elastischen Halbraumes", *Ingenier-Archiv*, Vol. 7, pp. 381-396, December 1936.

[12] Veletsos, A.S. and Wei, Y.T., "Lateral and Rocking Vibration of Footings", *Journal of the Soil Mechanics and Foundations Division*, ASCE, Vol. 97, No. SM9, pp. 1227-1248, 1971.

[13] Kausel, E., "Forced Vibrations of Circular Foundations on Layered Media", Report No. R74-11, MIT Dept. of Civil Engineering, Cambridge, Massachusetts, 1974.

[14] Wolf, John P. *Foundation Vibration Analysis Using Simple Physical Models*. New Jersey: PTR Prentice Hall, 1994.

[15] D'Appolonia Consulting Engineers*, Seismic Input and Soil-Structure Interaction*. Pittsburgh, PA, 1979.

[16] Hudson, Patrick J., *Wave-Induced Migration of Grounded Ships*, Doctoral Dissertation, Johns Hopkins University, 2001.

[17] Whitman, R.V., and Richart, F.E., Jr., "Design Procedures for Dynamically Loaded Foundations*," Journal of the Soil Mechanics and Foundations Division, ASCE* 93 (SM6), 169-193, 1967.

[18] Wolf, John P., *Dynamic Soil-Structure Interaction*. New Jersey: Prentice-Hall, Inc., 1985.

[19] Pais, Artur & Eduardo Kausel, *Stochastic Response of Foundations.* Research Report R85-6 sponsored by the National Science Foundation Grant CEE-8211021 and LNEC and INVOTAN in Lisbon, Portugal. Massachusetts: Massachusetts Institute of Technology, 1985.

[20] Kramer, Steven L., *Geotechnical Earthquake Engineering*. New Jersey: Prentice-Hall Inc., 1996.

[21] Abascal, R., *Estudio de Problemas Dina`micos en Interaccio`n Suelo-Estructura por el Me`todo de los Elementos de Contorno*, Doctoral Thesis, Escuela Te`nica Superior de Ingenieros Industriales de la Universidad de Sevilla, 1984.

[22] Dominguez, J., *Dynamic Stiffness of Rectangular Foundations*, Report No. R78-20, MIT, Cambridge, Massachusetts, 1978.

[23] Wong, H. L. and Luco, J. E., Tables of Impedance Functions and Input Motions for Rectangular Foundations, Report No. CE78-15, University of Southern California, 1978.

[24] Wolf, John P. and Weber B., "Approximate Dynamic Stiffness of Embedded Foundation Based on Independent Thin Layers With Separation of Soil", *Proceedings of the 8th European Conference on Earthquake Engineering*, pp.5.6/33-5.6/40, 1986.

[25] Gazetas, G., "Analyis of Machine Foundation Vibrations: State of the Art", *International Journal of Soil Dynamics and Earthquake Engineering*, Vol. 2, No. 1, pp. 2-42, 1983.

[26] Salvesen, N., Tuck, E.O., Faltinsen, O.M., "Ship Motions and Sea Loads*",* *SNAME Transactions*, Vol. 78, 1970

[27] Lloyd, ARJM. *Seakeeping: Ship Behaviour in Rough Weather*. Published by ARJM Lloyd, Hampshire, United Kingdom. 1998.

[28] *Principles of Naval Architecture*, Vol. 3, Society of Naval Architects and Marine Engineers, Jersery City, NJ, 1989

[29] Newman, J.N., *Marine Hydrodynamics*, Masschusettes Institute of Technology Press, Cambride, Massachusettes, 1977.

[30] Ursell, F., "On the Heaving Motion of a Circular Cylinder on the Surface of a Fluid," *Quarterly Journal of Applied Mathematics*, Vol. 2, 1949.

[31] Frank, F. and Salvesen, N., "The Frank Close-Fit Ship Motion Computer Program", *Naval Ship Research and Development Center Technical Note 105*.

[32] Bretschneider, C.L., "Maximum Sea State for the North Atlantic Hurricane Belt", *Ocean Industry*, September 1967.

[33] Herbert Engineering Corp., *HECSALV Ship Salvage Engineering Software Instruction Manual version 5.00*. San Francisco: April 15, 1995.

[34] Grim, O. and Kirsch, M., "Program zur Berechnung der Hyrodynamischen Krafte, der Bewegungen und des Biegemomentes fur ein Schiff in Langslaufden Wellen", 1966.

[35] Loukakis, Theodore A. *Computer Aided Prediction of Seakeeping Performance in Ship Design*. Report No. 70-3 prepared under MIT Contract No. DSR 71377 and sponsored by Maritime Administration United States Department of Commerce Contract No. MA-2710 Task Order No. 10. . Massachusetts: Massachusetts Institute of Technology, August 1970.

[36] Demanche, J. F., “Added Mass and Damping Coefficient for Cylinders with a Bulb-like Cross Section Oscillating in a Free Surface”, M.Sc. Thesis, M.I.T., Department of Naval Architecture and Marine Engineering, 1968.

Appendix I

Table I

	Abascal (1)	Dominguez (14)		Wong & Luco (59)		Value Taken
		a)	b)	$\nu=1/3$	$\nu=0.45$	
$\frac{K^o_H(2-\nu)}{GB}$	9.41	9.47	9.35	9.22	9.16	9.2
$\frac{K^o_V(1-\nu)}{GB}$	4.75	4.88	4.75	4.66	4.57	4.7
$\frac{K^o_R(1-\nu)}{GB^3}$	4.38	3.85	3.79	4.17	4.04	4.0
$\frac{K^o_t}{GB^3}$	8.71	7.53	7.48	8.31	8.42	8.31
$\frac{K^o_{RH}}{GB^2}$	—	—	—	0.508	0.302	0

a) Relaxed boundary conditions
b) Non-relaxed boundary conditions

Table II

Mode		L/B=1	L/B=2	L/B=3	L/B=4
Vertical $\frac{K^o_V(1-\nu)}{GB}$	Wong ($\nu=1/3$)	4.66	6.73	8.56	10.22
	Dominguez	4.88	7.0	8.9	10.7
	Formula	4.70	6.81	8.66	10.36
Horiz.-x $\frac{K^o_{Hx}(2-\nu)}{GB}$	Wong ($\nu=1/3$)	9.22	12.95	16.19	19.15
	Dominguez	9.47	13.1	16.3	19.3
	Formula	9.20	13.07	16.29	19.14
Horiz.-y $\frac{K^o_{Hy}(2-\nu)}{GB}$	Wong ($\nu=1/3$)	9.22	13.75	17.79	21.48
	Dominguez	9.47	14.0	18.1	21.8
	Formula	9.20	13.87	17.89	21.54
Rocking-x $\frac{K^o_{Rx}(1-\nu)}{GB^3}$	Wong ($\nu=1/3$)	4.17	7.18	10.30	13.18
	Dominguez	3.85	6.8	9.75	12.8
	Formula	4.0	7.20	10.40	13.60
Rocking-y $\frac{K^o_{Ry}(1-\nu)}{GB^3}$	Wong ($\nu=1/3$)	4.17	20.21	52.26	104.21
	Dominguez	3.85	19.6	50.6	105.3
	Formula	4.0	19.96	52.37	104.18
Torsion $\frac{K^o_t}{GB^3}$	Wong ($\nu=1/3$)	8.31	28.32	67.41	131.03
	Dominguez	7.53	26.8	65.7	129.2
	Formula	8.31	27.28	66.77	130.95

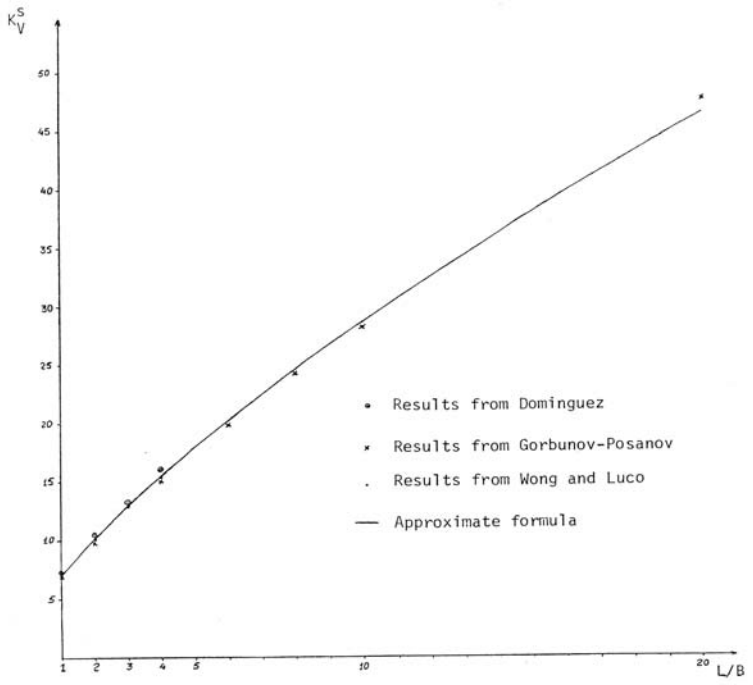

Fig. 15 - Variation of the vertical static stiffness with the shape of the foundation

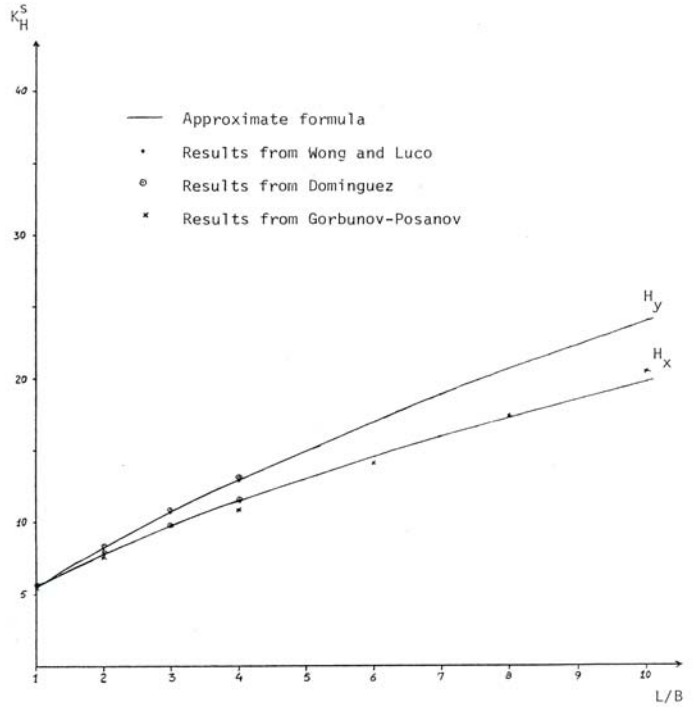

Fig. 16 - Variation of the horizontal data stiffnesses with the shape of the foundation

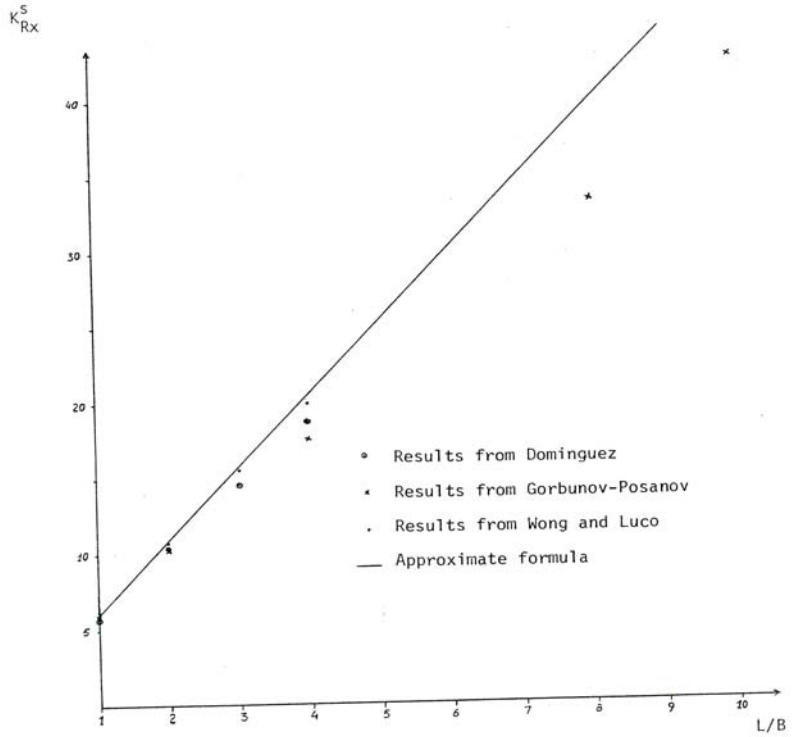

Fig. 17 - Variation of the rocking static stiffness with the shape of the foundation

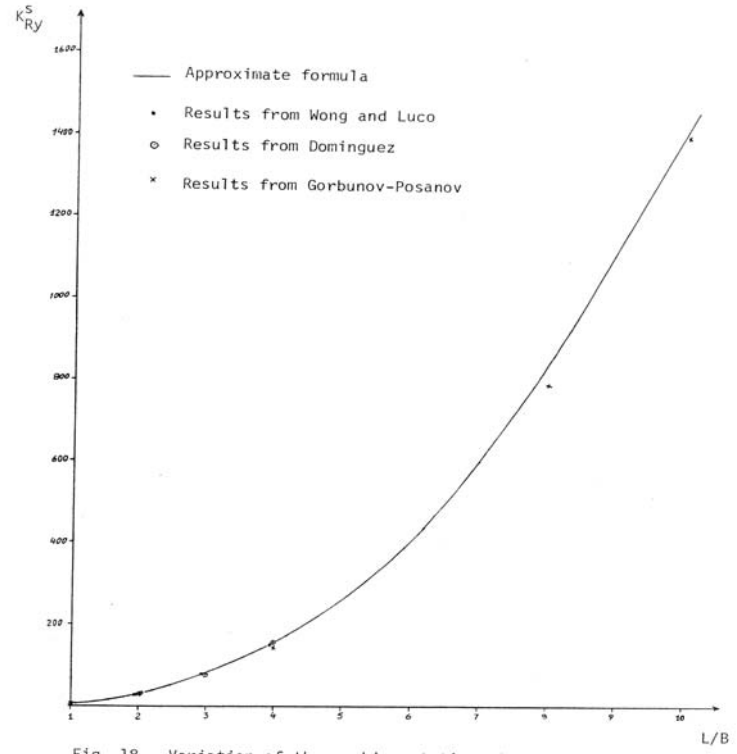

Fig. 18 - Variation of the rocking static stiffness with the shape of the foundation

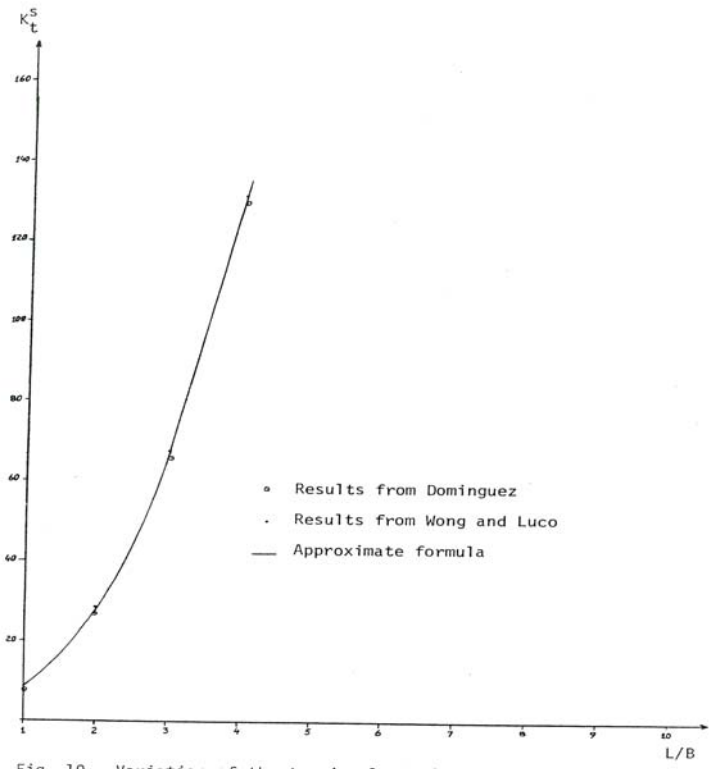

Fig. 19 - Variation of the torsional static stiffness with the shape of the foundation

Appendix II

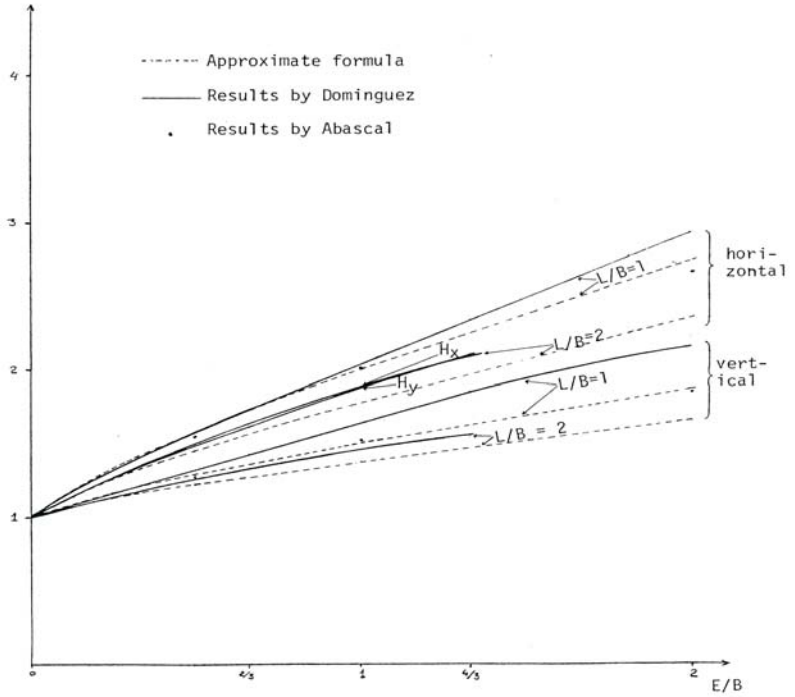

Fig. 34 - Variation of the static stiffnesses with the embedment - horizontal and vertical

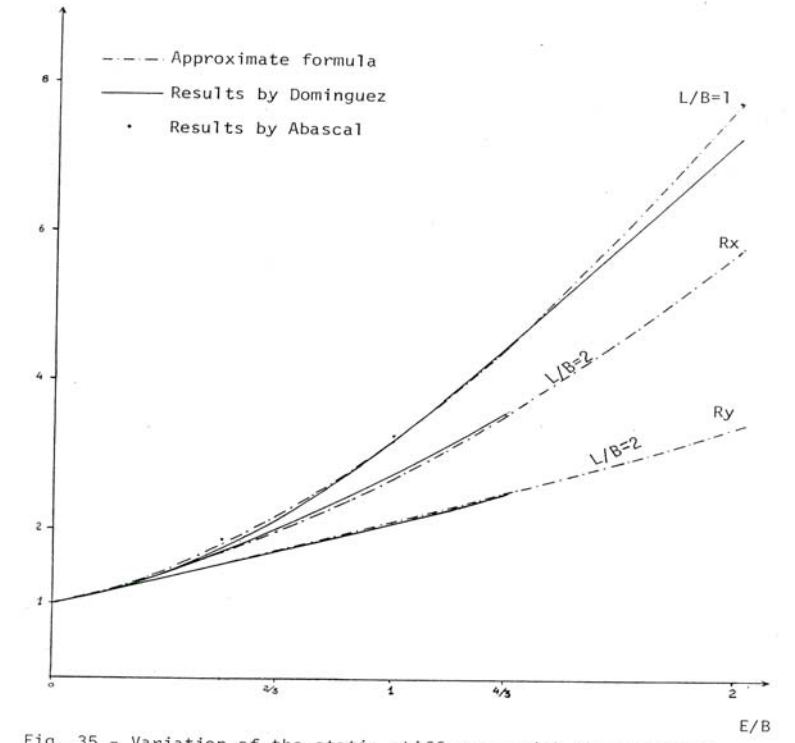

Fig. 35 - Variation of the static stiffnesses with the embedment - rocking

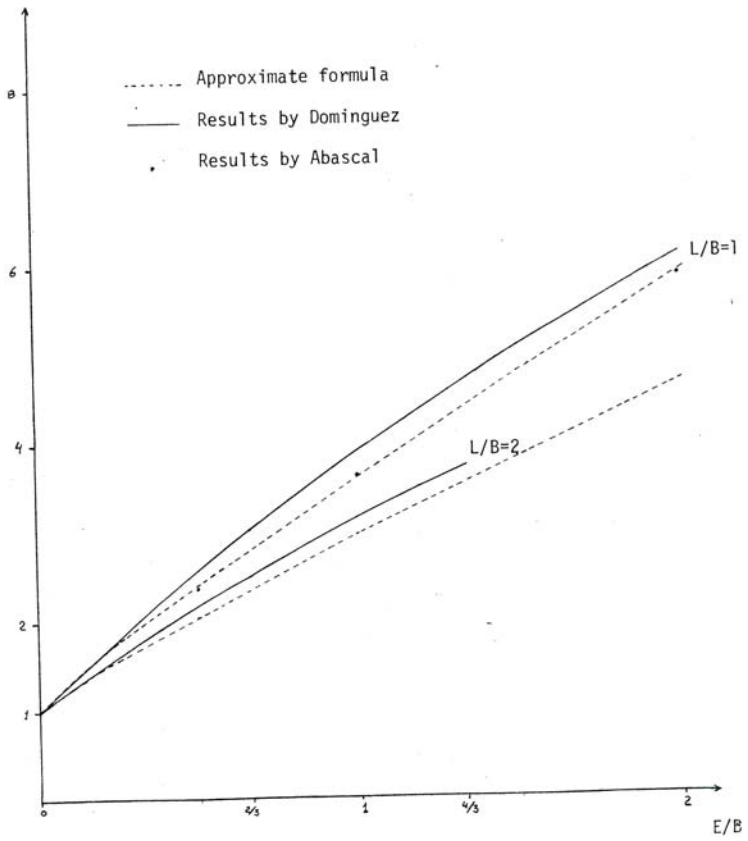

Fig. 36 - Variation of the static stiffness with the embedment - torsion

Appendix III

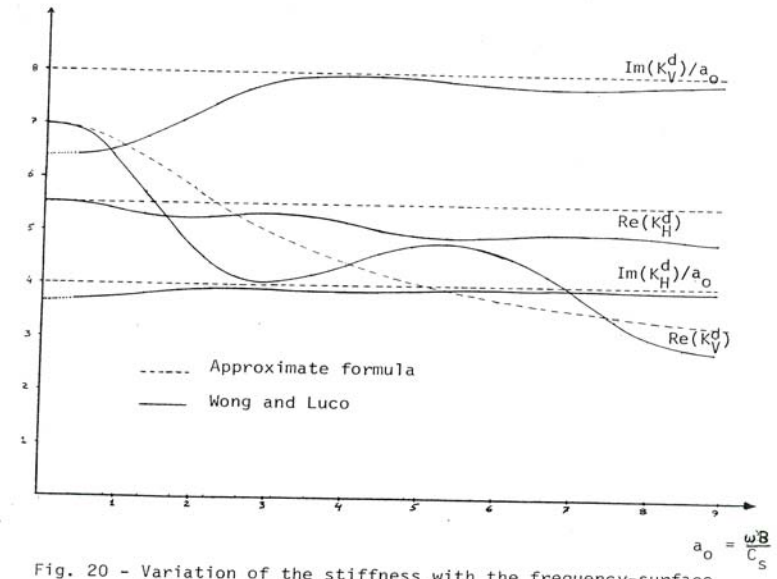

Fig. 20 - Variation of the stiffness with the frequency-surface foundation L/B = 1. (vertical and horizontal modes)

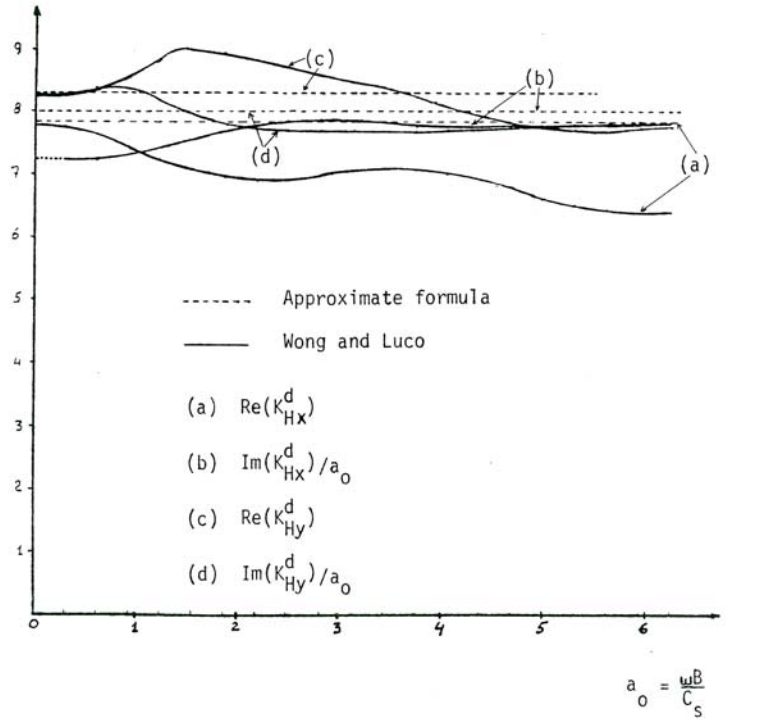

Fig. 21 - Variation of the stiffness with the frequency-surface foundation L/B = 2 (horizontal mode)

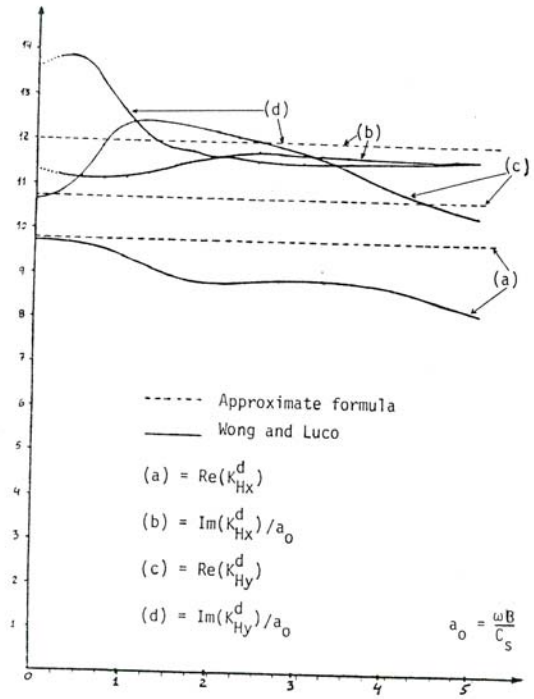

Fig. 22 - Variation of the stiffness with the frequency- surface foundation L/B = 3 (horiz. mode)

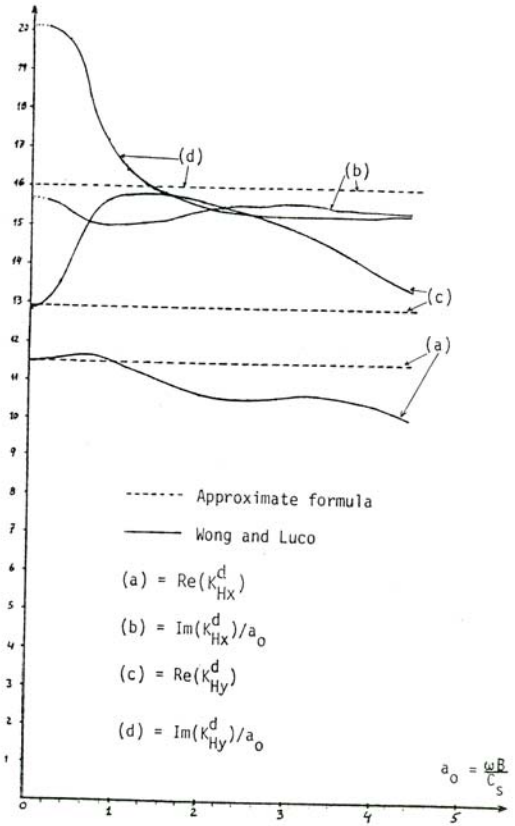

Fig. 23 - Variation of the stiffness with the frequency- surface foundation L/B = 4 (horiz. mode)

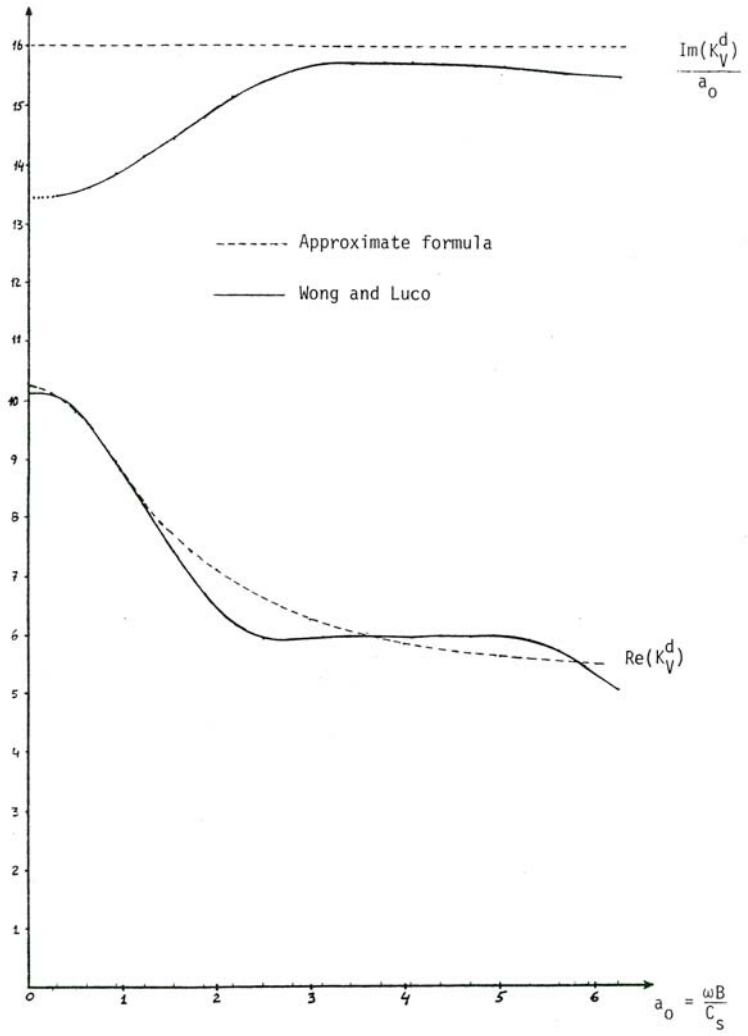

Fig. 24 - Variation of the stiffness with the frequency-surface foundation L/B = 2 (vertical mode)

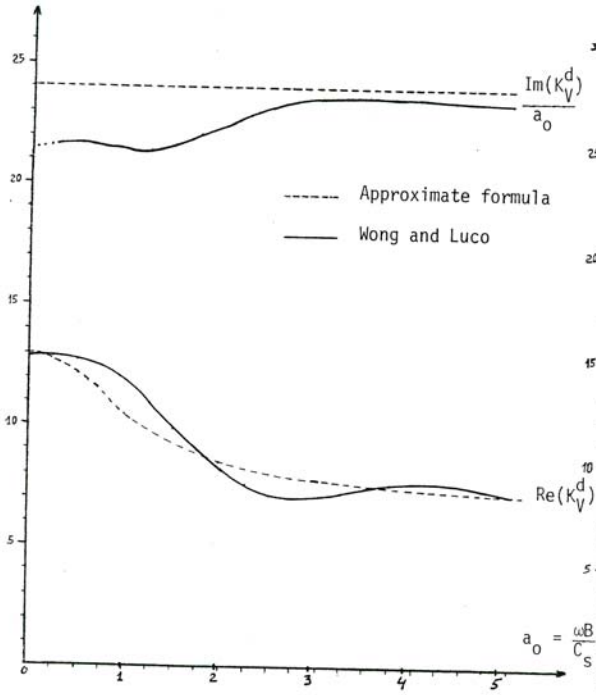

Fig. 25 - Variation of the stiffness with the frequency- surface foundation L/B = 3 (vert. mode)

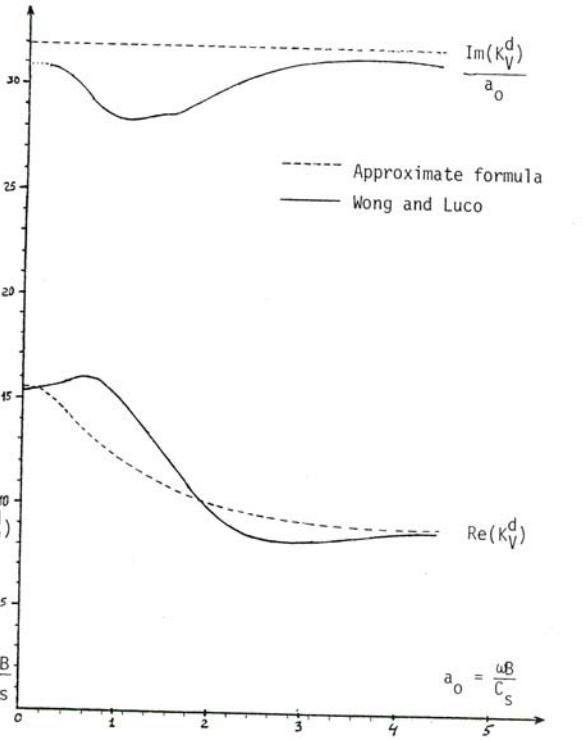

Fig. 26 - Variation of the stiffness with the frequency surface foundation L/B = 4 (vert. mode)

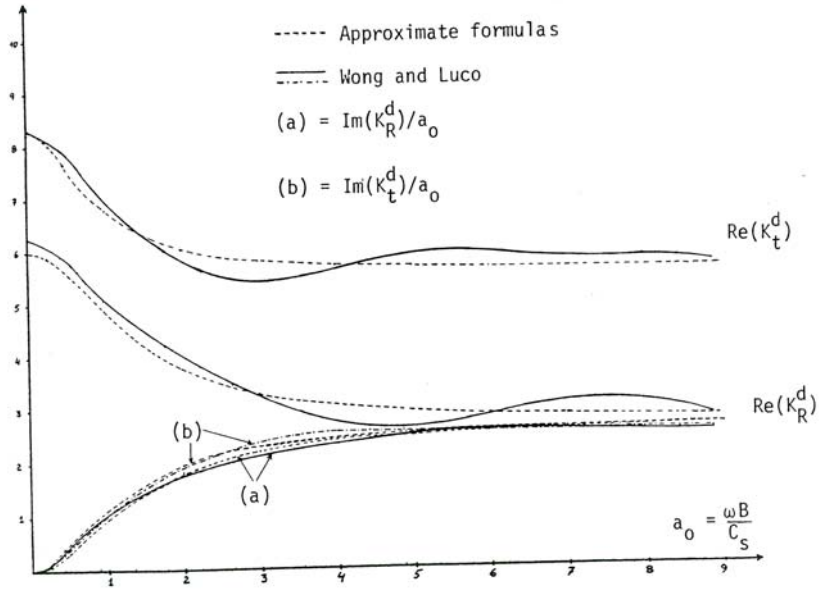

Fig. 27 - Variation of the stiffness with the frequency-surface foundation L/B = 1 (rocking and torsion)

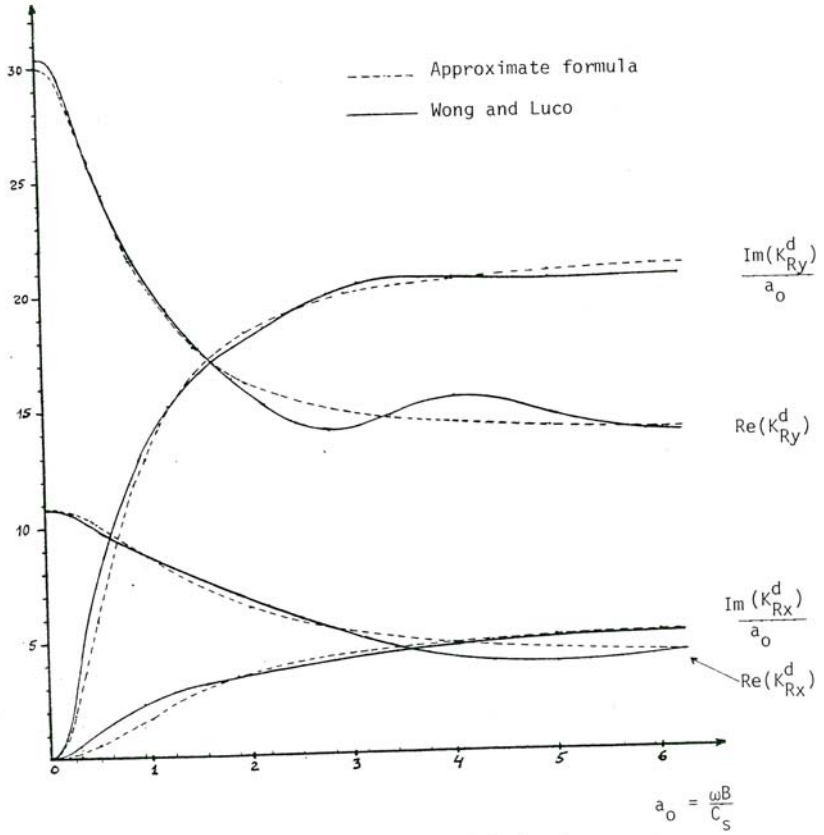

Fig. 28 - Variation of the stiffness with the frequency-surface foundation L/B = 2 (rocking)

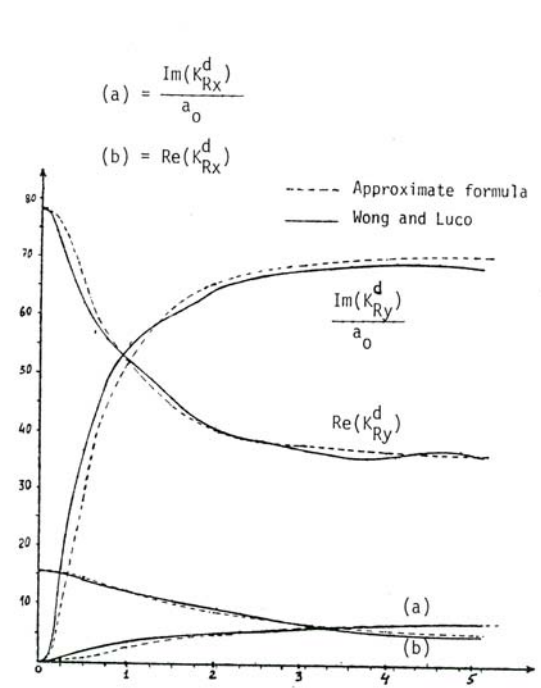

Fig. 29 - Variation of the stiffness with the frequency-surface foundation L/B=3 (rocking)

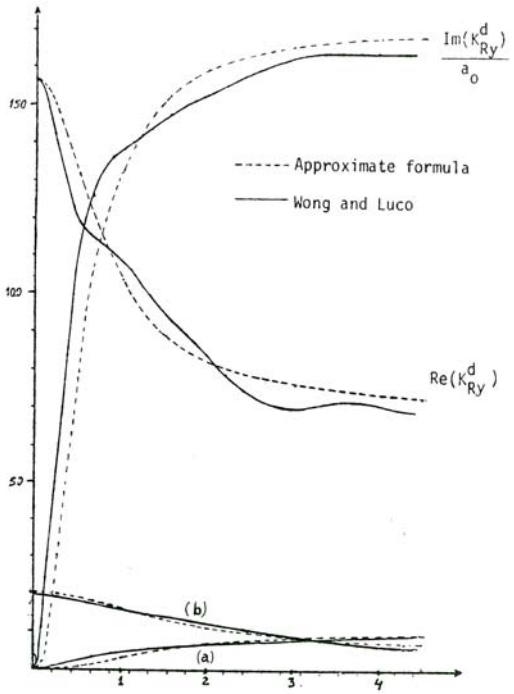

Fig. 30 - Variation of the stiffness with the frequency-surface foundation L/B = 4 (rocking)

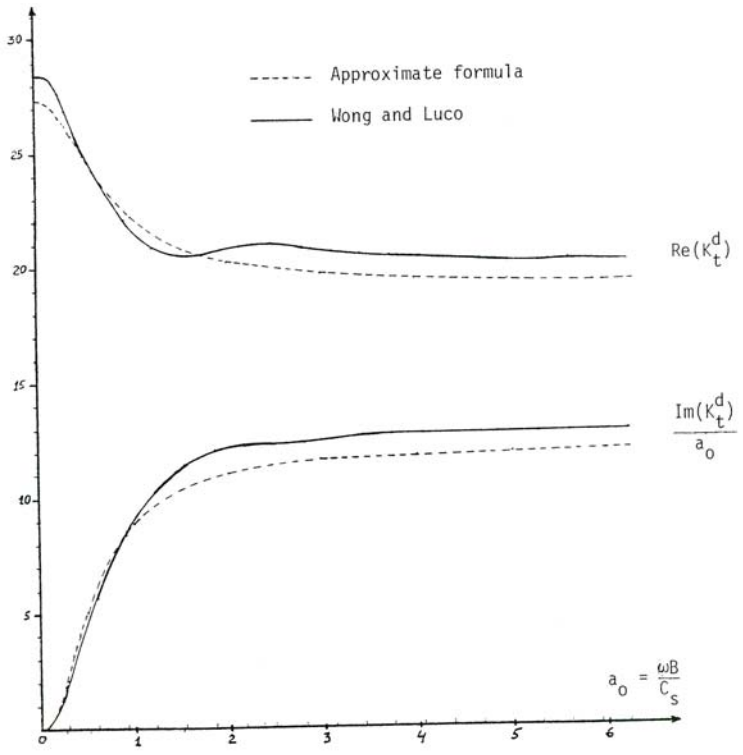

Fig. 31 - Variation of the stiffness with the frequency-surface foundation L/B = 2 (torsion)

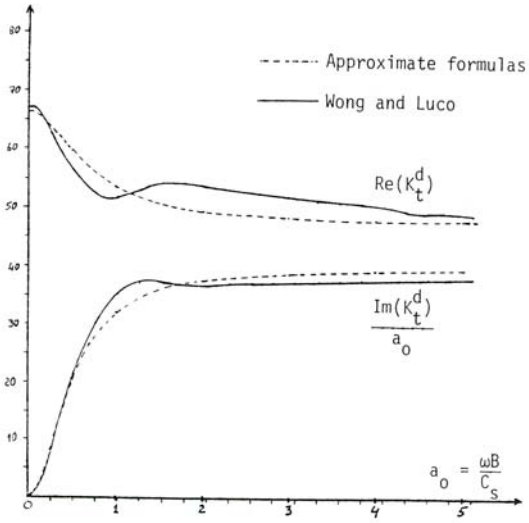

Fig. 32 - Variation of the stiffness with the frequency-surface foundation L/B = 3 (torsion)

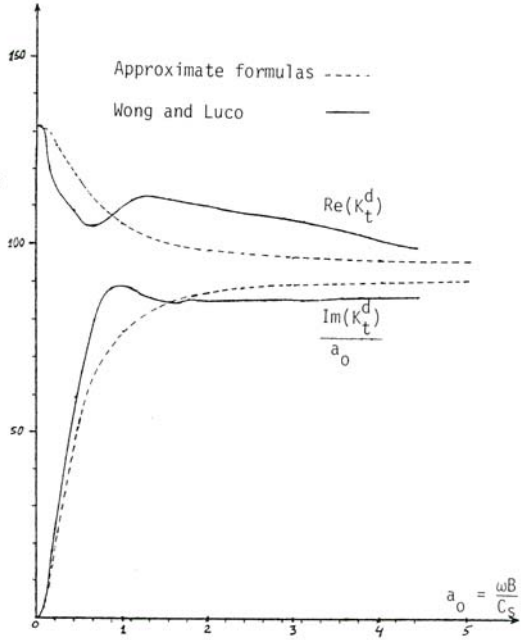

Fig. 33 - Variation of the stiffness with the frequency-surface foundation L/B=4 (torsion)

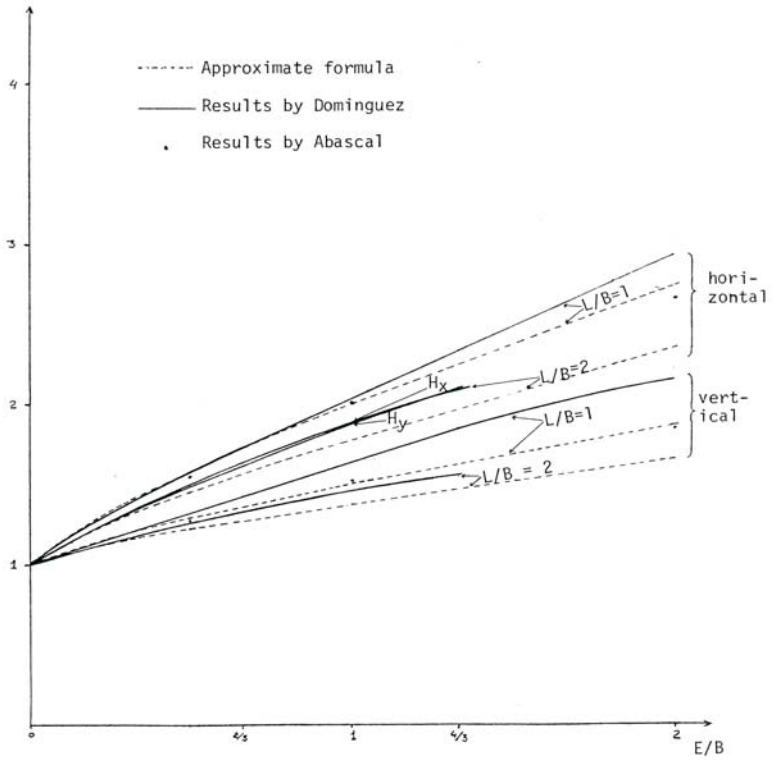

Fig. 34 - Variation of the static stiffnesses with the embedment - horizontal and vertical

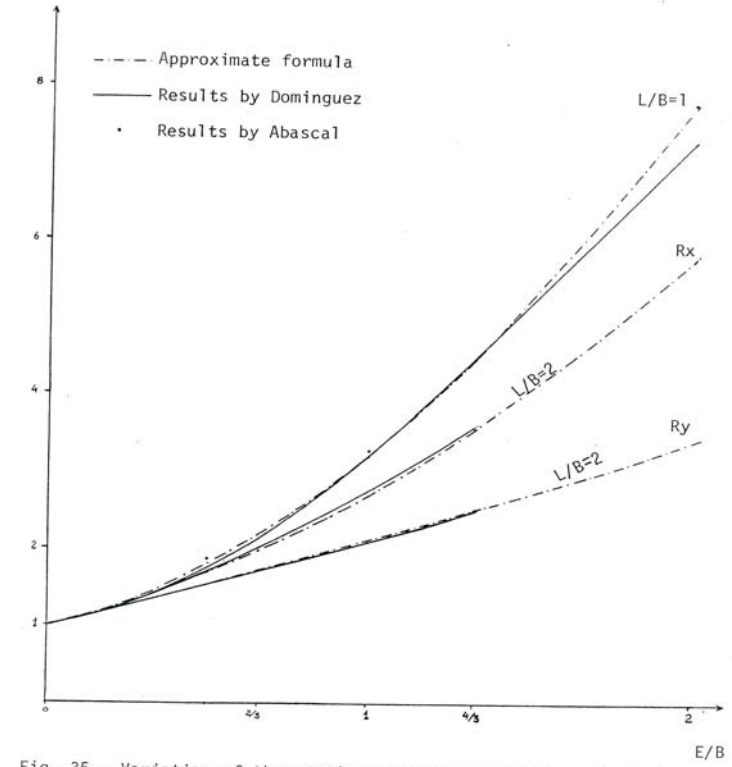

Fig. 35 - Variation of the static stiffnesses with the embedment - rocking

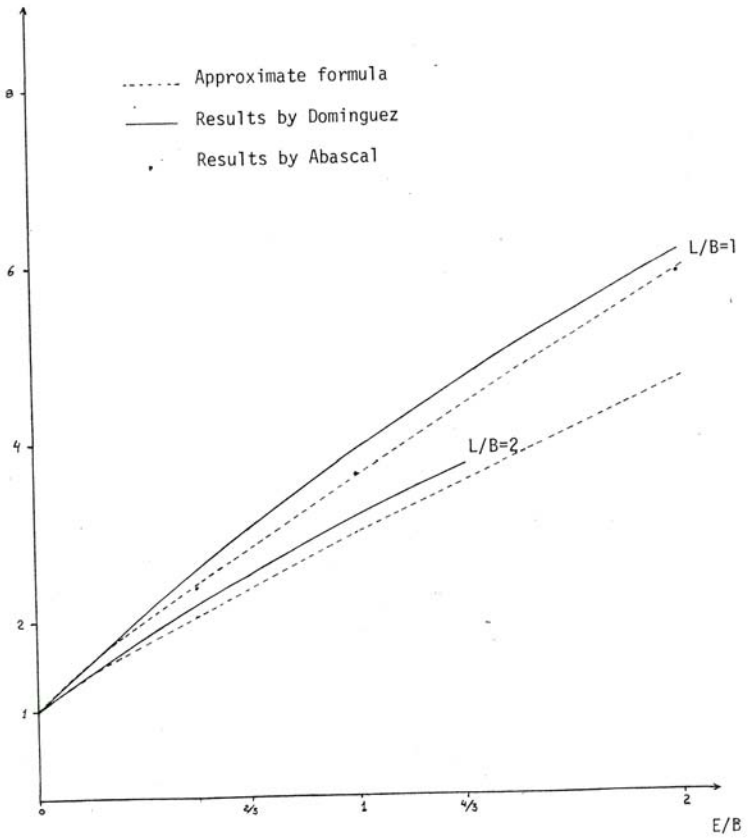

Fig. 36 - Variation of the static stiffness with the embedment - torsion

Vitae

Jeffrey McQuillan, LT, CEC, USNR

Education

B.S. (Aerospace Engineering), United States Naval Academy, 1998

Employment

United States Navy 1998-2002

Professional Affiliations

The Society of American Military Engineers

The Society of Naval Architects and Marine Engineers

The American Institute of Aeronautics and Astronautics

The National Space Society

The Planetary Society

The National Air and Space Society